PMM/A-42

COMISION NACIONAL DE ENERGIA ATOMICA
DEPENDIENTE DE LA PRESIDENCIA DE LA NACION

SEXTO CURSO PANAMERICANO DE METALURGIA

Dentro del Programa Multinacional de Metalurgia
(Programa Regional en Ciencia y Tecnología - OEA)

FRACTURE

Prof. Dr. W.H. Irvine

Departamento de Metalurgia
Buenos Aires - Argentina

1970

PMM/A-42

COMISION NACIONAL DE ENERGIA ATOMICA
DEPENDIENTE DE LA PRESIDENCIA DE LA NACION

SEXTO CURSO PANAMERICANO DE METALURGIA

Dentro del Programa Multinacional de Metalurgia
(Programa Regional en Ciencia y Tecnología - OEA)

FRACTURE

Prof. Dr. W.H. Irvine

Departamento de Metalurgia
Buenos Aires - Argentina

1970

FRACTURE*

LECTURE No. 1

INTRODUCTION

1. One of the most important factors in the development of new technologies, such as space exploration and nuclear power, is pressure vessel integrity. In considering the adequacy of existing practice for these new applications, it is prudent to take into account the differences which may exist in service conditions and consequences of failure. The main differences between say nuclear reactor pressure vessels and conventional vessels is as follows:-

(a) Because of the much greater consequences of failure in the case of nuclear reactor vessels there is a need for much greater reliability.

(b) Operational inspection is important in detecting defects which could otherwise develop in service and cause a major rupture. Approximately 90% of all failures in conventional plant are detected during such inspection, yet most nuclear reactor pressure vessels constructed up to this time are not directly accessible for periodic inspection.

A recent examination of the failure statistics of conventional pressure vessels in the U.K.(1) is summarised in Table I and this suggests that the average rate of explosive failure in such plant, <u>if it was not periodically inspected</u>, would be 1 in 10^3 to 10^4 plant years. Such a rate is not likely to be acceptable for nuclear reactor vessels in a large power programme.

2. The older codes of practice tended to evolve by the writing of a new rule for each distress as it occurred. This process is being increasingly modified as these newer technologies develop and the idea that pressure vessel design should take into account possible modes of failure has now gained a moderate amount of acceptance. Knowledge of possible patterns of failure should, of course, be obtained directly from service experience and until fairly recently such experience was largely hidden behind a veil of secrecy. However, more enlightened policies are gradually being introduced here as well and the recent survey of pressure vessel

....

* U.K.A.E.A., England

failures mentioned above shows that at least 89% of service failures are by cracking and about 50% of these are caused by fatigue assisted mechanisms. Thus it would appear that the majority of pressure vessel failures may be considered to follow a common path, i.e., crack initiation, crack growth to critical size and fast fracture.

3. The three possible phases may exist in differing proportions. Examples are:-

(a) Brittle fracture during fabrication provides initial defect. Defect may, or may not, be extended by a number of pressure cycles. E.g., Cockenzie Steam Drum - failure during pressure test (5 cycles).(Figs 1 and

(b) Small weld crack of uncertain origin associated with brittle material. Defect may, or may not, be extended by a number of pressure cycles. E.g., Immingham Ammonia Vessel - failure during pressure test.(4 cycles). Figs. 3, 4 and 5).

(c) Crack initiation and growth from stress concentration during service. E.g., German Boiler Drum. (Figs 6 and 7)

From these and other cases, it is obvious that component life is dependent on:-

(1) The initial size of crack present at the commissioning of the plant.

(2) The growth rate of this crack under operating conditions.

(3) The critical size to which the crack has to grow for fast fracture under operating conditions.

Reasons for Improving Technology

4. There are other reasons for improving pressure vessel technology other than obtaining a satisfactory failure rate, although these are more closely related to economic considerations than those of safety. There is obviously an ever present pressure to reduce capital costs by raising stress levels and thus making vessels thinner and lighter. Thus, in the last fifteen years design stress levels in mild steel atmospheric temperature have increased from one quarter of ultimate tensile strength (about 5 T.s.i.) to two thirds of the yield stress (about 10 T.s.i.).

Obviously such a trend is only permissible if it is accompanied by comparable improvements in the understanding of the pattern of failure behaviour, the increased use of stress analysis techniques (theoretical and experimental) and the more rational and rigorous inspection and testing of all the materials of construction and of the finished pressure vessel.

5. Although the important role of operational inspection has been emphasised earlier, it is important to recognise that this is itself a very expensive procedure in terms of the down time of the plant. It is therefore a direct reduction in plant availability unless it can be carried out concurrently with some other basic operation on the plant such as re-fuelling. Here again, the emphasis is on improving the technology through an improved understanding of failure behaviour, thus leading to the development of methods of indirect inspection and a minimal amount of direct inspection.

6. The different phases of vessel failure have been described in para. 3. In a pressure vessel of welded construction it is impossible to be completely sure that there are no cracks present in the finished construction. Consequently, by quantifying these various stages of crack development by use of a fracture mechanics approach, it is possible to achieve the objective described above. The details of such analyses are dealt with in subsequent lectures.

Consequences of Failure

7. Once the fast propagation of the crack has commenced, the extent of propagation is controlled by the amount of energy contained in the pressure vessel and by its availability at the crack. The amount of energy in a compressible fluid such as gas will be high, while for a relatively incompressible fluid such as water, it will be low. The strain energy in the steel vessel itself will be negligible compared with the gas energy, but of the same order as the water energy. The availability of the stored energy is also important, e.g., in a long gas pipe of ductile material it is possible for a propagating crack to arrest due to loss of pressure and stress caused by the difference in the speed of the crack front and the decompression wave in the gas

8. In cases where the material behaves in a brittle manner, either because it is intrinsically brittle, or because of the high strain rate produced by high energy availability, fragmentation due to branching of the crack may occur. Thus, the containment of compressible fluids under pressure, constitutes the greatest potential hazard, both from the point of view of complete disruption of the container, loss of its contents and the formation of high velocity missiles.

9. It is important to realise however that large amounts of energy may be stored in fluids which are relatively incompressible such as water where the volume involved is large. In such a situation the consequences of failure can still be hazardous with extensive crack propagation and possibly missiles. An additional hazard could be the tidal wave produced by the sudden release of a large volume of fluid. Figs 8 and 9 show such a failure which occurred to a Sizewell Atomic Power Station boiler shell.

10. The two extremes of compressibility may be thought of in terms of a constant deflection versus a constant load model. (Fig. 8). Here, it will be seen that in the constant strain case, the strain energy decreases as the crack extends, while in the constant load case, the strain energy increases by the same numerical amount and the work done by the external load is twice the change in strain energy. This, of course, means that the energy being released at the crack is the same in both cases.

General Summary of Methods of Avoiding Fast Fracture

11. The occurrence of fast fractures in steel bridges, ships and pressure vessels has led to numerous investigations of this phenomena and the usually brittle appearance of the fracture surface led to the term 'brittle fracture' being adopted. The materials involved usually exhibited adequate ductility in a tensile test but when tested in the form of a notched bar such as in the Charpy, Izod, or notched tensile (Tipper) test, the fracture surfaces of the test piece underwent a transition from brittle to ductile appearance as the test temperature was raised. The other test parameters such as energy absorbed, contraction in thickness at the tip of the notch etc., also underwent a sudden change in the same temperature region. Thus it was originally thought that this temperature represented the boundary line

between brittle behaviour and ductile behaviour in the presence of a notch or crack and it became known as the transition temperature. However, the transition temperature as measured by various tests varied somewhat depending on the type of test piece, speed of testing etc., and a large number of tests were developed each one with its own individual claims to realism in reproducing practical conditions. The more prominent of these tests are described in the next lecture. Later work showed that the general idea of transition temperature is a myth and the mechanical parameters of stress level, energy content and availability, size of crack, etc., are equally, if not more important than notch ductility.

12. The transition temperature approach is still widely used and involves keeping the component above the transition temperature as indicated by the particular test in vogue.

13. Griffith[2] developed his original theory for glass which could be treated as elastic. He considered the stability of a crack by equating the energy which would be absorbed in an incremental extension of the crack, in creating new fracture surfaces to the strain energy which would be released. He was of the opinion that crack extension would occur when the stress at the crack tip reached a certain value, but was unable to use a direct stress approach because the elastic analysis of a crack predicts infinite stress at this point.

14. Griffith's original model has since been modified and other methods have been developed and are described later. The use of a crack model to describe crack extension in terms of crack size, stress level, material properties and geometrical parameters has come to be known as fracture mechanics. It is usually used in conjunction with the onset of fast fracture. However, there seems to be no valid reason why it should not be used also to cover crack growth.

TABLE I

The total number of failures reported is related to about 100,300 vessel years.

The distribution of the causes of all service failures is:-

		No. of Cases	%
(i)	Cracks	118	89.3
(ii)	Corrosion (including stress corrosion, assisted fatigue and wastage)	2	1.5
(iii)	Maloperation (including water shortage, control malfunction)	8	6.1
(iv)	Pre-existing from manufacture (e.g., material or fabrication causes)	3	2.3
(v)	Creep failure	1	0.8

The distribution of the defects amongst the various detection methods is:-

		No. of Cases	%
(i)	Visual examination	75	56.9
(ii)	Leakage	38	28.8
(iii)	Non-destructive testing methods	10	7.5
(iv)	Hydraulic test	2	1.5
(v)	Catastrophic failure	7	5.3
		132	100.0

The majority of failures (89.3%) were due to cracks and most of these were at branches and fillet welds. Since a large proportion of the incidents were due to cracks, these have been examined separately.

The distribution of the cause of the cracks is as follows:-

		No.	%	% Total
(i)	Fatigue (including mechanical and thermal fatigue)	47	40.0	35.6
(ii)	Corrosion (including stress corrosion, assisted fatigue and wastage)	24	20.3	18.2
(iii)	Pre-existing from manufacture	10	8.4	7.6
(iv)	Not ascertained	35	29.6	26.5
(v)	Miscellaneous	2	1.7	1.5
		118	100.0	89.4

REFERENCES

1. PHILLIPS, C.A.G., WARWICK, R.G. A Survey of Defects in Pressure Vessels Built to High Standards of Construction and its Relevance to Nuclear Primary Circuits. AHSB(S)R 162, 1968

2. Report on the Brittle Fracture of a High Pressure Boiler Drum at Cockenzie Power Station. South of Scotland Electricity Board, January, 1967.

3. B.W.R.A. Bulletin, Vol. 7, No. 6, June, 1966

4. Von. K. WELLINGER, D.UEBING. Festigkeitsuntersuchungen an einer nahtlosen Kesseltrommel aus Th 31 R.

5. Special Report on Failure of a Boiler during Hydrostatic Test at Sizewell Nuclear Power Station. West of Scotland Iron and Steel Institute, 1964.

6. OROWAN, E. Energy Criteria of Fracture. The Welding Journal, Welding Research Supplement, p. 1575, March, 1955.

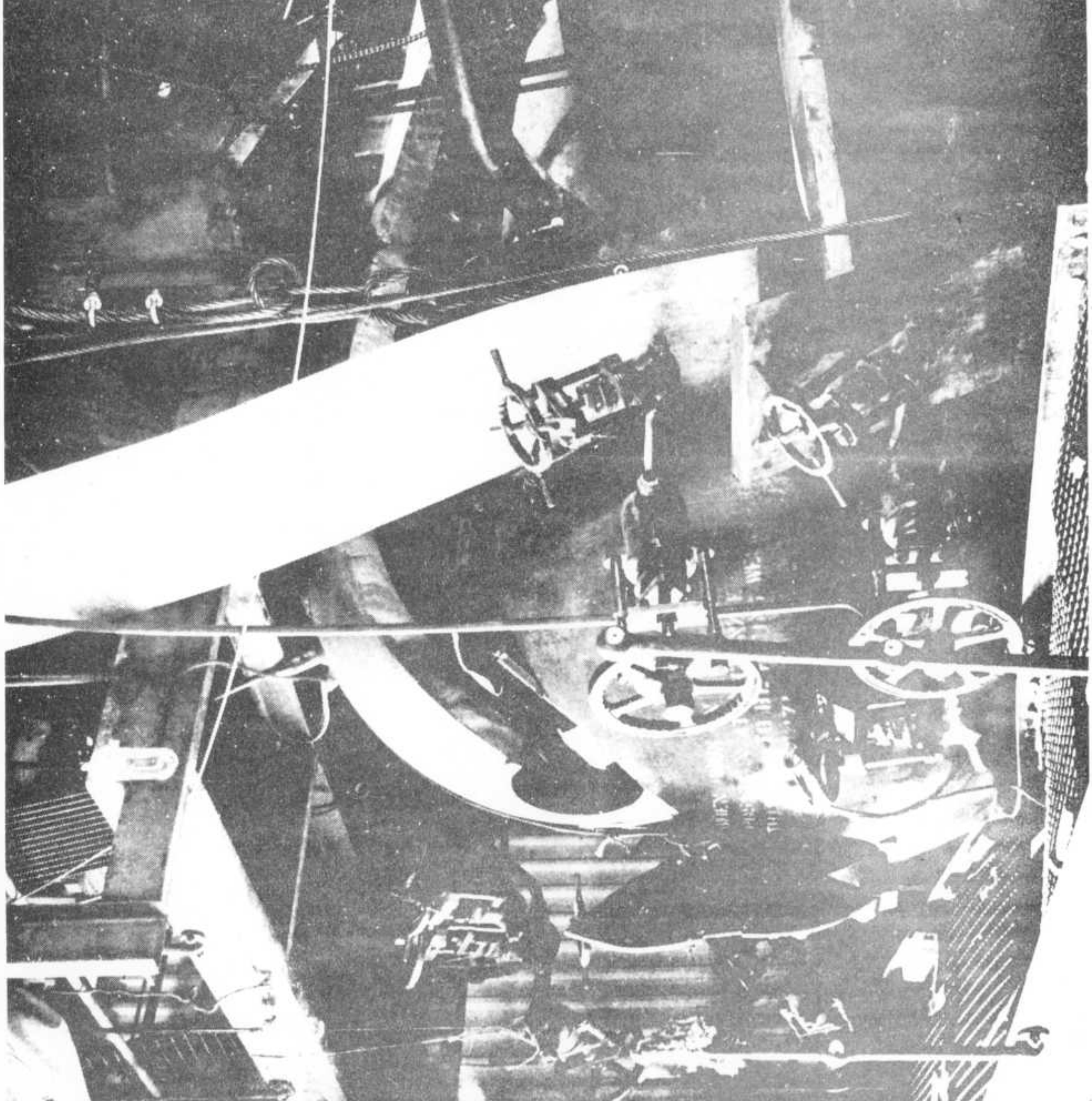

Fig. 1

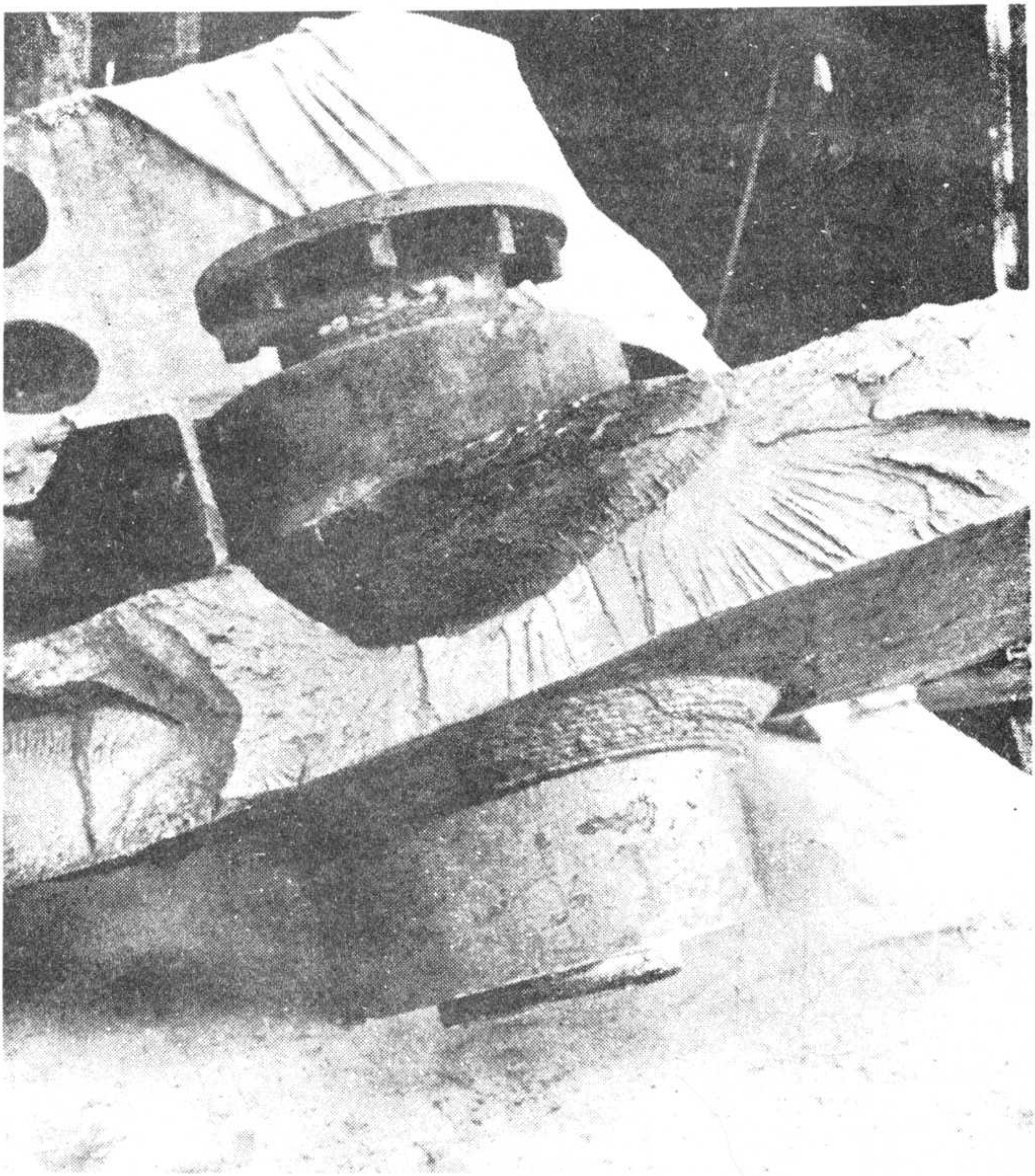

Fig. 2 : *Blackened surface of crack associated with economiser nozzle.*

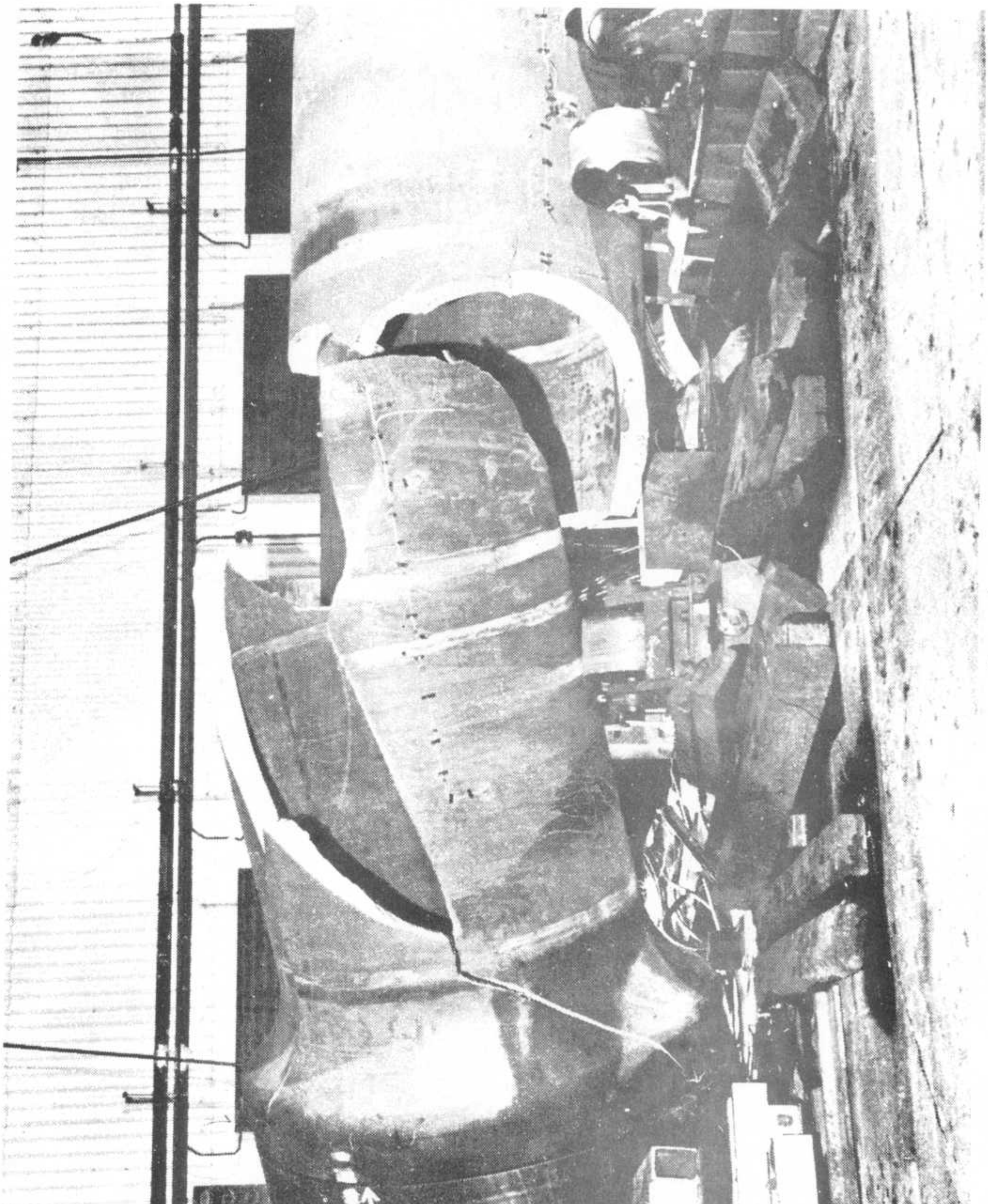

Fig. 3

Fig. 4

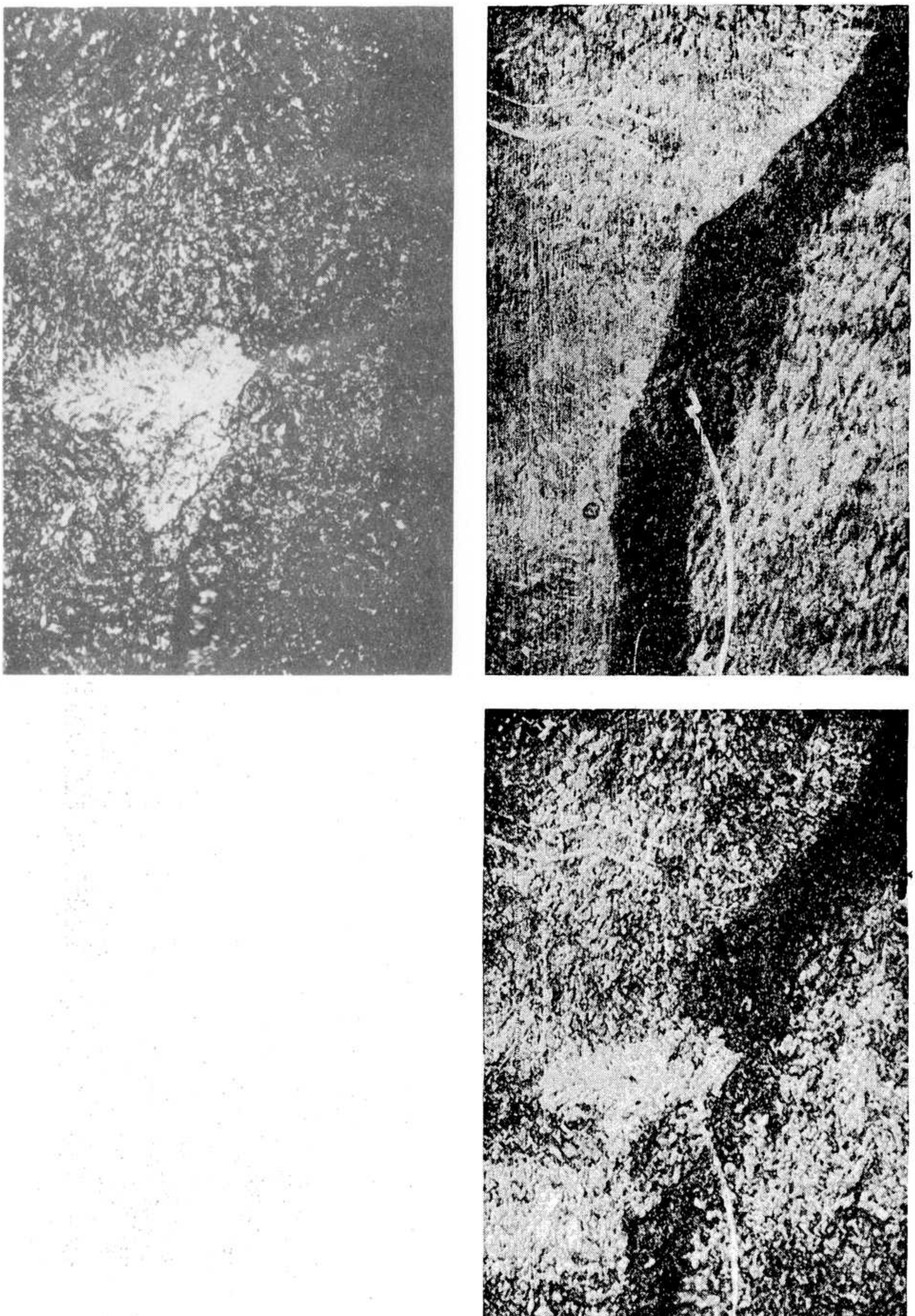

a

b

Fig. 5

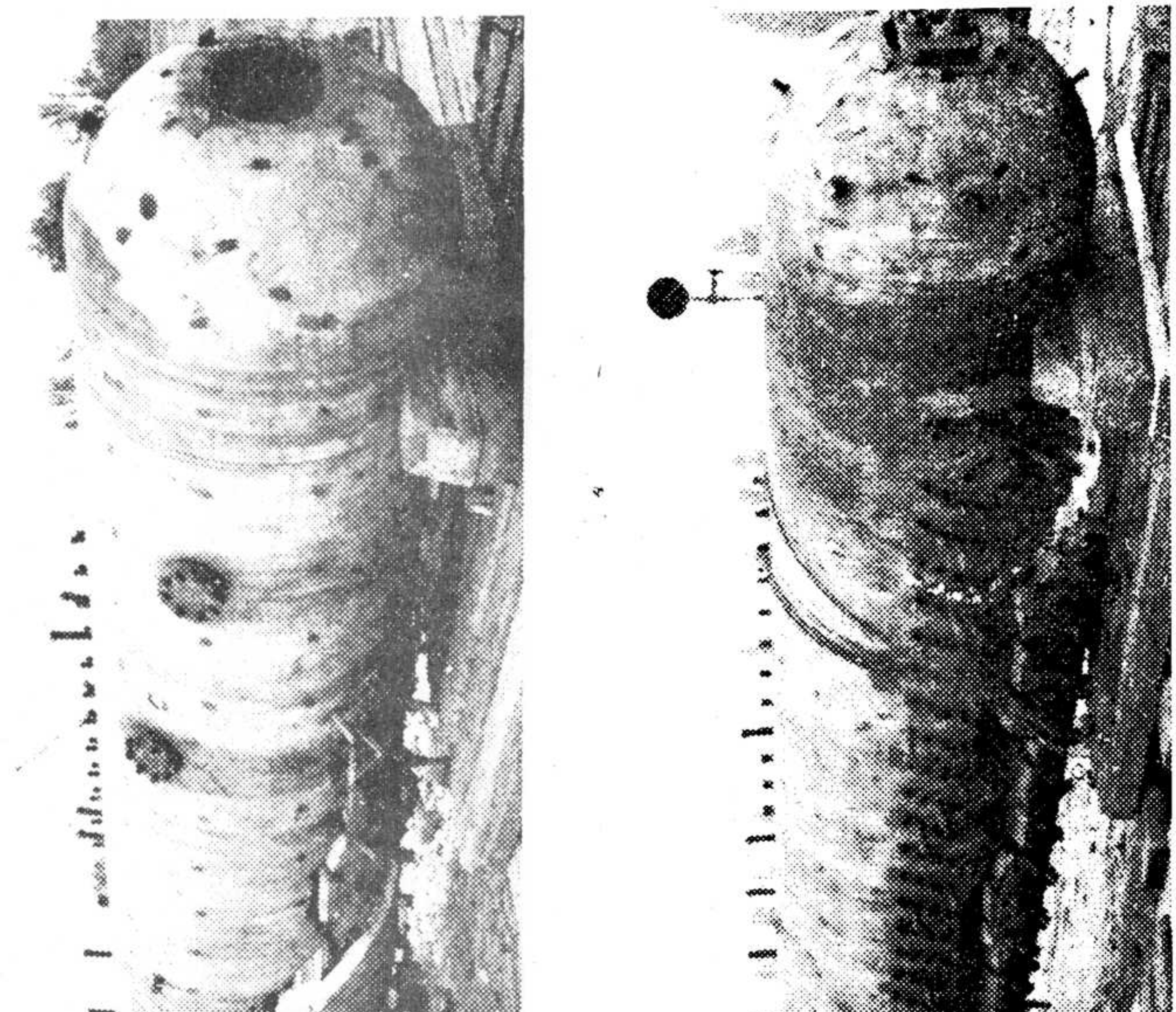

Fig. 6

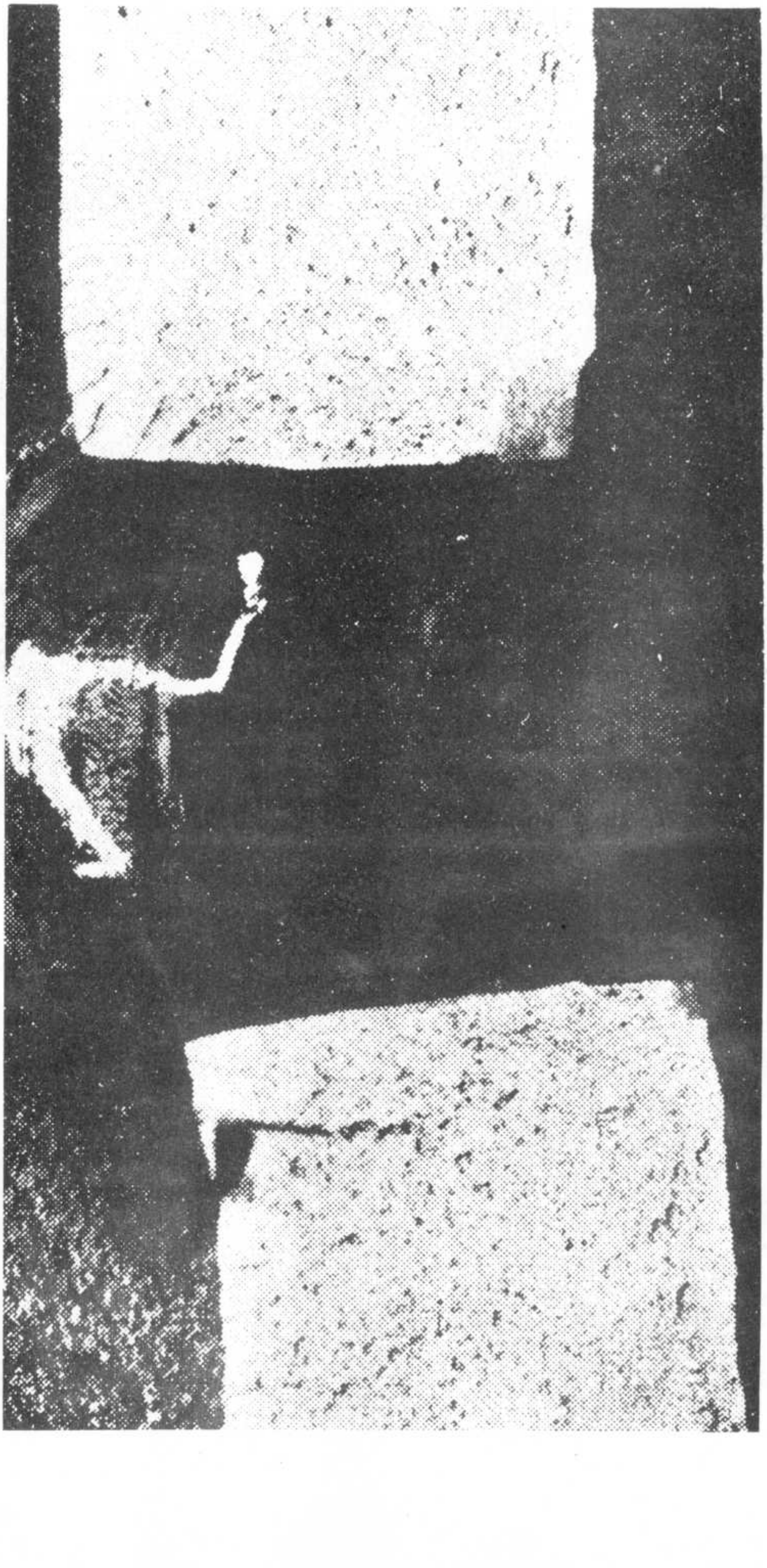

Fig. 7

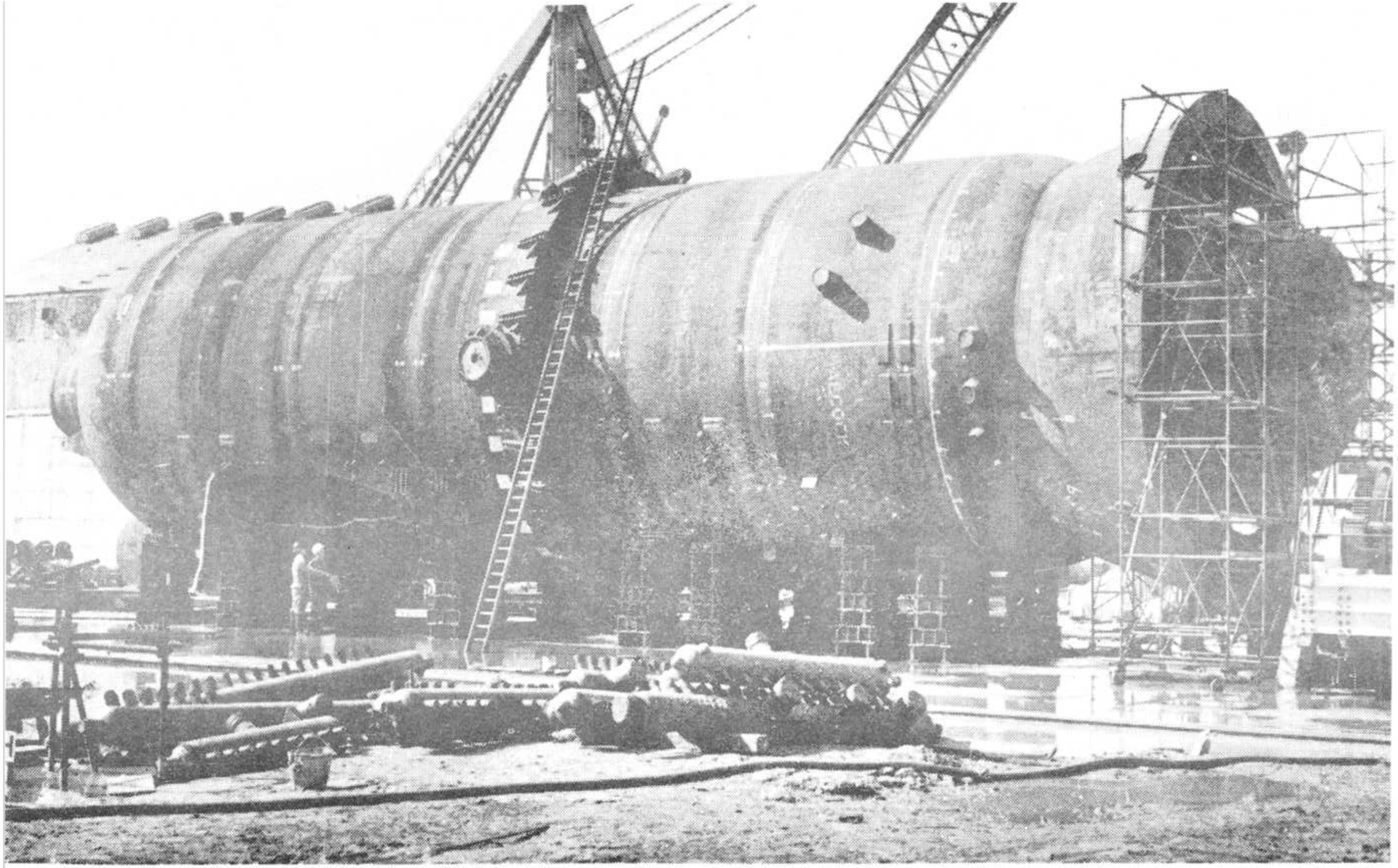

Fig. 8 : Failure of boiler No. 2A under hydrostatic test.

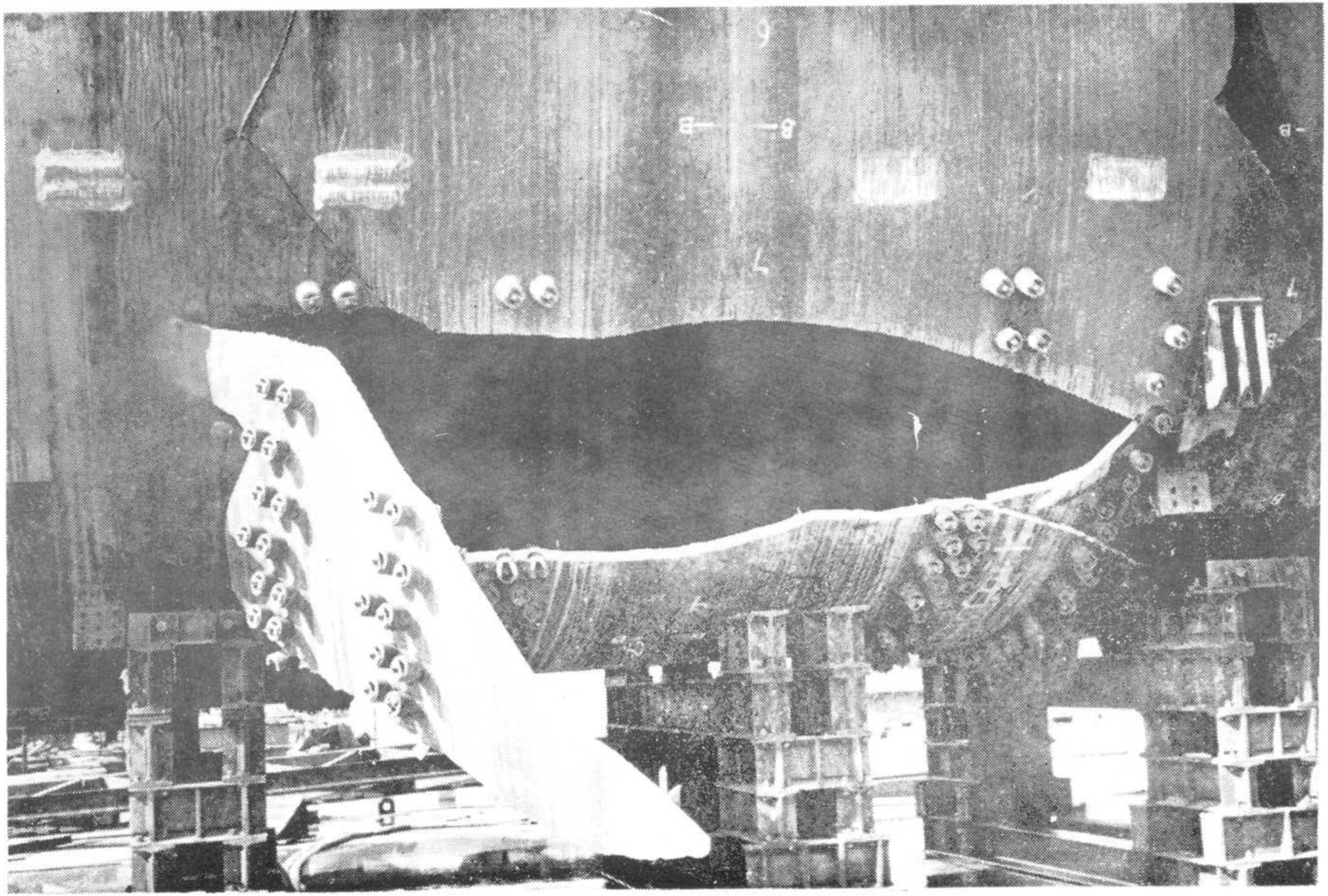

Fig. 9 — *Failure of boiler No. 2A under hydrostatic test.*

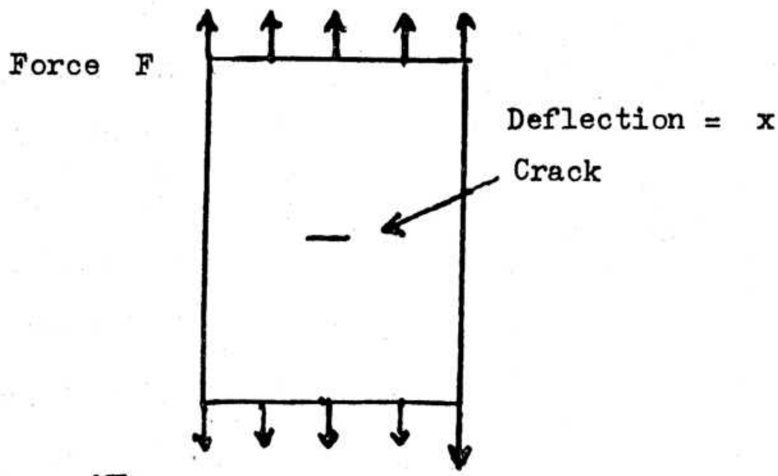

$$x = MF$$

$$\text{Strain energy } U = \int_{x=0}^{x=MF} F\,dx = \frac{MF^2}{2}$$

then

$$dU = \frac{F^2}{2}\,dM + MF.\,dF \qquad \ldots \qquad \ldots \qquad \underline{1}$$

If crack increases with grips fixed

$$x = MF = \text{Const.}$$

$$dx = MdF + FdM = 0$$

putting $MdF = -FdM$ in $\underline{1}$

gives

$$dU = -\frac{F^2}{2}\,dM \qquad \ldots \qquad \ldots \qquad \underline{2}$$

On the other hand for Const. load F

$$dF = 0$$

$\underline{1}$ gives

$$dU = \frac{F^2}{2}\,dM \qquad \ldots \qquad \ldots \qquad \underline{3}$$

and F does the work. $Fdx = dW$

$$dW = F^2\,dM \qquad \ldots \qquad \ldots \qquad \underline{4}$$

Fig. 10

LECTURE No. 2

FAST BRITTLE FRACTURE

TRANSITION TEMPERATURE APPROACH

Introduction

1. Until the early 60's the philosophy of safe operation of reactor pressure vessels was, to a large extent, dominated by the consideration of avoidance of brittle fracture. Although creep and stress rupture, etc., were taken into account in design, brittle fracture was considered to be the only practical means by which catastrophic failure of large pressure vessels could occur. High temperature failures due to creep, etc., were deemed to lead only to local leakage since a limited amount of theoretical work suggested that impractically large defects would be required to initiate catastrophic ductile failure. [1]

Classification of Type of Fracture - Brittle or Ductile

2. The classification of fracture type some ten or fifteen years ago, was based on the appearance of the fracture surface. Brittle fracture was defined as being of crystalline appearance (cleavage), with the fracture surface making an angle of 90° with the plate surface. Ductile fracture, where it occurred and was recognised as such, was defined as having fracture surfaces making an angle of 45° with the plate surface. There was a large body of expert opinion which completely denied the possibility of ductile fracture and in cases where it was observed, e.g., latter stage of fracture in Fawley tank failure, it was attributed to the 'arresting phase' of a brittle fracture.

More recently, mainly as a result of the rationalisation resulting from the application of fracture mechanics, it has come to be recognised that the appearance of a fracture is controlled by a number of factors such as material thickness, rate of loading (or rate of crack propagation), yield stress, etc. Thus it is possible for a fracture of brittle appearance to exist side by side with a fracture of ductile appearance in the same material, Fig. 1. The difference in this case, is that the ductile 45° fracture existed under the static conditions of crack initiation, whereas once the crack speed had increased to give a straining rate at the crack tip sufficient to increase yield stress and decrease plastic zone size beyond a certain level, the fracture took on the characteristics of a brittle fracture. Thus the differences in fracture type are mechanical rather than metallurgical.

Transition Temperature Approach

3. The bulk of earlier work on vessel safety was thus devoted to tests aimed at delineating some temperature limit for a given material below which the material was susceptible to brittle fracture and above which it was immune and hence, in the absence of gross over-pressure, free from any danger of catastrophic failure. These tests ranged from the relatively simple determination of transition temperatures using the Charpy V notch impact test, through drop weight tests using crack starters, to crack arrest tests in which large specimens, held in tension in hydraulically loaded machines, are brought to test temperature and then subjected to a fast running brittle crack induced at one locally chilled edge of the specimen.

Brittle Fracture Tests

4. Some of the more prominent tests are described below.

Charpy Test

The Charpy V notch test is probably the most widely used. The test piece is in the form of a 10 m.m. square bar with a 45° V notch in the middle. The notch is 2 m.m. deep and has 0.25 m.m. radius at its tip. Fig. 2. The test piece is broken in a pendulum type machine and the energy absorbed measured. The relative amounts of fibrous ('ductile') and cleavage ('brittle') fracture are usually observed directly from the fracture surface. There is also a change in the amount of lateral deformation at the tip of the notch [2] in the transition temperature range and this is sometimes measured. Standardised criteria have been used for choosing the transition, e.g., temperature for 20 ft. lbs., or temperature for 50% crystalline fracture. It is now fairly widely accepted that correlations of the temperature for a certain energy absorbtion with other tests, have no general validity.

Tipper Test (3)

This test has only been used very infrequently. It consists of a specimen of full plate thickness with V notches machined in the edges. The width to thickness ratio should be about 10 to one. The specimen is broken by a tensile stress applied at right angles to the notched cross section. See Fig. 3. The maximum stress and reduction in thickness are both plotted against temperature. The fracture appearance is recorded. The sudden change in reduction in thickness with temperature is probably the most useful indication.

Drop Weight Test (4) and (5)

This test has been developed and used by N.R.L., Washington, although other workers appear to have had similar ideas. The drop weight test piece is shown in Fig. 4. A plate like specimen is supported at its ends and is subjected to a rapidly applied load at mid span by a dropped weight. A brittle weld bead on the tension side of the specimen serves as a crack starter. The bead is nicked almost to the surface of the plate. As the specimen bends under the action of the load a crack forms at the base of this notch in the brittle weld bead. Further deformation may, or may not, cause this crack to propagate into the specimen depending on the degree of brittleness present. The deformation of the specimen is usually limited to an angle of bend of 3" by a stop at mid span. The highest temperature at which the specimen breaks into two pieces is termed the nil ductility transition temperature. (N.D.T.). The N.D.T. has been correlated with the Charpy V test, the impact energy varying with the type of material, i.e., from about 10 ft.lbs. for mild steel to 50 ft. lbs. in alloy steels.

The Explosion Bulge Test (4) and (5)

This test has been used to evaluate the crack propagation characteristics of materials. In this case the sample consists of a square plate (or weldment) with a brittle weld bead on the underside. The plate is placed on an open die and an explosive charge detonated over the plate. The nature and extent of the resulting deformation and cracks is used to rate the materials. When tested over a range of temperatures the performance of a given material changes from extensive plastic bulging, with or without some ductile shear tearing from the brittle weld bead, at high temperatures to a flat, brittle, shattering type of fracture at low temperatures. The high temperature, where extensive deformation without brittle cracking occurs, is referred to as F.T.P., fracture transition plastic. The temperature below which the cracking begins to extend beyond the deformed material, into the elastic loaded edge regions, has been designated F.T.E., fracture transition elastic. The brittle shattering type of fracture is obtained at the N.D.T. temperature. The relative positions of these transition temperatures, superimposed on a Charpy V notch impact energy curve, is shown schematically in Fig. 5. Practical considerations involved in conducting the esplosion test limits its use compared with the drop weight or Charpy impact tests.

Wells Wide Plate Test [(6) and (7)]

The test piece comprises of two rectangular plates joined by a butt weld. At the mid length of the butt weld a saw cut is made transverse to the weld axis before welding. (See Fig. 6). The specimen is loaded in tensile parallel to the axis of the weld by jacks acting on lugs attached to its ends. The failure stress for various test temperatures is noted along with the amount of plastic strain at failure.

Robertson Crack Arrest Test [(8)]

(a) Gradient Test

In this a large plate is loaded to a uniform tensile stress while a temperature gradient is maintained across the width of the plate. A crack is started by firing a bullet into the cold side of the plate and it runs up the temperature gradient until it reaches material which has sufficient 'toughness' to arrest it. The temperature at which this arrest occurs is known as the 'crack arrest temperature'. From a series of tests where the stress is varied a relationship of stress and temperature such as is shown in Fig. 7 is obtained.

(b) Isothermal Test

The Robertson test has been modified into a constant temperature test to eliminate uncertainties and possible complications caused by the temperature gradient. This test is similar to the S.O.D.(Standard Oil Development) test. There is a slight difference between the results of the gradient and isothermal tests. A typical Robertson Machine is shown in Fig. 8.

Limitations to the Validity of the Transition Temperature Approach

5. Tests such as are described above led to the concept of a minimum operating temperature, below which loading of the component was forbidden. This temperature was established by reference to a certain value of impact energy in the Charpy test, or by the addition of a temperature margin to the Nil Ductility Temperature or Crack Arrest Temperature. Pellini (9) summarised these ideas in his fracture analysis diagram and in addition incorporated in this a crude form of fracture mechanics, which recognised the relation between stress level and defect size.Fig. 9. This diagram clearly defined, in terms of nominal stress:-

1. The N.D.T. at which fractures can occur at nominal stresses between the yield stress and one fifth of the yield stress depending on defect size.
2. The F.T.E. (Fracture Transition Elestic) at which fractures can only occur above the yield stress and the stress levels are again dependent on defect size.
3. The F.T.P. (Fracture Transition Plastic) above which fracture cannot occur.

Pellini has since modified his original fracture analysis diagram in the light of some bursting test results which fell in the area where fractures were not supposed to propagate, i.e., to the right hand side of the C.A.T. curve. The first modification was to postulate that some materials could have low energy tear characteristics (such as poor weld heat affected zone properties). The second modification was to suggest that the long defects which existed in the bursting tests had, because of bulging in the region of the defect, amounted to gross plastic overload, and that it was thus permissible to plot these results as having failed at the ultimate tensile strength, Fig. 10.

Obviously, both of the effects mentioned above are important. It is difficult however, to believe that there are just low and high tear energies. Surely it is more likely that there is a whole range of possible toughness. Again, even in a flat plate, where bulging is impossible, there are high stresses at the crack tip and these must reach the fracture stress if failure is to occur. It would be just as logical therefore, to plot all failures at fracture stress level, not just the cases where bulging occurs.

However, since the ordinate is nominal stress it seems rather that the explanation is in the method of derivation of the C.A.T. curve. Both the Robertson and Wells type of wide plate machines really apply a strain or deflection to the specimen, and therefore, as the crack propagates across the specimen, it does so under constant strain or 'fixed grip' conditions rather than under constant load conditions. Orowan's analysis of these two conditions was described in Lecture 1. Therefore, the occurrence of an 'arrest' in the above tests is purely due to the relaxation of the general stress field as the crack traverses the plate and the C.A.T. curve of Fig. 9 is only valid for structural members which are operating under this type of loading, i.e., redundant members. The apparent anomolous behaviour in the bursting tests referred to earlier, can therefore be explained in terms of the high energy contained in the pressurising air. Similar behaviour has been observed in experiments which will be described later. Considerations similar to the above led to the development of the idea of a continuous range of behaviour from the most brittle of material failing at small defect sizes and low stress levels to the most ductile material failing at relatively large defect sizes and high stress levels.

<u>The Experiments of Sopher et al on 9 ft. Spheres</u> [10]

6. These experimental results were published in 1959 and by using Charpy value as a measure of material fracture toughness G in the Griffith equation:-

$$f^2 l = \frac{EG}{\pi}$$

in conjunction with the 9 ft. sphere experiments the author was able to construct the generalised diagram for mild steel shown in Fig. 11.

These predictions indicated that ductile failures could occur in mild steel pressure vessels under gas pressurisation with stress levels of two thirds of yield and crack lengths of one or two feet.

Thus, if the diagram of Fig. 11 was proved to be correct in principle, then the possibility of fast ductile fracture originating at defects would render the minimum operating temperature concept invalid as an all-embracing defence against catastrophic failure. Even in the event of the theoretical possibility of such a failure mode proving to be valid, the practical significance of such a mode would depend entirely on the actual size of the necessary initiating defects and the feasibility of the slow growth of defects to critical dimensions without displaying early signs of their existence, for instance by leakage.

REFERENCES

1. COTTRELL, A.H. Theory of Brittle Fracture in Steel and its Application to Radiation Embrittlement. CONF BRIT/P.P.1. 1958.

2. ORNER, G.M. Charpy Brittle-Fracture Transitions by the Lateral Expansion-Energy Relationship. The Welding Journal, Research Supplement p. 201S, May, 1958.

3. BAKER, J.F. TIPPER, C.F. The Value of the Notch Tensile Test. Proc. Inst. Mech. Engineers, Vol. 170, No. 1, 1956

4. PUZACK, P.P., ESCHBACHER E.W., PELLINI, W.S. Initiation and Propagation of Brittle Fracture in Structural Steels. Welding Journal Research Supplement Vol. 31, No. 12. p. 561S, December, 1952.

5. PUZACK, P.P. SCHUSTER, M.E., PELLINI, W.S. Crack Starter Tests of Ship Fracture and Project Steels. Welding Journal Research Supplement, Vol. 33 No. 10, p. 481S, October, 1954.

6. WELLS, A.A. Trans. Inst. Naval Arch. 1956, Vol. 98, p. 296.

7. WELLS, A.A. British Welding Journal, 1957, Vol. 4, p. 529.

8. ROBERTSON, T.S. Conference on the Properties of Materials at High Rates of Strain. Proc. Inst. Mech. Engineers, 1957.

9. PELLINI, W.S., PUZACK, P.P. Practical Considerations in Applying Laboratory Fracture Test Criteria to the Fracture-Safe Design of Pressure Vessels.

10. SOPHER, R.P., LOWE, A.L.,MARTIN, D.C., RIEPPEL, P.J. Evaluation of Weld Joint Flaws as Initiating Points of Brittle Fracture. Welding Journal Research Supplement, November, 1959.

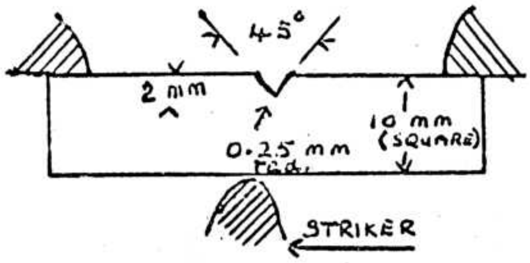

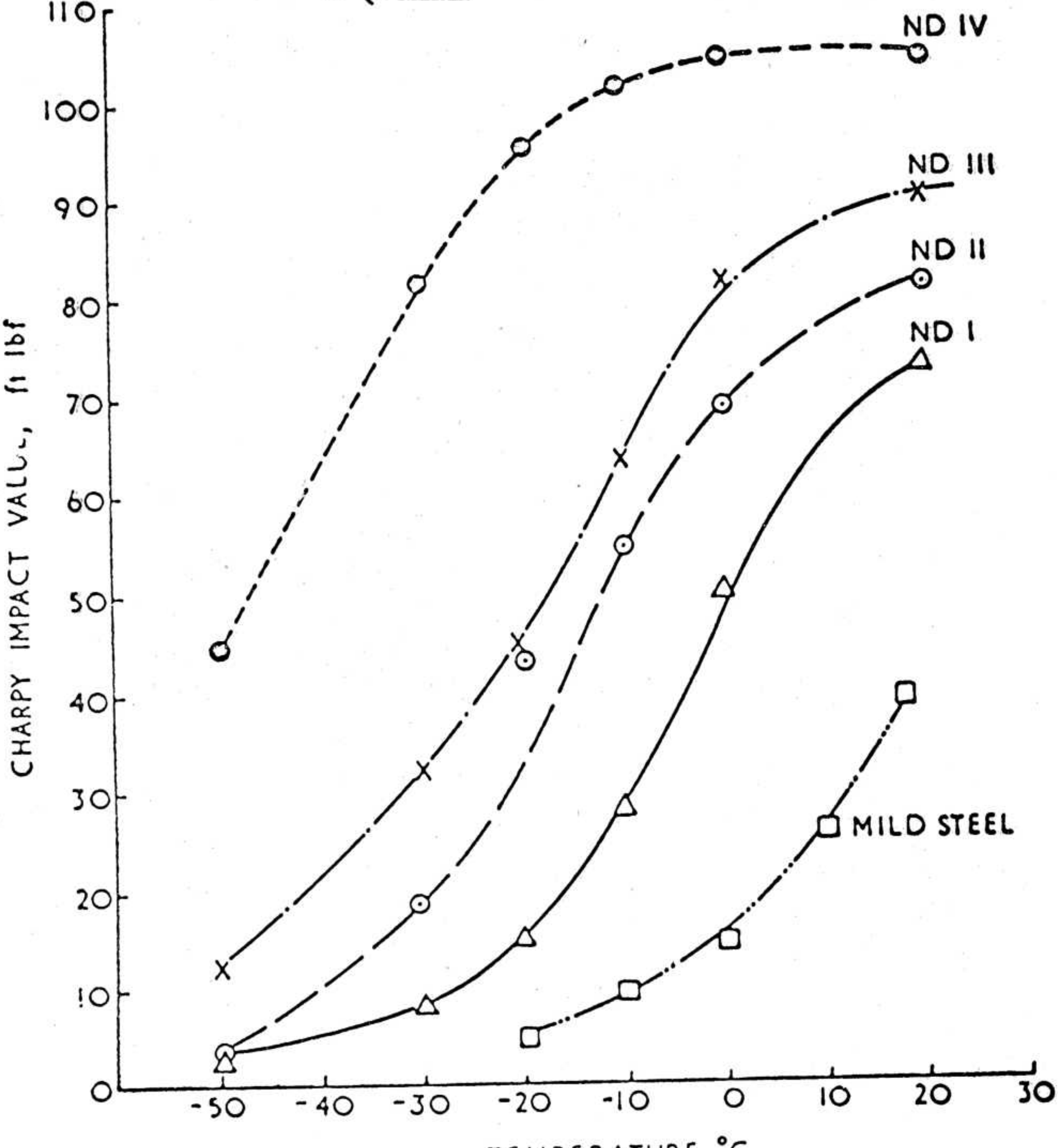

Effect of metallurgical factors on charpy V-notch **transition** curves of low-carbon high-manganese plate **steels.**

ND I. Semi-killed steel in as-rolled condition.
ND II. As ND I but normalized.
ND III. Silicon-killed steel, normalized.
ND IV. Aluminium-treated (fine grain) steel, normalized.

FIG. 2

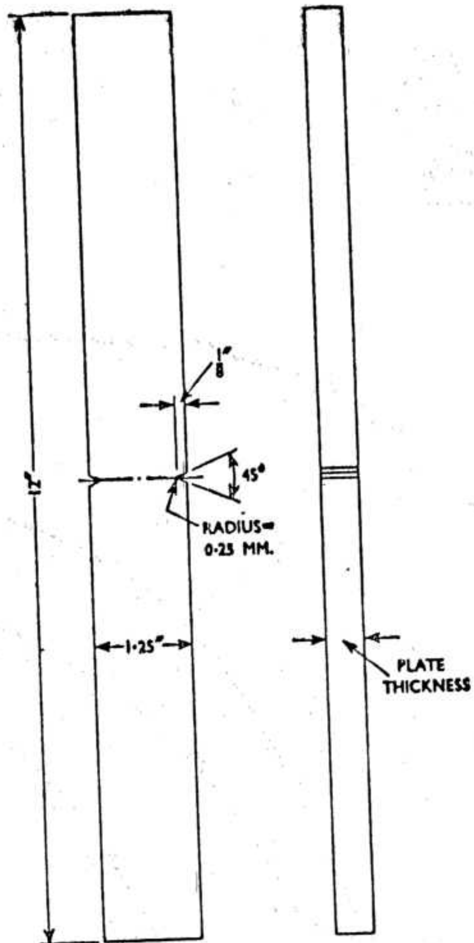

Notch Tensile Test, Standard Dimensions

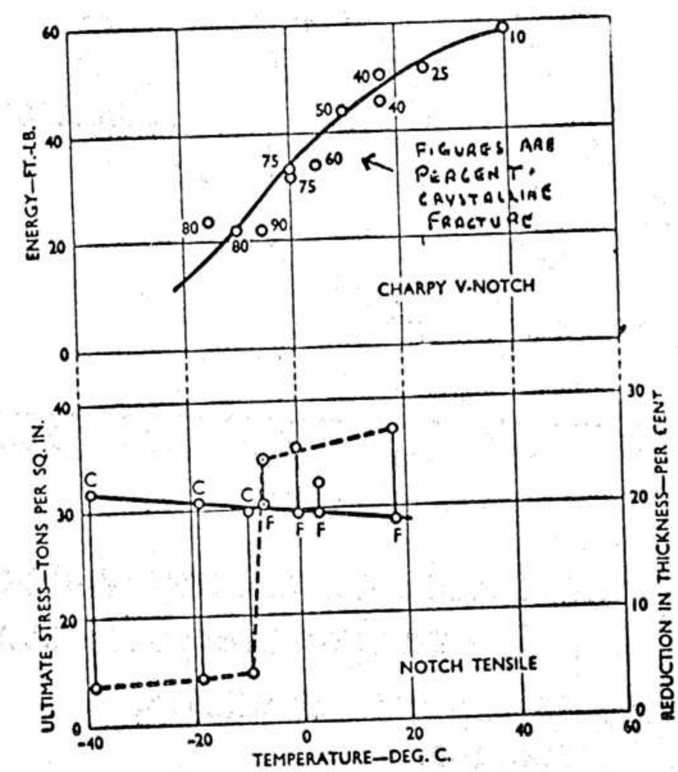

Charpy and notch tensile.
Plate 46A2B, 0·37 inch thick.

FIG. 3

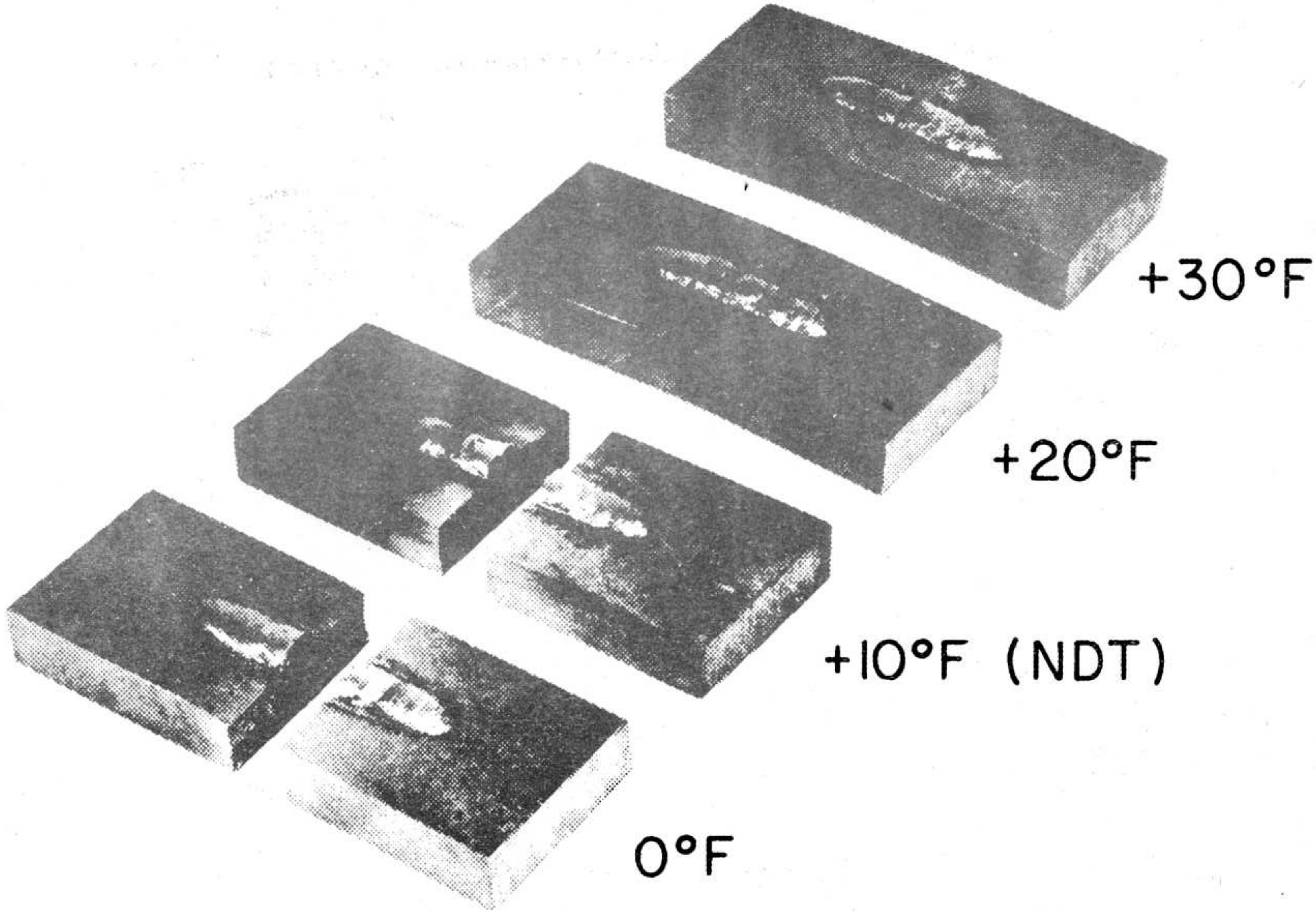

Fig. 4 — Typical drop-weight test series, illustrating an NDT at 10°F

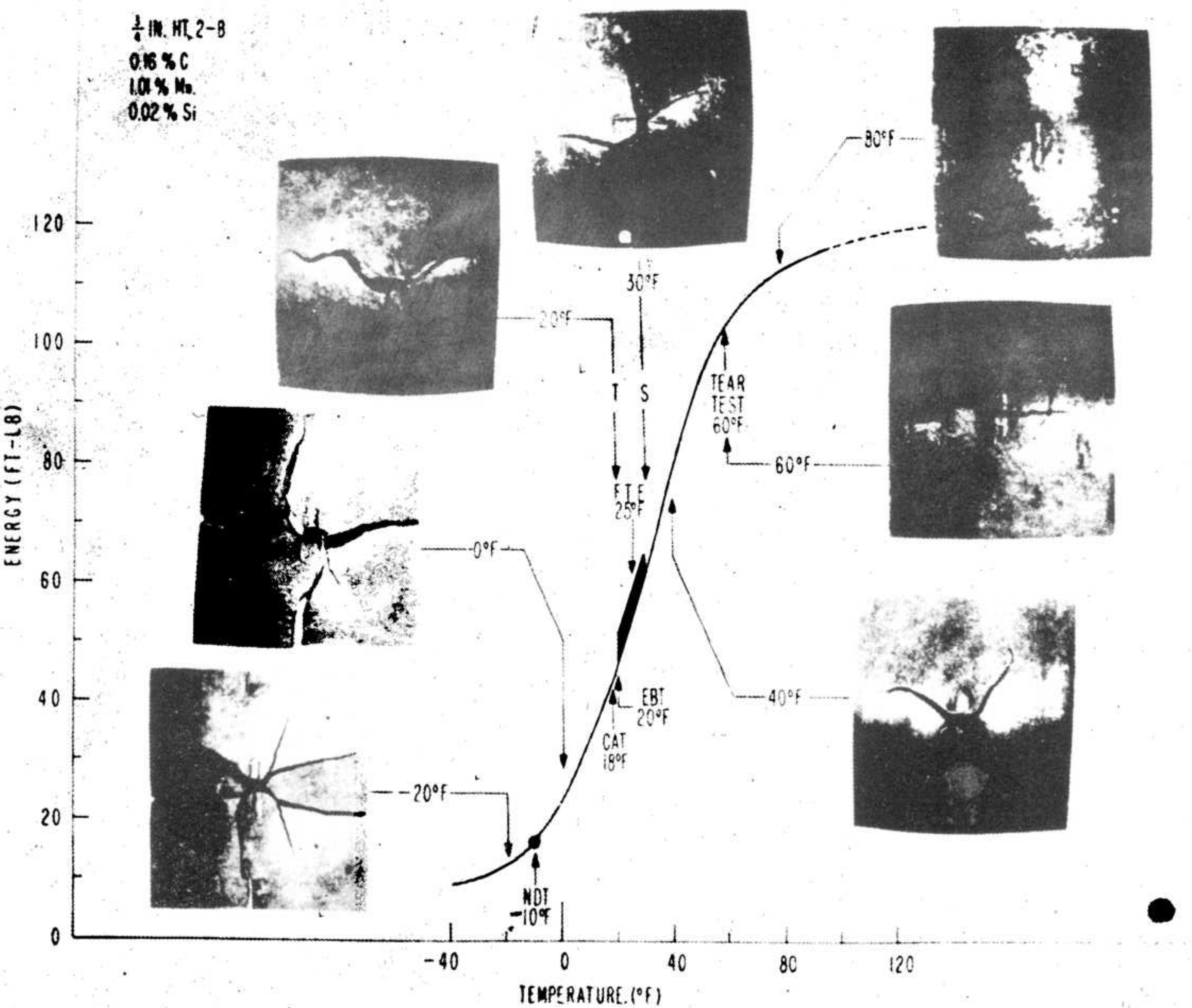

Fig. 5 : VARIOUS TRANSITION TEMPERATURES OBTAINED ON A GIVEN PLATE OF STEEL [81].

P A.8

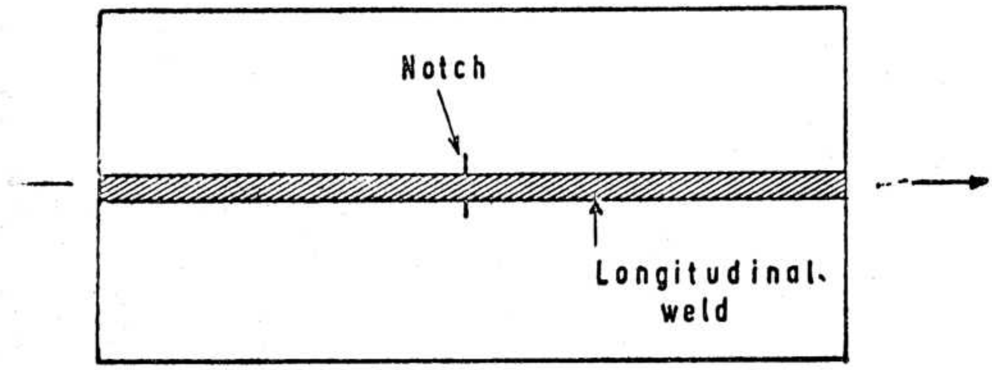

General testing arrangement.

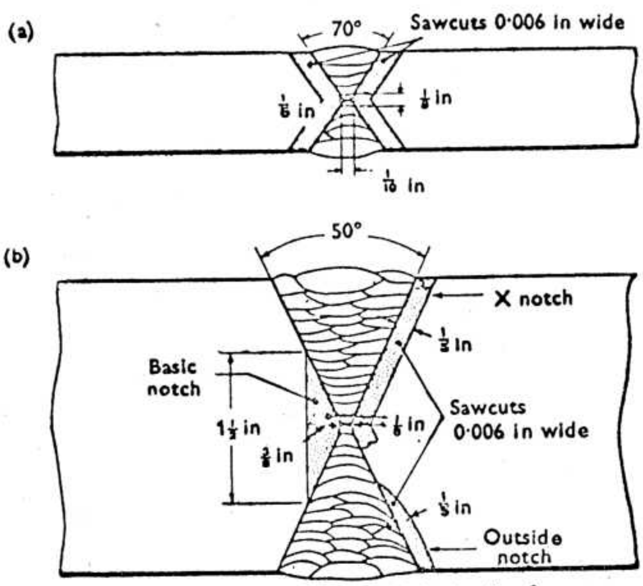

—(a) 2 in thick specimen. Weld details: 2 runs No. 8 s.w.g. electrode, 170 A. Subsequent runs No. 6 s.w.g. electrode, 220 A. (b) 3 in thick specimen. Weld details: 2 runs No. 8 s.w.g. electrode, 170 A. Subsequent runs No. 6 s.w.g. electrode 230 A.

FIG. 6

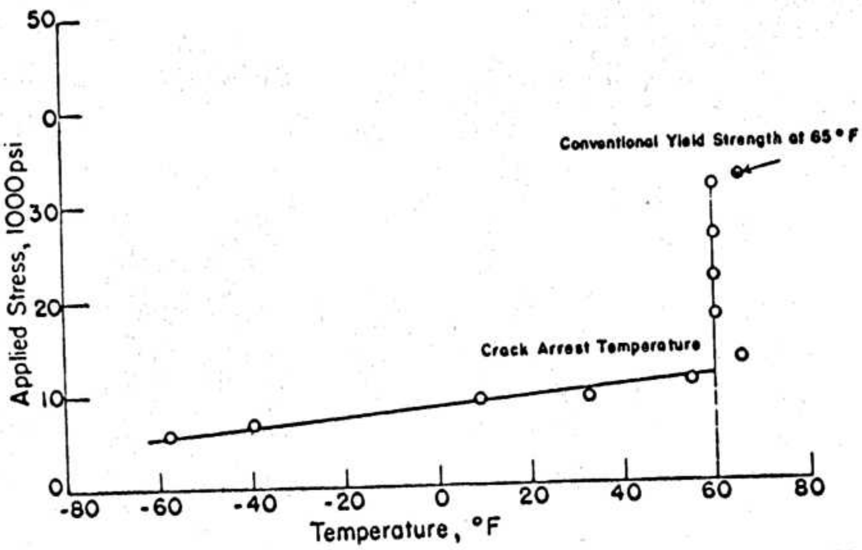

THE EFFECT OF TEMPERATURE ON THE STRESS REQUIRED FOR THE PROPAGATION OF A CRACK IN 1 INCH THICK MILD STEEL PLATE [73].

FIG. 7

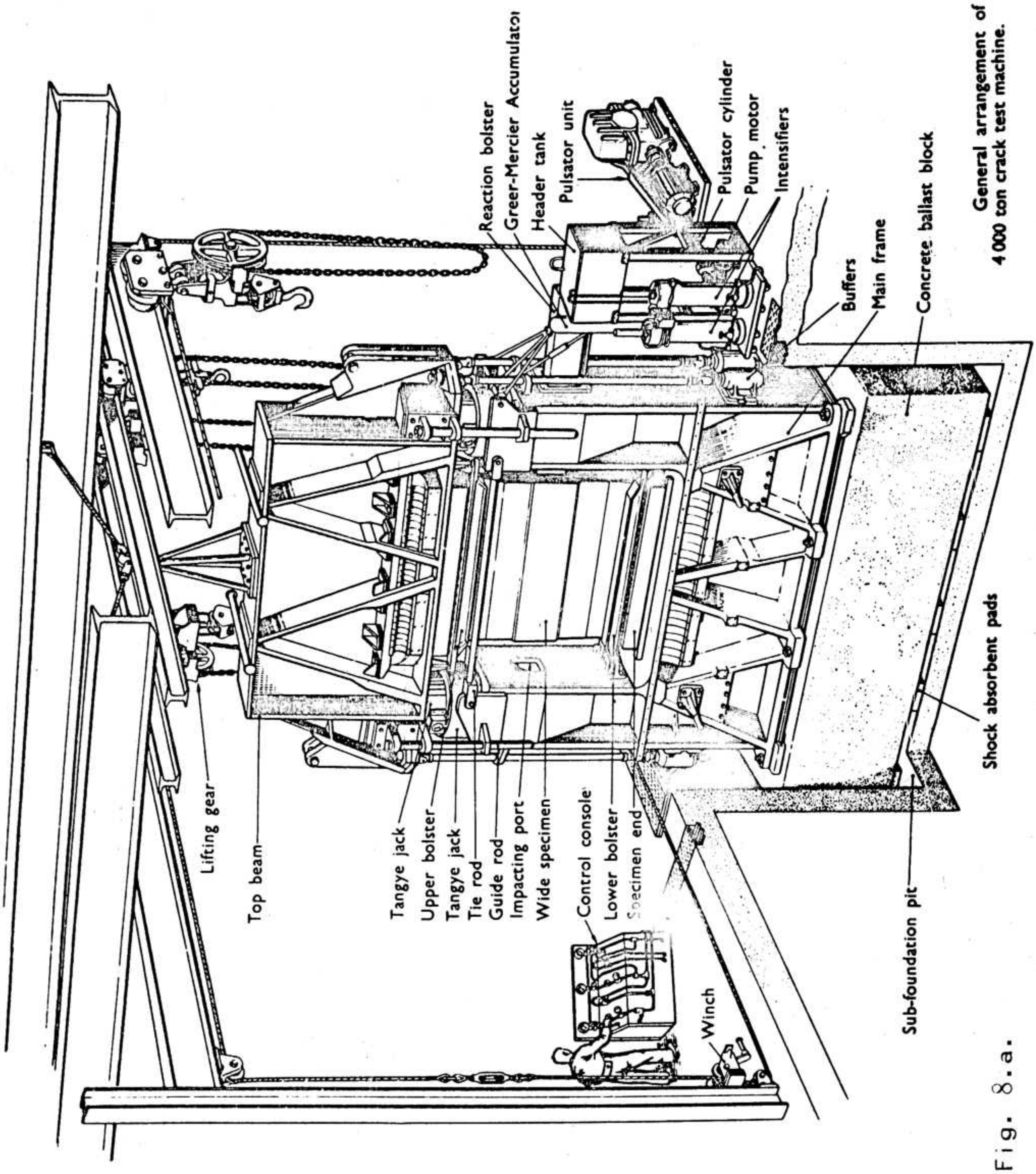

General arrangement of 4 000 ton crack test machine.

Fig. 8.a.

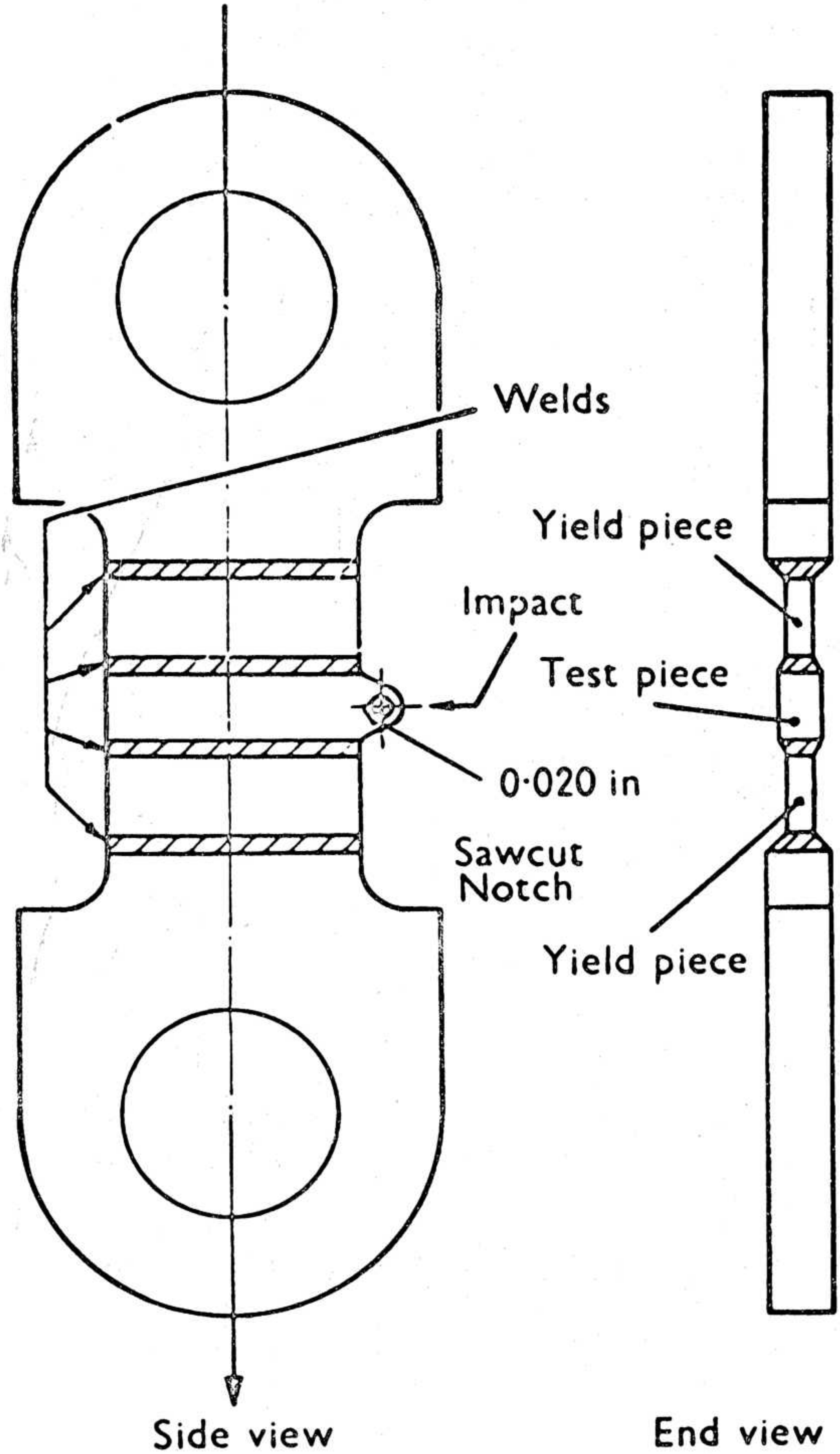
Welds
Yield piece
Impact
Test piece
0·020 in
Sawcut
Notch
Yield piece
Side view
End view

FIG. 8b

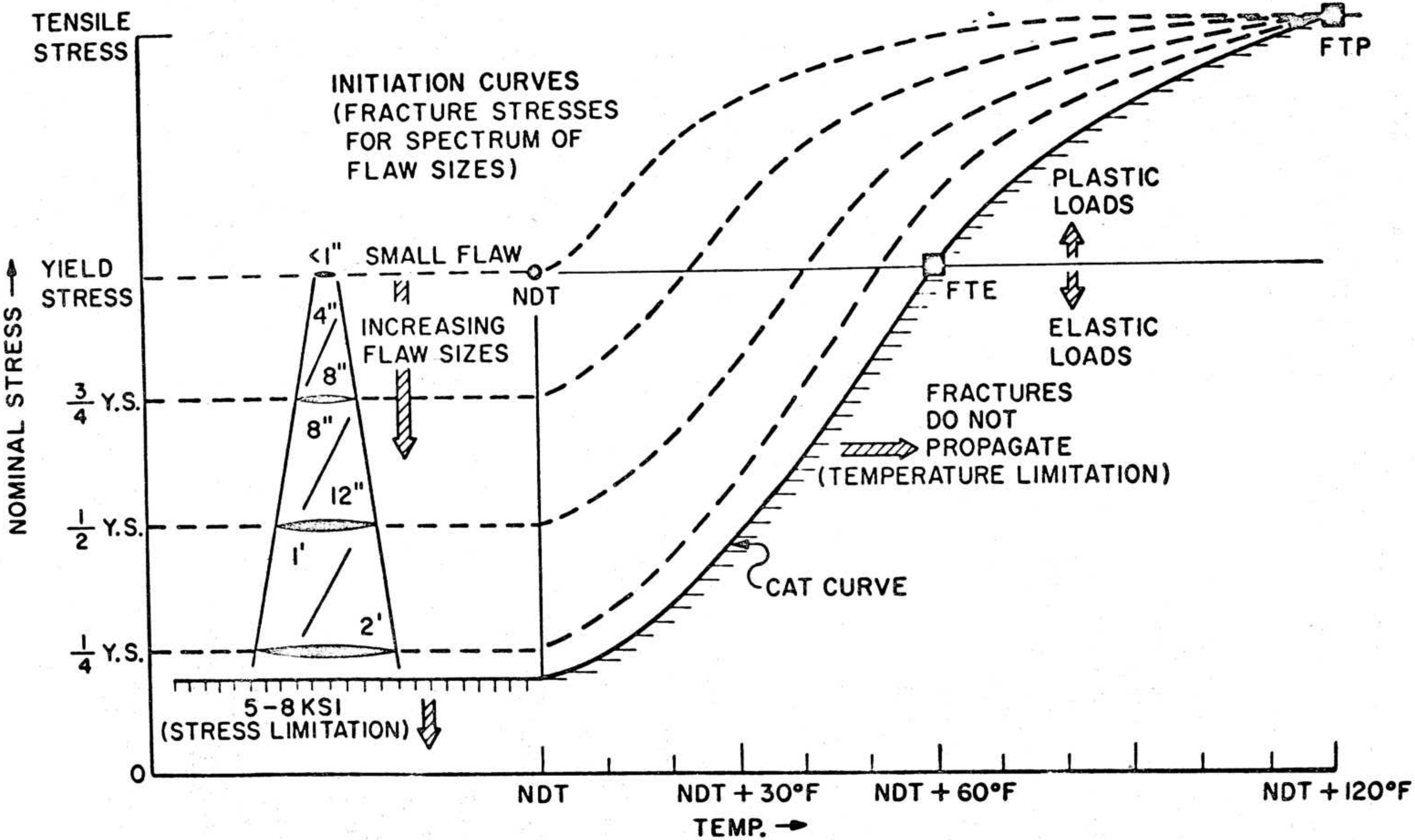

Generalized fracture analysis diagram, as referenced by the NDT temperature

FIG. 9

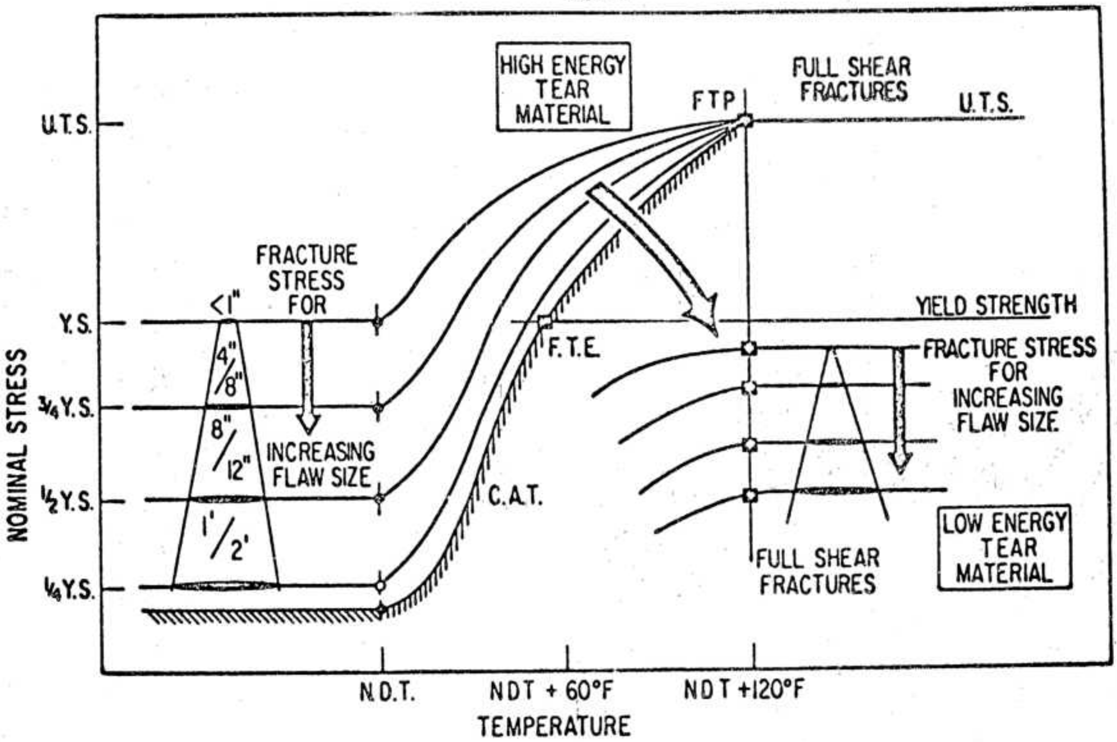

Fig. 10a - Features of fracture analysis diagram modifications for steels of "low energy tear" characteristics

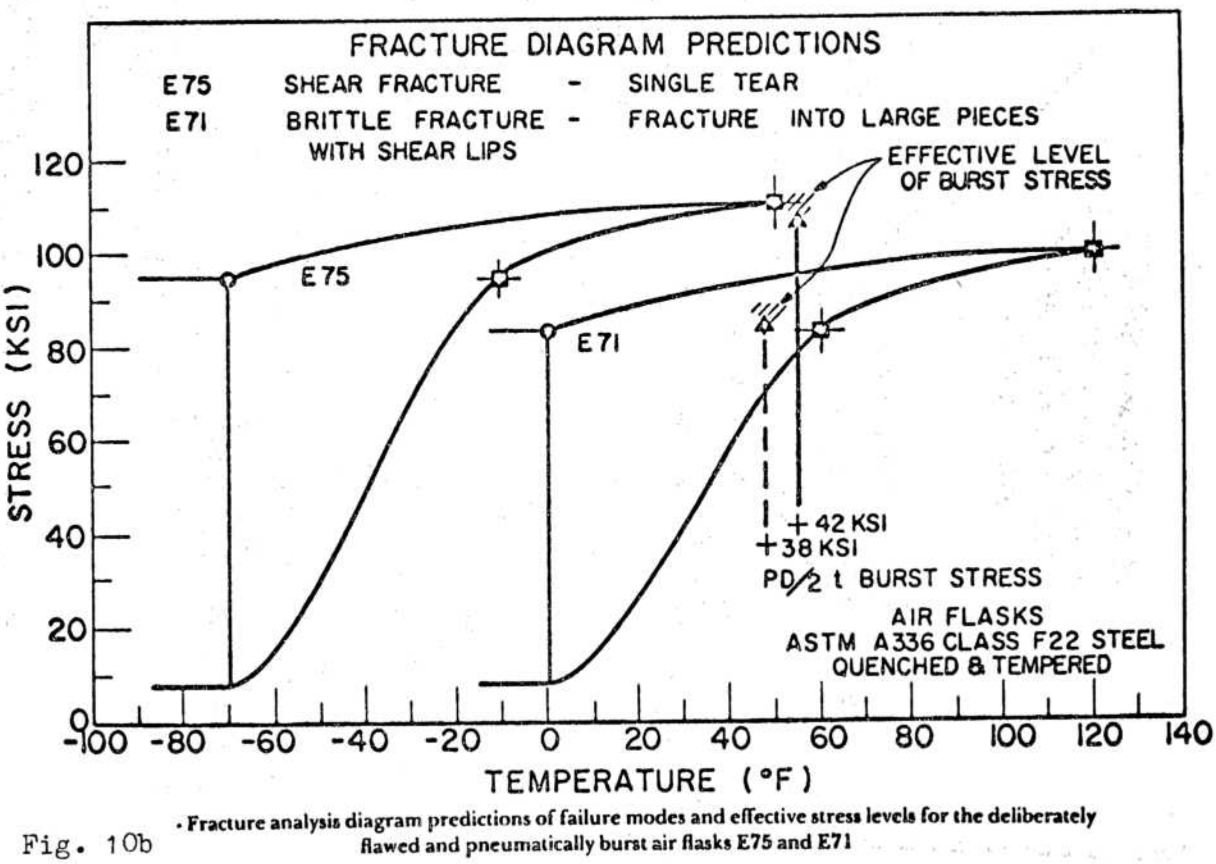

Fig. 10b - Fracture analysis diagram predictions of failure modes and effective stress levels for the deliberately flawed and pneumatically burst air flasks E75 and E71

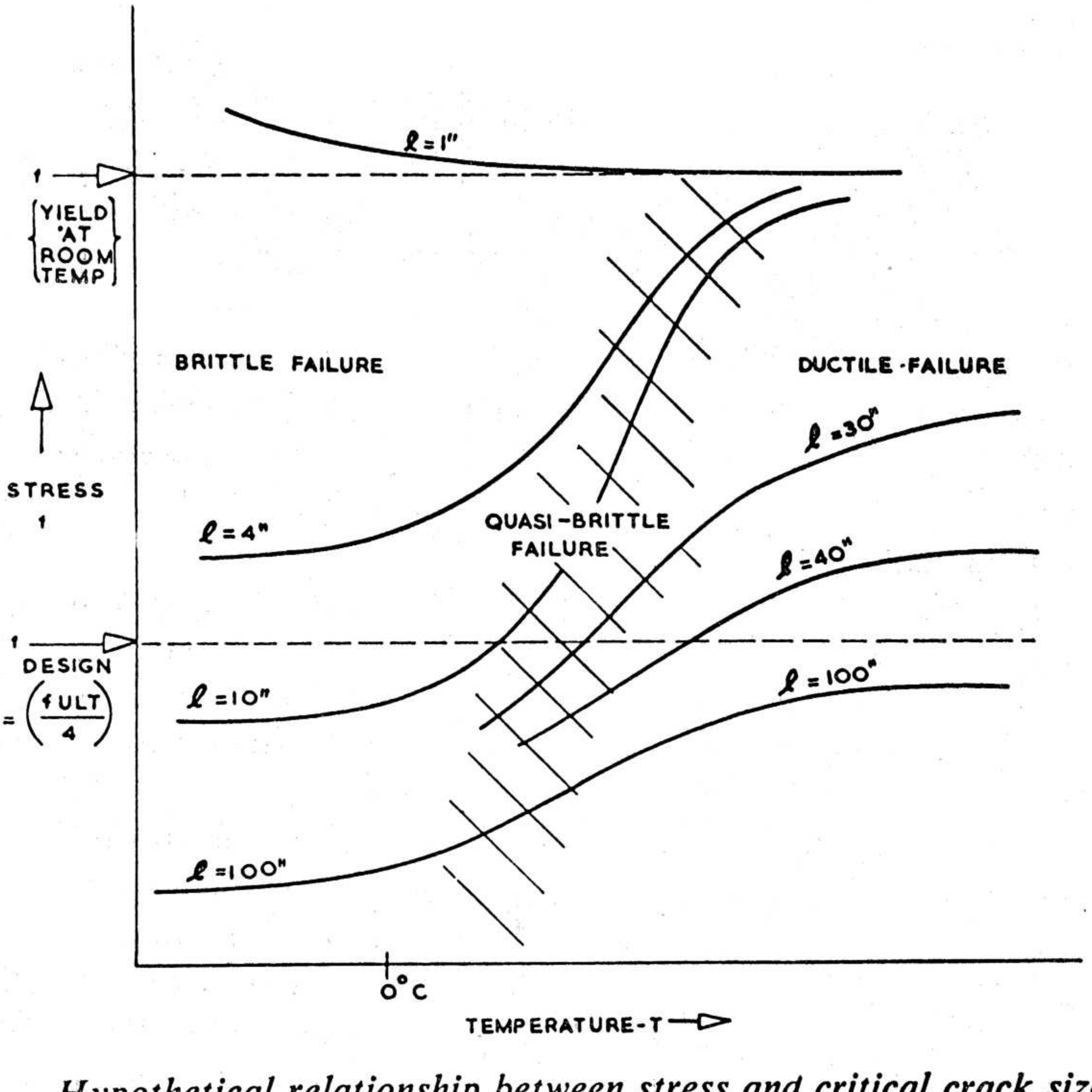

Hypothetical relationship between stress and critical crack size for mild steel plate

FIG. 11

LECTURE No. 3

EXPERIMENTAL PROGRAMME
TO STUDY FAST FRACTURE

Reasons for Experimental Programme

1. In Ref. 1 it was recognised that with the materials and relatively low nominal stress employed in reactor vessels, faults may need to be of considerable length for instability to occur, but in dealing with large vessels with complex design features, large areas of secondary stress, subject to thermal and pressure stress cycles, the ultimate appearance of such defects could not be ruled out.

In these circumstances it was evident that an almost complete lack of relevant experimental data in this field would need to be remedied and consequently, the Authority Health and Safety Branch of the United Kingdom Atomic Energy Authority, embarked on an investigation of the behaviour of artificially-faulted large pressure vessels[2].

Details of Experimental Arrangements

2. The vessels were 14 ft. long x 1 in. wall thickness cylinders, mainly of 5 ft. internal diameter, but also including vessels of 3 ft. and 9 ft. 6 in. internal diameter, closed by torispherical ends (Fig. 1.). The faults consisted of longitudinal slits of full wall thickness, ending in 0.008 in. wide, jewellers saw cuts and sealed internally with metal and neoprene patches.

The initial objective of the programme was to obtain a relationship between nominal hoop stress and fault length over a temperature range covering both the brittle and ductile ranges, as determined by the usual Charpy, Nil Ductility and Crack Arrest Temperature Tests. In order to realise this within the hydraulic test temperature range, a special steel was made in which by adjustment of composition and heat treatment, the transition and Crack Arrest Temperatures were elevated sufficiently, whilst still retaining the tensile properties of a typical boiler quality steel. Later the work was extended to include actual pressure vessel steels.

Results of Experiments

3. The test results are shown in Fig. 2, the main features of which are:-

(a) for the fault length range studies (6 in. - 24 in.) the nominal hoop stresses at failure rise evenly throughout the brittle and ductile ranges, remaining below general yield stress at temperatures well in excess of the Crack Arrest Temperature.

(b) As discussed later the failure stress is independent of the means of pressurisation.

In obtaining these curves certain observations were made regarding the extent and mode of failure under given loading conditions.

At low temperatures hydraulic pressurisation gave an unequivocal end point and catastrophic failure (Fig. 3.).

At higher temperatures hydraulic loading leads to limited damage due to a tear-volume increase-pressure drop mechanism and led initially to questions of the interpretation of such results. These doubts were, however, resolved by high temperature pneumatic loading which causes failure at the same pressure as for hydraulic loading for a given fault and temperature, but leads to catastrophic failure (Fig. 4).

These tests, comparing the consequences of the use of hydraulic or pneumatic loading in the ductile temperature range, are particularly instructive, in that they shed light on the results obtained in crack arrest tests and the invalidity of such tests when applied to vessels containing compressible fluids.

In the crack arrest test using a specimen stressed by, in effect, a large tensile machine and in the hydraulically loaded vessel, the energy available is largely confined to the strain energy of the metal itself. In both cases deformation associated with extension of the crack leads to unloading of the specimen and hence the crack stops for lack of driving energy.

In the pneumatically loaded case however, deformation accompanying crack extension produces virtually no unloading and indeed the stress level rises due to the reduction of load bearing area. Only by massive leakage will the crack driving force be removed and although this may limit the extent of damage in components of high surface/volume ratio such as pipelines where the depressurisation wave may out-pace the crack propagation, catastrophic failure becomes increasingly likely as one goes to large pressure vessels.

Different Fracture Modes

4. As regards modes of failure, three distinct types were observed, depending on relative influence of the principal stresses acting at the fault tip. The designation of these stresses is made clear in Fig. 5.

The failure modes are:-

(A) Brittle - perpendicular to surface and to P_1 and governed by value of P_1; Fig. 6.

(B) 1st Shear - approximately 45° to surface proceeding in longitudinal direction governed by $P_1 - P_3$.

(C) 2nd Shear - proceeding in direction lying between P_1 and P_2 and governed by value of $P_1 - P_2$.

Modes (A) and (B) are not influenced by the bulging produced by internal pressure load acting along the unsupported edge of the through crack, but in Mode (C), this load causes sufficient bending at the crack tip to produce a longitudinal compressive stress at the outer surface which overcomes the normal longitudinal tensile stress P_2 due to the internal pressure. Hence $P_1 - P_2$ exceeds $P_1 - P_3$ ($P_3 = 0$ at surface) and thus $P_1 - P_2$ controls failure and produces the failure mode observed. A $P_1 - P_2$ type failure is shown in Fig. 7.

Fracture appearance in vessels may, however, prove misleading, if one thinks only in terms of a clearly defined brittle-ductile transition temperature as derived by a specific type of mechanical test.

Fig. 8 shows an example of brittle and ductile fractures appearing side by side at a single temperature in a partial pneumatic test carried out on a faulted steel vessel.

Plastic Zone Phenomena

5. The explanation of this behaviour is believed to lie in the existence of a plastically strained zone which develops and extends from the tip of the fault as the stress level increases. Various methods have been employed to measure this zone, including brittle lacquer and photo-elastic coatings. Fig. 9 shows an example of the latter.

The size of the plastic zone has been found to correlate quite well with Dugdale's equation (3):-

$$\frac{S}{S + L} = 2 \operatorname{Sin} \frac{\pi}{4} \frac{f_g}{f_y}$$

Where S = plastic zone diameter; L = Crack half length

f_g = nominal applied stress; f_y = yield stress

Returning to Fig. 8. The size of the plastic zone prior to and following rapid propagation of the defect may be seen from the thickness contours shown in Fig. 10. It will be seen that the transformation from shear to fast fracture coincides with the virtual disappearance of the plastic zone at the tip of the running crack. This may be explained in terms of the Dugdale equation by the dynamic elevation of the yield stress due to the high rates of strain at failure.

An examination of Dugdale's equation will suggest that at higher temperatures due to the reduction in f_y; the plastic zone size should increase. In addition, there is evidence that failure arising from a defect must be preceded by additional yielding. These two observations suggest that once a fault has been stressed and a plastic zone created at its tip then the fault should remain stable up to this stress level at lower temperatures. This "hot pre-stress" effecthas in fact been observed in our work, but was absent in cases where failure was by the $P_1 - P_2$ mode.

Correlation of Results with Material Mechanical Properties

6. The first attempt in this direction was to check the applicability of the Griffith-type equation, (stress^2 x crack half length - constant for constant material properties), to the results. The fact that they did not fit comes as no surprise when one realises that Griffith's original treatment was for completely brittle materials and here we are dealing with a ductile material, which upon

stressing, is capable of exhibiting large and demonstrably complex plastic zones at the tips of defects.

It was found however, that for constant properties, the expression $f_g^3 l^2$ = constant, where f_g = applied stress and l = crack half length, gave a better fit and a plot of $f_g^3 l^2$ against the energy absorbtion in the Charpy V notch energy absorbtion, other properties remaining constant, was linear for failure of the brittle and 1st Shear modes. Fig. 11. From Fig. 12 which includes a wider range of results, down to pipes of 1 ft. diameter, it will be seen that vessel geometry playes an important role in defining the failure condition. Changes in those factors which increase the tendency to the bulging type of failure (2nd Shear mode), namely, increased crack length, reduced wall thickness and diameter, cause this mode to intervene at progressively lower levels of Charpy energy and it will be seen as the parameter $\frac{l}{tD}$ increases, the failure curves lie increasingly closer and parallel to the abscissa. Thus, the change in failure pattern as one goes from large diameter, thick walled vessels to small size, thin wall pipes, will be generally from flat fractures, originating at defects showing little if any gaping, to 2nd mode shear failures preceded by wide gaping of the defect. It will be recognised that this gaping type of failure is somewhat artificial, in that internal sealing is necessary to enable such a failure to be produced. For the practical case of tubes in the absence of gross over-pressure, fast fracture without prior leakage is conceivable only in the event of a high degree of embrittlement, in which case the critical crack size may be very small, or in the presence of a long partial penetration defect which grows radially through the wall thickness.

An early analysis of the test results[4], led to the postulation of failure equations of the general form:-

$$f_g^3 l^2 = f_y^d f_u^e (C + D\phi)$$

where f_g = nominal applied stress; l = crack half length

f_y = yield stress; f_u = ultimate tensile stress ; ϕ = Charpy impact energy;

d, e, C + D are constants.

However, examination of a large number of experimental results and further analysis of the forces acting at the crack tip [5], now suggest that the above equation is a good approximation to a more general equation of the form:-

$$f_u = f_g (Al + 1)$$

where f_u, f_g and l are as defined earlier; and A is a material parameter incorporating yield stress and Charpy energy.

This equation is based on an expression derived by Seaman[6], to describe crack instability in aluminium alloy sheet containing defects transverse to the applied load, which involves a stress concentration factor $K = Al + 1$ and a criterion for failure that $Kf_g = Bf_u$.

Whence $f_g(Al + 1) = Bf_u$; where A and B are constants and f_g vs $f_g l$ will give a linear plot.

In Fig. 13 plots of log l against log f_g/f_u are shown first using Seaman's values for A and B, i.e., ($A = 2.4$; $B = 1/0.82$) and then putting $B = 1$, i.e., U.T.S. as the failure criterion. The figure also shows lines corresponding to $f_g^3 l^2 = \text{Const.}$ and $f_g^2 l = \text{Const.}$

It may be seen that $f_g^3 l^2 = \text{Constant}$ is a close approximation to the curves for values of f_g/f_u between 0.17 and 0.7 using Seaman's values of A and B, and for values of f_g/f_u between 0.14 and 0.6 putting $B = 1$. One will also note that at high values of f_g/f_u, $f_g^2 l$ is a better fit.

REFERENCES

1. IRVINE, W. H. Fast Fracture in Reactor Pressure Vessels. (AHSB(S)R. 46) Revised from AHSB Memo 38, January, 1960.

2. BEVITT, E., STOTT, A. L. Fast Fracture of Pressure Vessels: Tests on 5' Diameter Cylindrical Vessels. TRG R.477(C) March, 1963.

3. DUGDALE, D. S. Yielding of Steel Sheets Containing Slits. Journal of Mech. and Phys. Solids, Vol. 8, No. 2, May, 1960.

4. IRVINE, W. H., QUIRK, A., BEVITT, E. Fast Fracture of Pressure Vessels. Journal, British Nuclear Energy Society, January, 1964.

5. QUIRK, A. A Maximum Stress Theory for the Failure of Pressure Components Containing Through Thickness Defects. AHSB(S)R.134, 1967.

6. SEAMAN, L. A Stress Criterion for Crack Growth. Proc. Soc. for Experimental Stress Analysis, Vol. 22, No. 2.

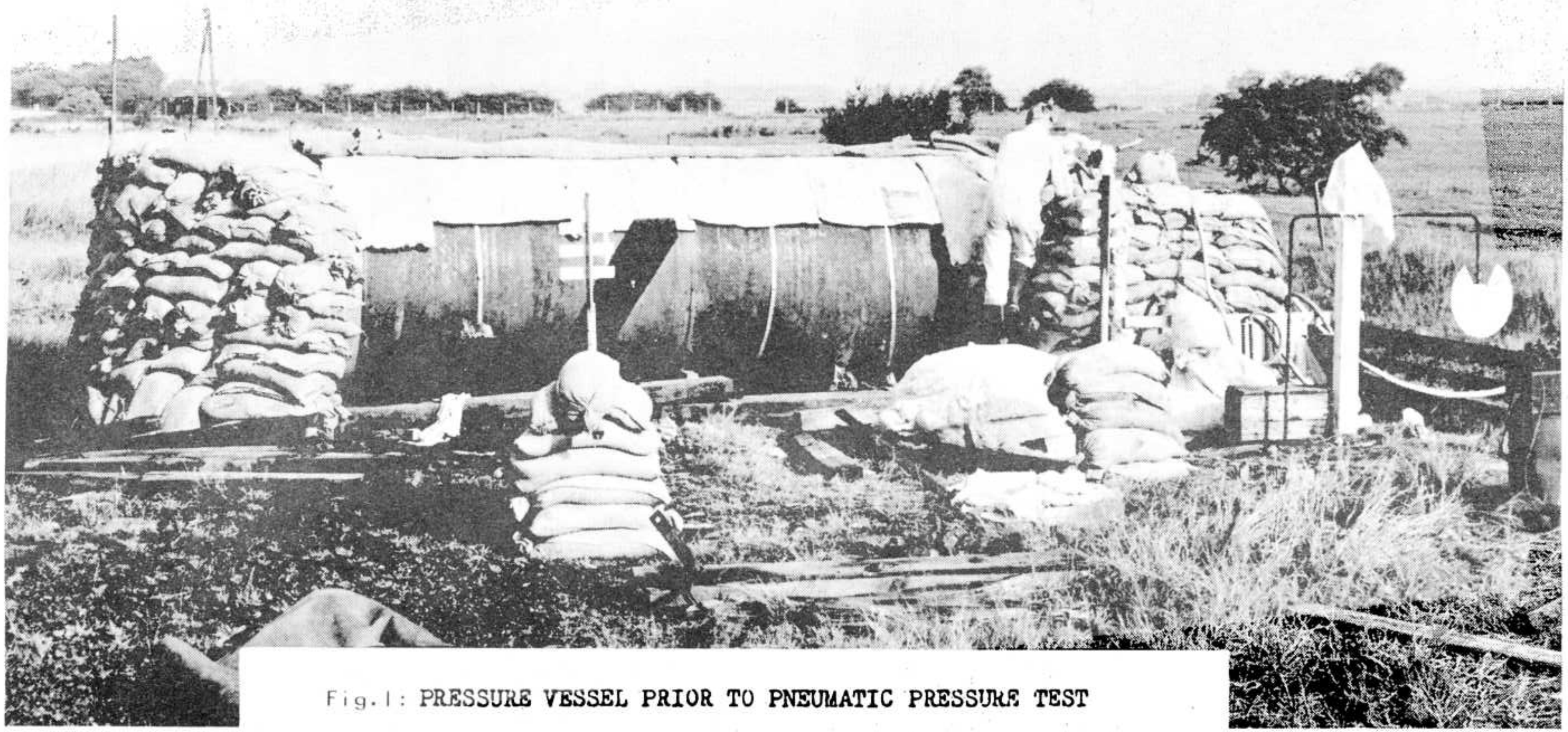

Fig.1: PRESSURE VESSEL PRIOR TO PNEUMATIC PRESSURE TEST

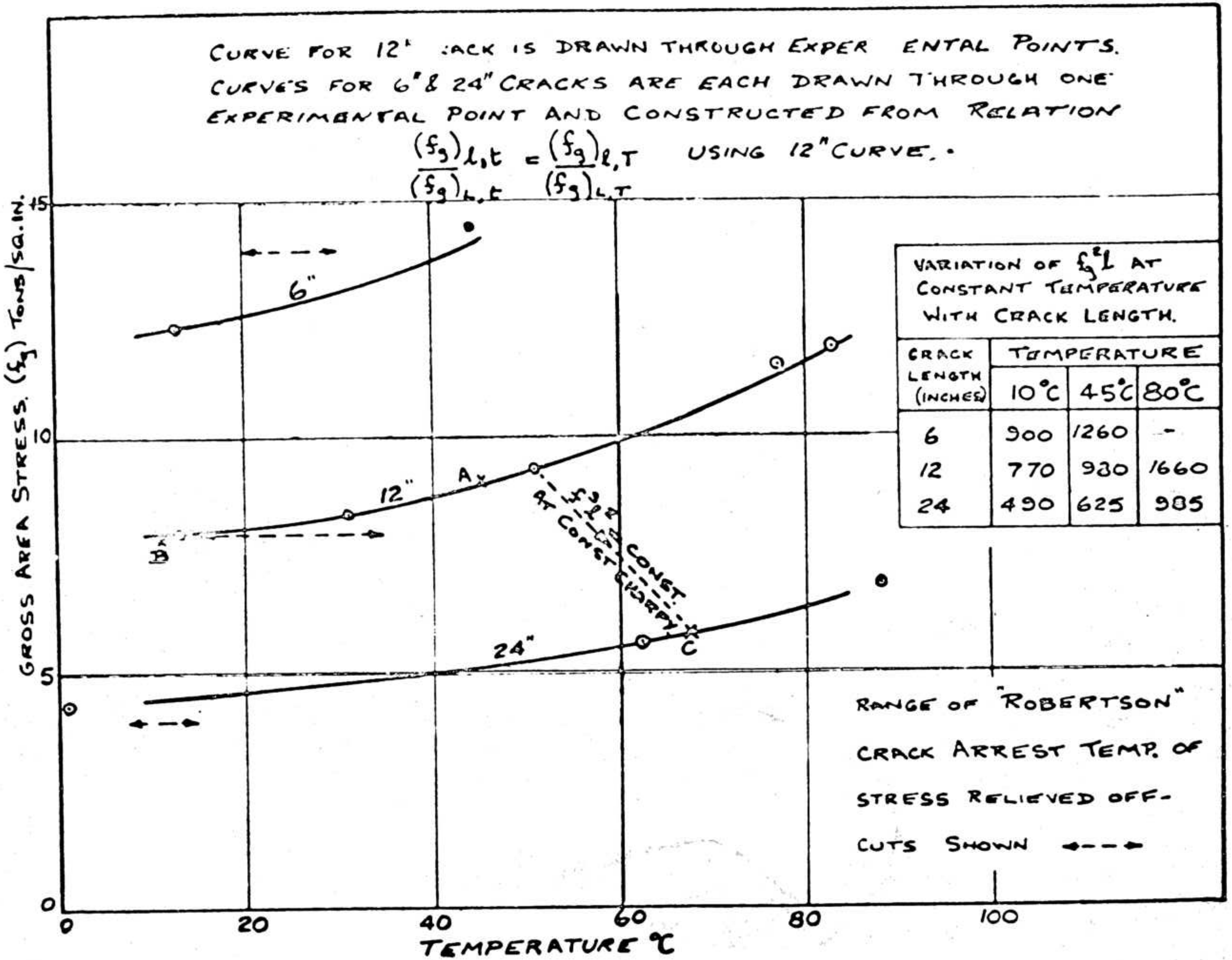

CRACK LENGTH (INCHES)	TEMPERATURE 10°C	45°C	80°C
6	900	1260	-
12	770	930	1660
24	490	625	985

Vessel failure stress v. *temperature for* 6 *in.*, 12 *in. and* 24 in. *cracks*

FIG. 2

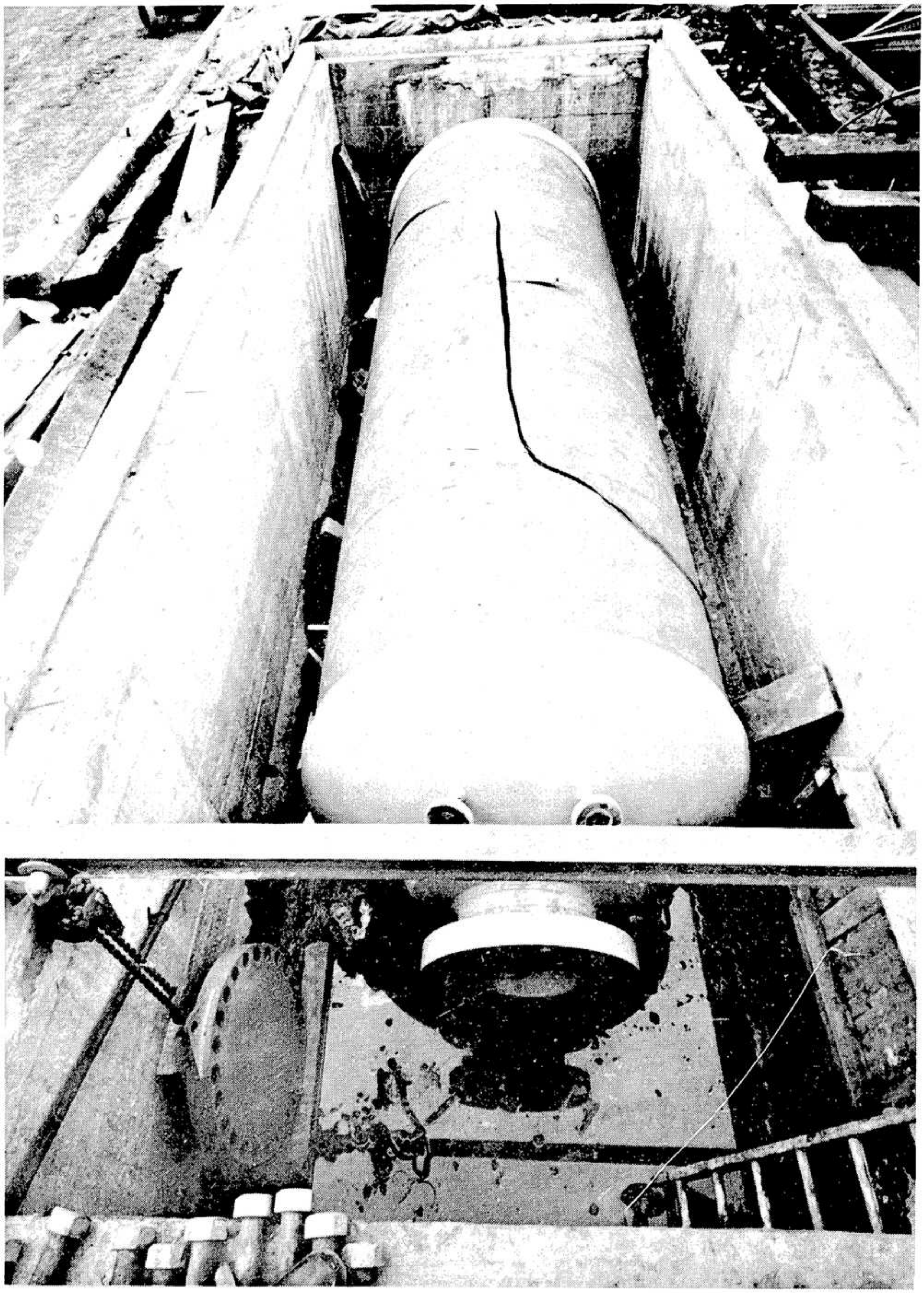

Fig. 3

Fig. 4 : DIFFERENCE IN CRACK PROPAGATION BETWEEN HYDRAULIC AND PNEUMATIC PRESSURISATION IN TWO SIMILAR VESSELS AT APPROXIMATELY SAME TEST CONDITIONS

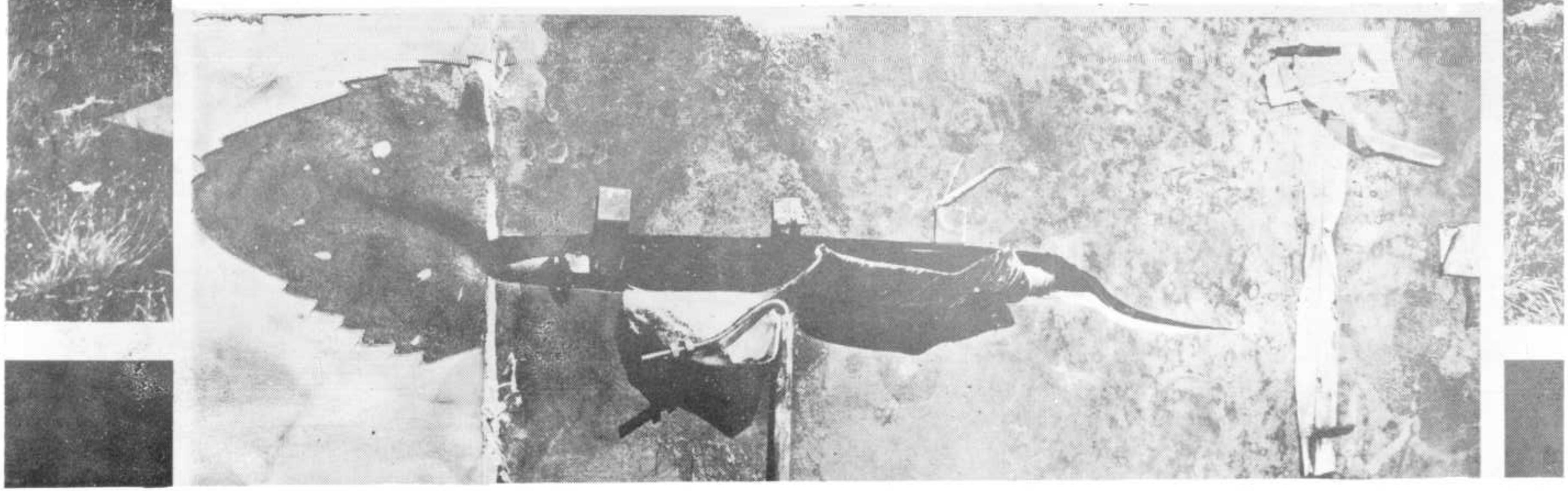

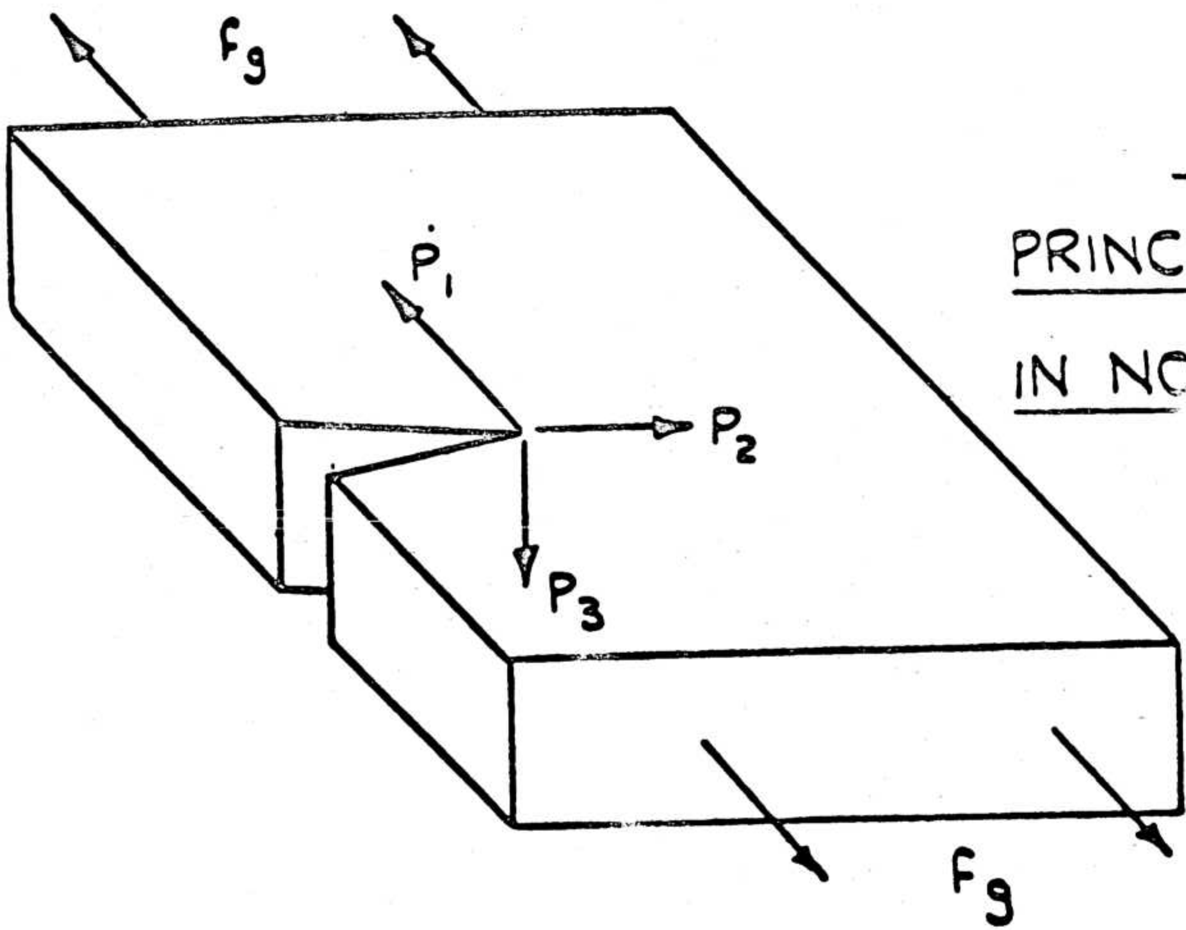

NOMENCLATURE OF
PRINCIPAL STRESS SYSTEM
IN NOTCHED PLATE.

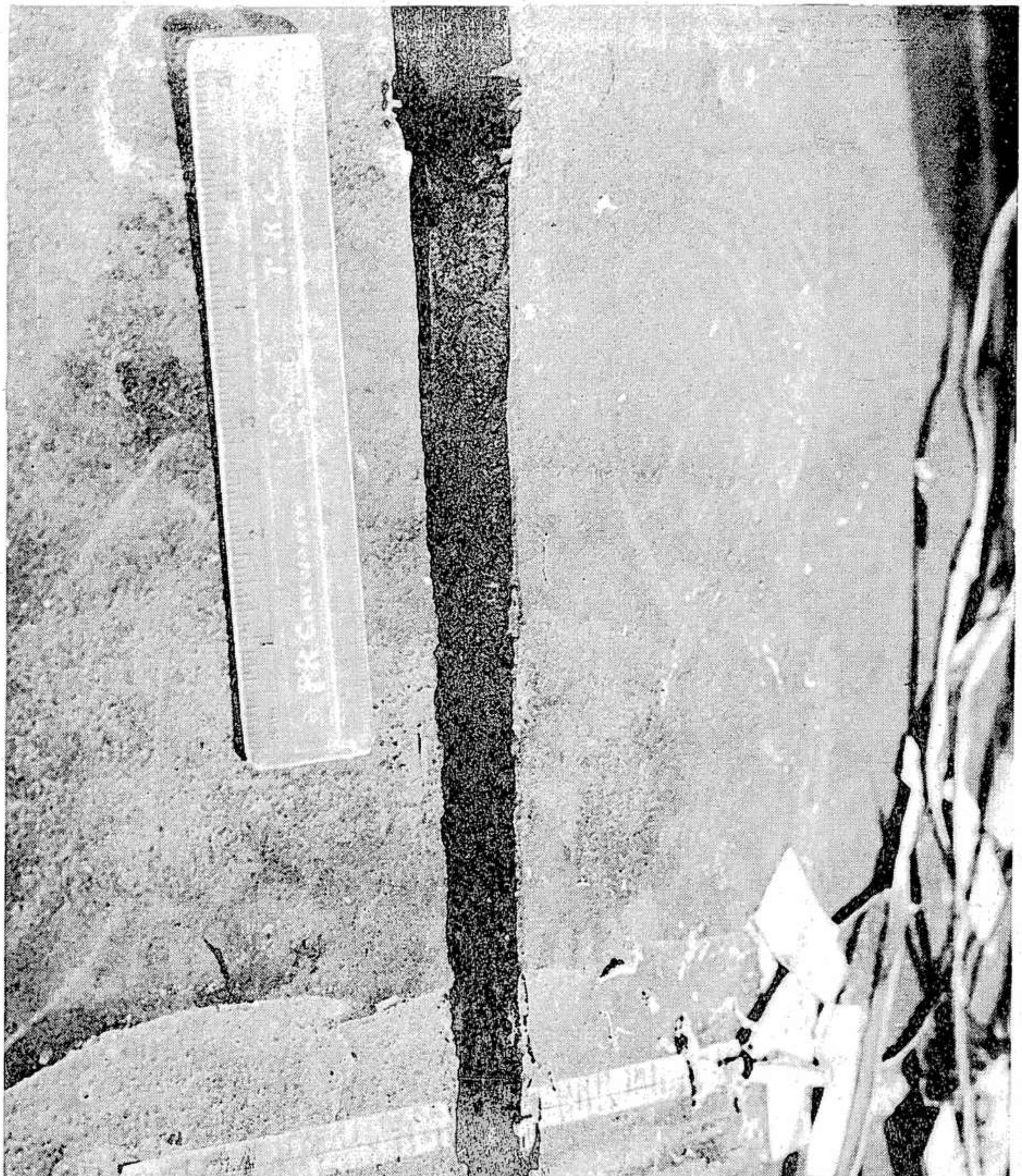

Fig. 6

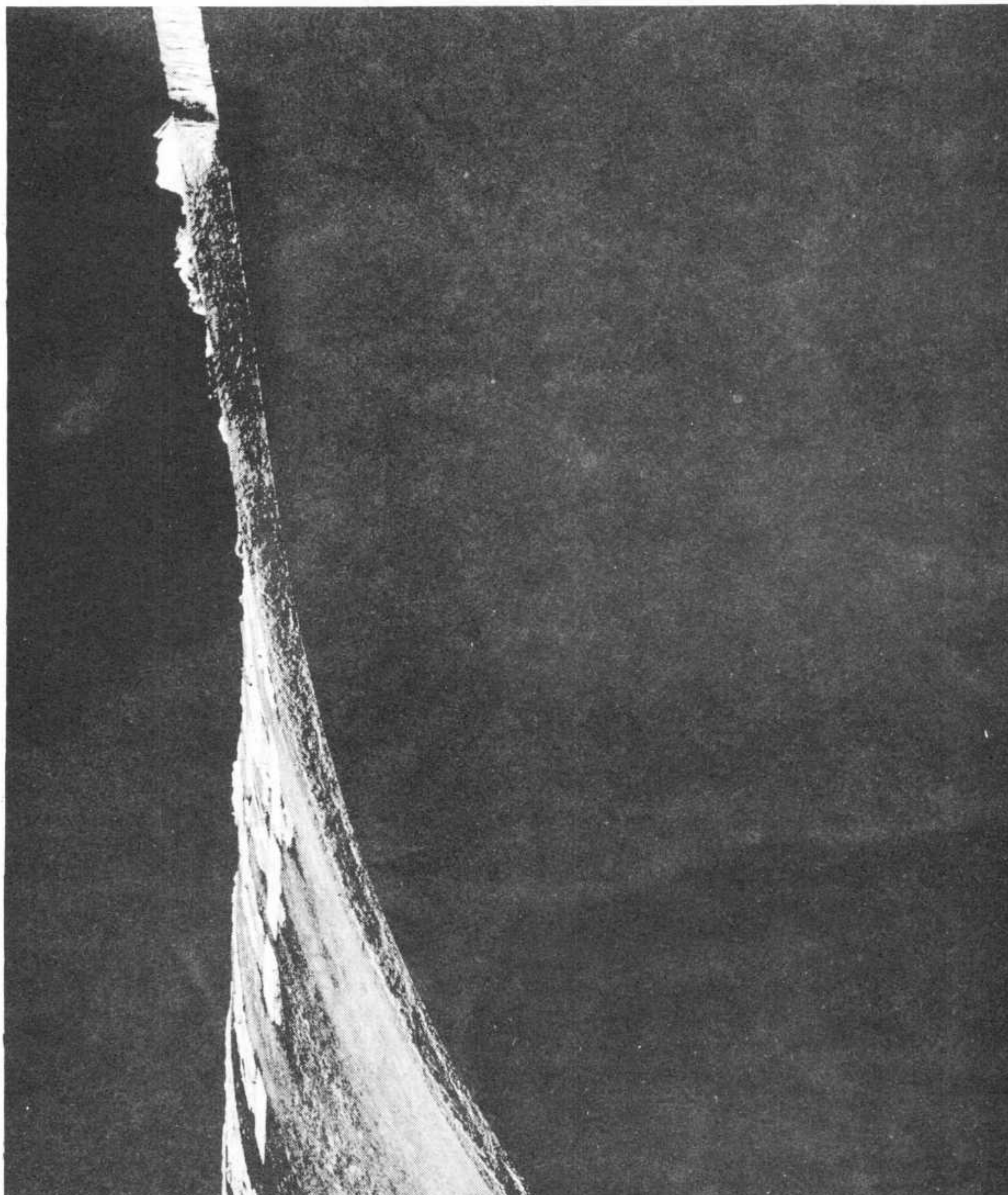

Fig. 7

Fig. 9

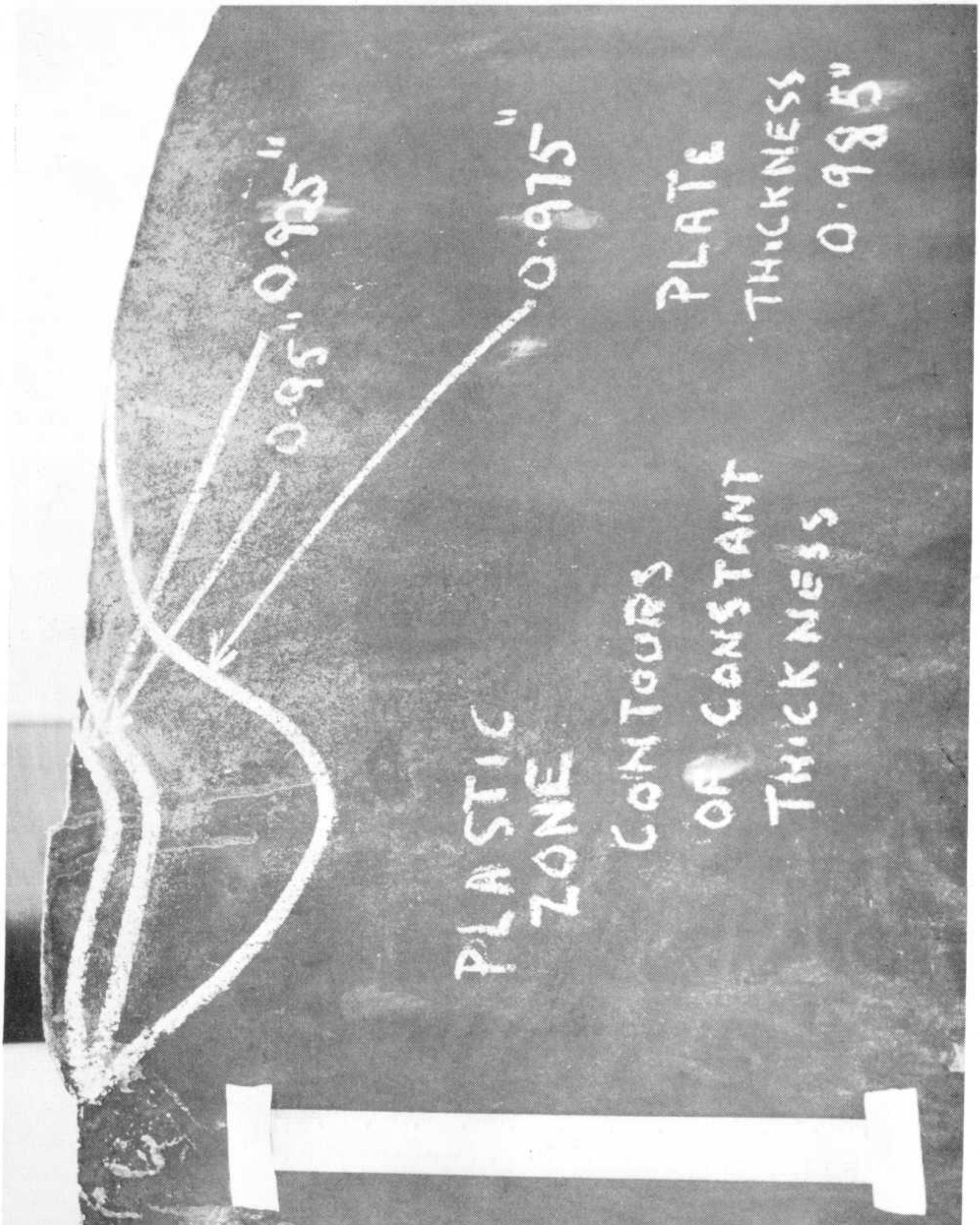
PLASTIC ZONE
CONTOURS OF CONSTANT THICKNESS
0.95"
0.975"
PLATE THICKNESS 0.985"

Fig. 10

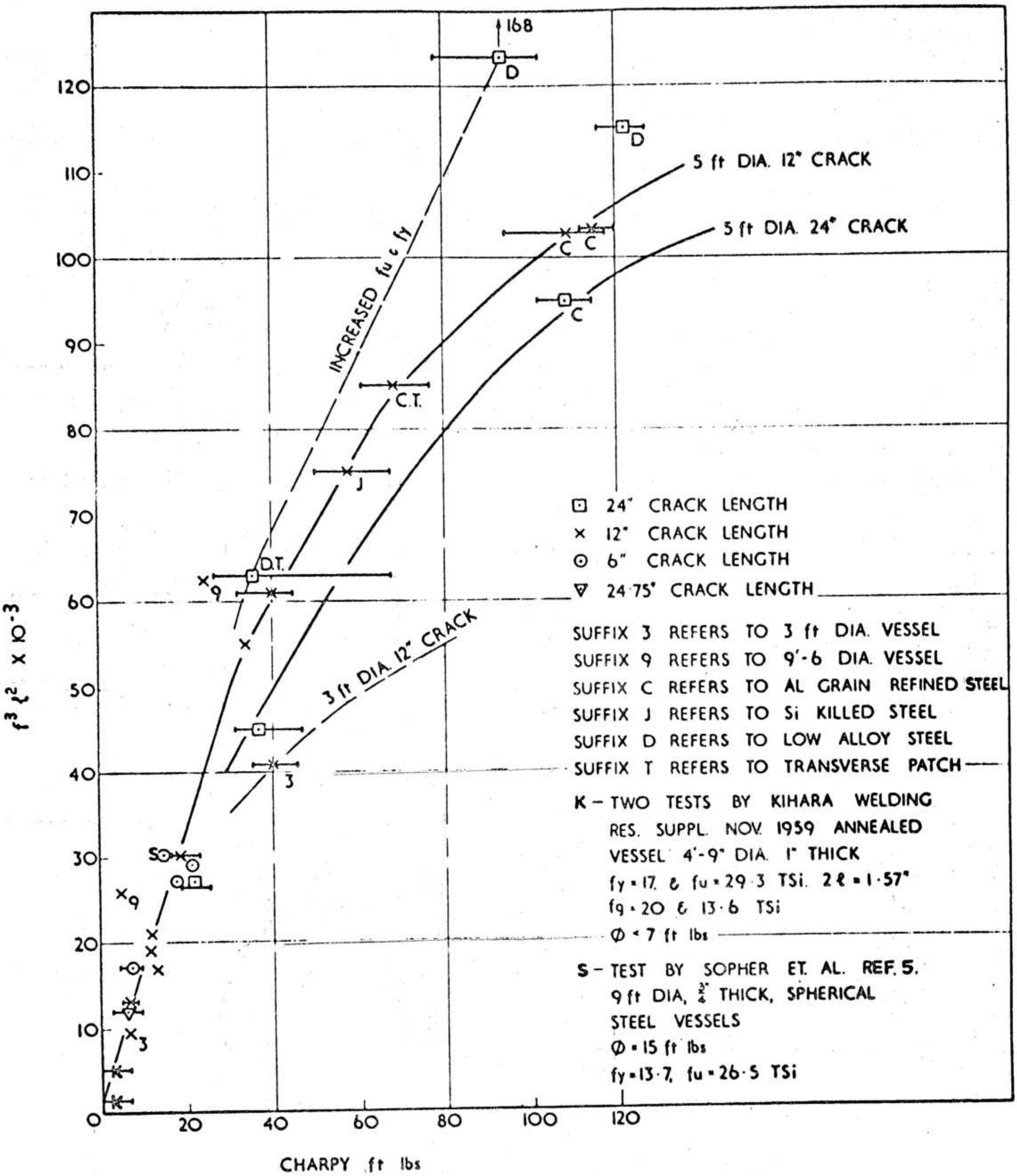

CHARPY v $f^3 \ell^2$ FOR TEST VESSELS.

FIG. 11

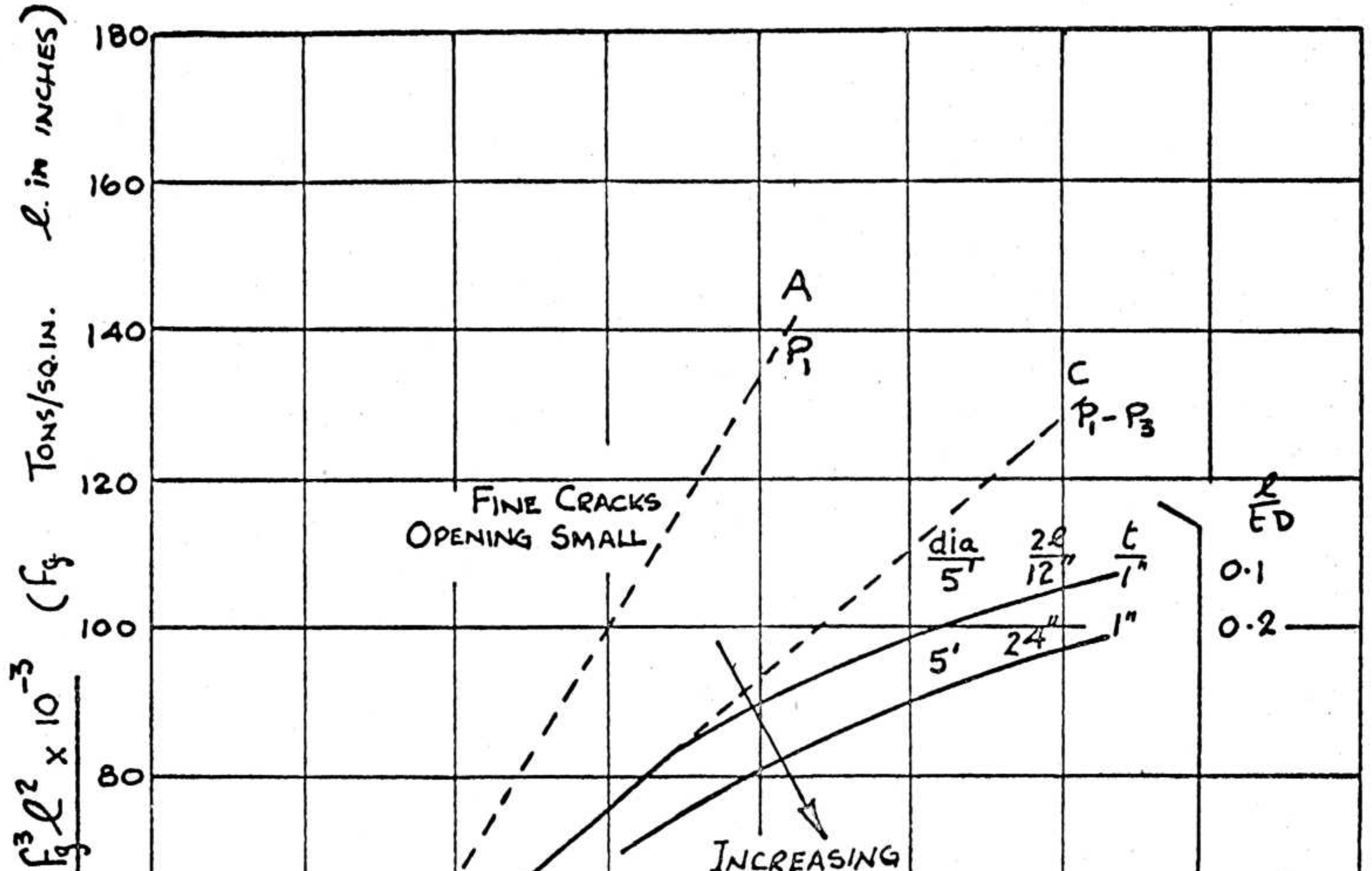

FAILURE DIAGRAM

FIG. 12

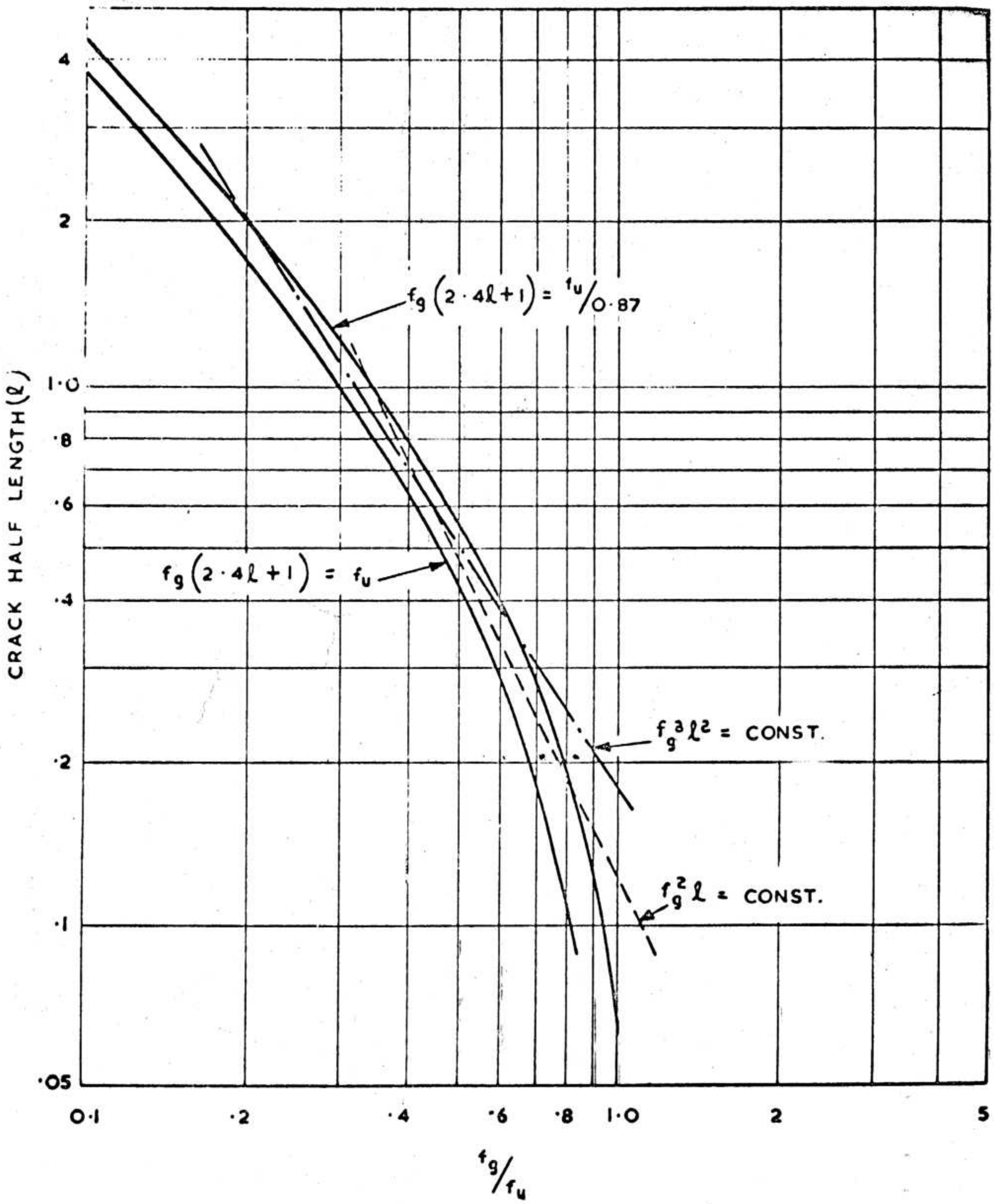

SEAMANS EQUATION $f_g(2 \cdot 4\ell + 1) = f_u/{\cdot}87$ PLOTTED AS LOG ℓ V LOG f_g/f_u

FOR COMPARISON WITH $f_g^3 \ell^2$ = CONST., AND ALSO $f_g(2 \cdot 4\ell + 1) = f_u$

FIG. 13

LECTURE 4

Experimental Programme to Study Crack Growth

Reason for Crack Growth Experiments

1. The main reason for the programme was to provide information on the growth rate of cracks at 50-100% of their critical size, since in 1964 there was no such experimental data available. It was also expected that since each test would terminate in a fast fracture, information would be obtained on the difference in behaviour, if any, of natural fatigue cracks and the artificial slits used in the fast fracture programme. Another aspect of interest was the eefect of one cycle of loading to a significantly higher pressure, on the subsequent growth behaviour of a crack.

Details of Experimental Arrangements

2. The materials tested were those used in the fast fracture tests, namely, 0.36%C and BS 1501-151 steels. Two sizes of vessel were used, 2 ft. diameter, 1 in. thick and 5 ft. diameter, 1 in. thick. The main difference in the experimental arrangement related to the need for cyclic pressurisation, continuous crack length measurement and safety. Cyclic pressurisation of the 5 ft. diameter vessels at temperatures near atmospheric was carried out using mains water as the pressurising medium. The cycling rate was about 3 cycles/hour. Testing was carried out in a concrete lined pit, the top of which was covered by a layer of wooden railway sleepers tied together by steel bars. Measurement of crack length was made directly by travelling microscope every 10 cycles with the vessel depressurised. For temperatures higher than 100°C, air was used as the pressurising medium and to keep pumping requirements to reasonable proportions while maintaining a similar cycling rate to that mentioned above, the 2 ft. vessels were fitted with internal packing in the form of a hollow steel cyclinder. See Fig. 1. Reduction of the pressurised volume also reduced the effects of final explosive failure. The requirement was for temperatures up to 400°C and therefore the equipment had to withstand the effects of fatigue and creep.

The 2 ft. diameter vessels were housed in underground test cells designed to contain the explosive failure under pneumatic pressurisation. Continuous crack measurement was achieved in the case of the 2 ft. diameter vessels by a system of remote viewing, using mirrors and an astronomical telescope. Occasional direct checks were made with the vessel depressurised. The method of preparing the initial defects and sealing them was similar to that employed in the fast fracture experiments. Test pressure cycle was from zero to maximum, with hold period, then back to zero. Cycling was controlled automatically.

Results of Experiments

3. The test programme is still proceeding; however, the measurements taken during the first six tests are given in Ref. 1 and the crack growth behaviour of these materials appears to be a reasonable fit to an equation of the type:-

$$N = C - D \exp(-Bl) \qquad \text{Eqn. (1)}$$

Where l is the half length of the crack

N is the number of cycles to increase crack length from l_o to l

D and B are constants and $C = D \exp(-Bl_o)$

The crack growth behaviour for these materials is shown diagramatically in Fig. 2. Other experimental work on higher strength materials, as yet unpublished, also fits this type of description.

Conclusions

4. The first, and possibly the most important conclusions is that the "end point" is the same in both the cyclic loading and in the "once off" loading fast fracture experiments - the same correlation being obtained between crack length, maximum stress level and material properties.

Secondly, it appears that the crack growth mechanism is not dependent on the fast fracture parameters. Thus, in one experiment the critical crack was varied by increasing the test temperature through the transition range for the material without any effect on the growth rate being observed. There is however, a sudden increase in crack growth rate over that predicted by Eqn. (1) over the last few cycles before fast fracture and it may be that this would be influenced by say, Charpy value. There is yet insufficient evidence to resolve this question.

Thirdly, three fracture modes have been observed which are analogous to those occurring in fast fracture, i.e., are flat or 90° mode and two shear modes, the crack growth rate being lowest in the former.

Fourthly, in one experiment on a 5 ft. diameter vessel at atmospheric temperature, the pressure for one cycle was raised 10% above the normal maximum pressure for the test. No further crack growth occurred until after about 15 cycles of normal cycling. The crack extension during the one overpressure cycle was much greater than during a normal cycle and it appears that the subsequent total length - total cycles curve is approximately the same whether an overpressure cycle is carried out or not. See Fig. 3.

Finally, the materials tested so far appear to show crack growth characteristics which are insensitive to moderate changes in material properties. Much more work is needed however, particularly on materials of low ductility, such as weld metals and heat affected zone material.

Reference 1.

IRVINE W. H., QUIRK, A., BEVITT, E. An Elasto-Plastic Approach to Fracture Mechanics. (AHSB(S)R.142)

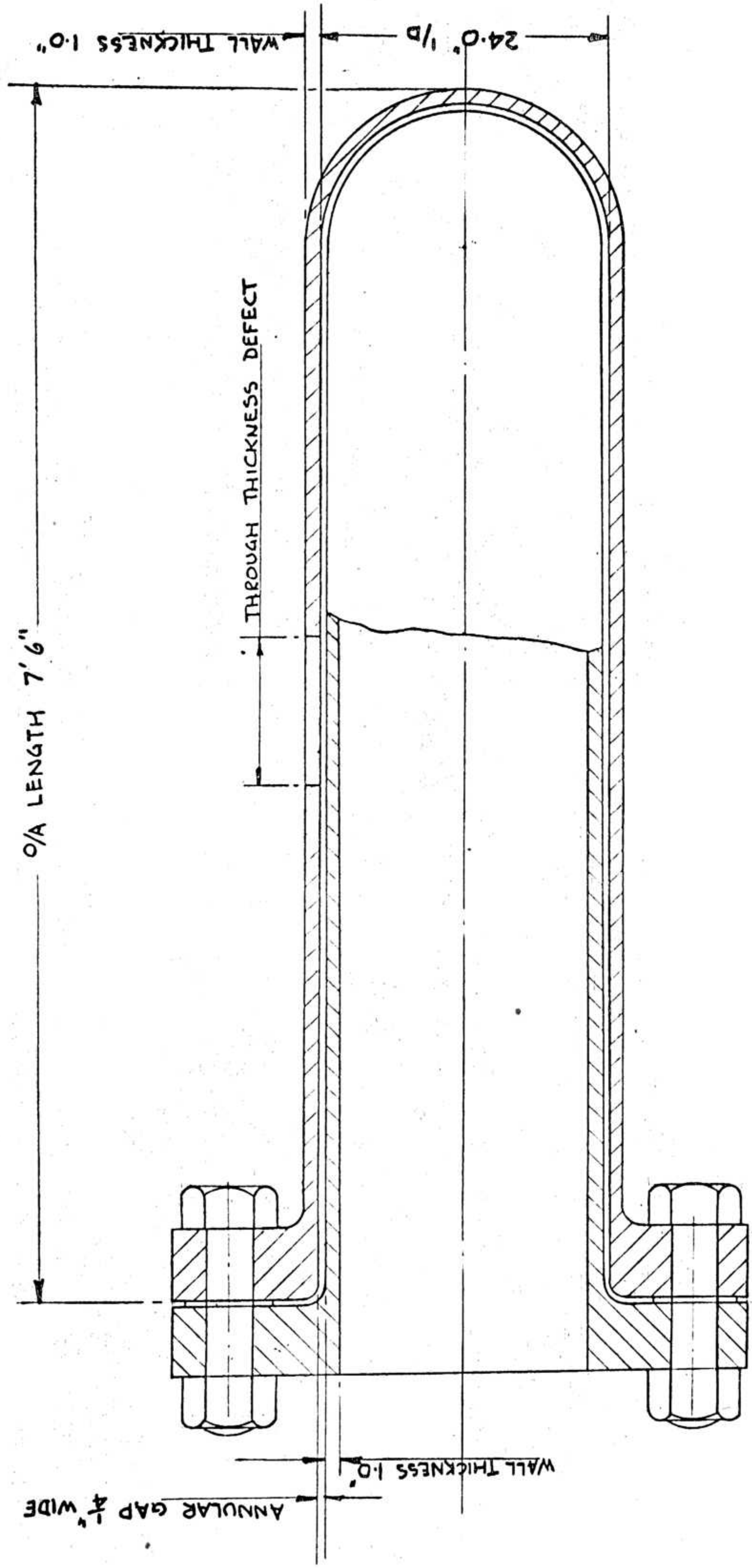

2Ft. DIA TEST VESSEL WITH PACKING

FIG. 1

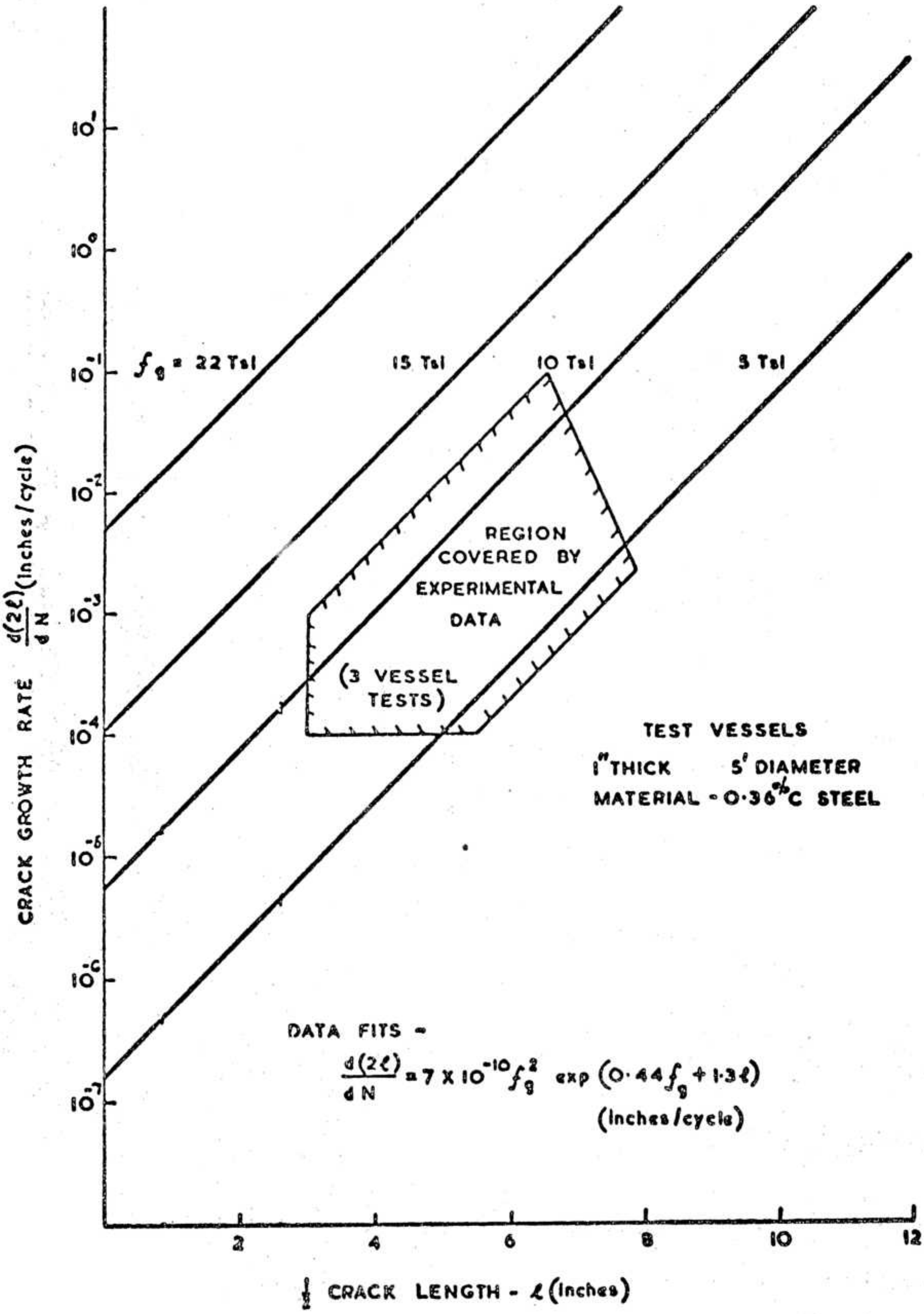
CRACK GROWTH RATE $\frac{d(2\ell)}{dN}$ (inches/cycle)
10^{1}
10^{0}
10^{-1}
10^{-2}
10^{-3}
10^{-4}
10^{-5}
10^{-6}
10^{-7}
f_g = 22 Tsi
15 Tsi
10 Tsi
5 Tsi
REGION COVERED BY EXPERIMENTAL DATA
(3 VESSEL TESTS)
TEST VESSELS
1" THICK 5' DIAMETER
MATERIAL - 0·36% C STEEL
DATA FITS -
$\frac{d(2\ell)}{dN} = 7 \times 10^{-10} f_g^2 \exp(0{\cdot}44 f_g + 1{\cdot}3\ell)$
(inches/cycle)
2
4
6
8
10
12
$\frac{1}{2}$ CRACK LENGTH - ℓ (inches)

FIG. 2.

NOTE:- FOR CLARITY THE EFFECT OF OVERPRESSURE IS NOT TO SCALE

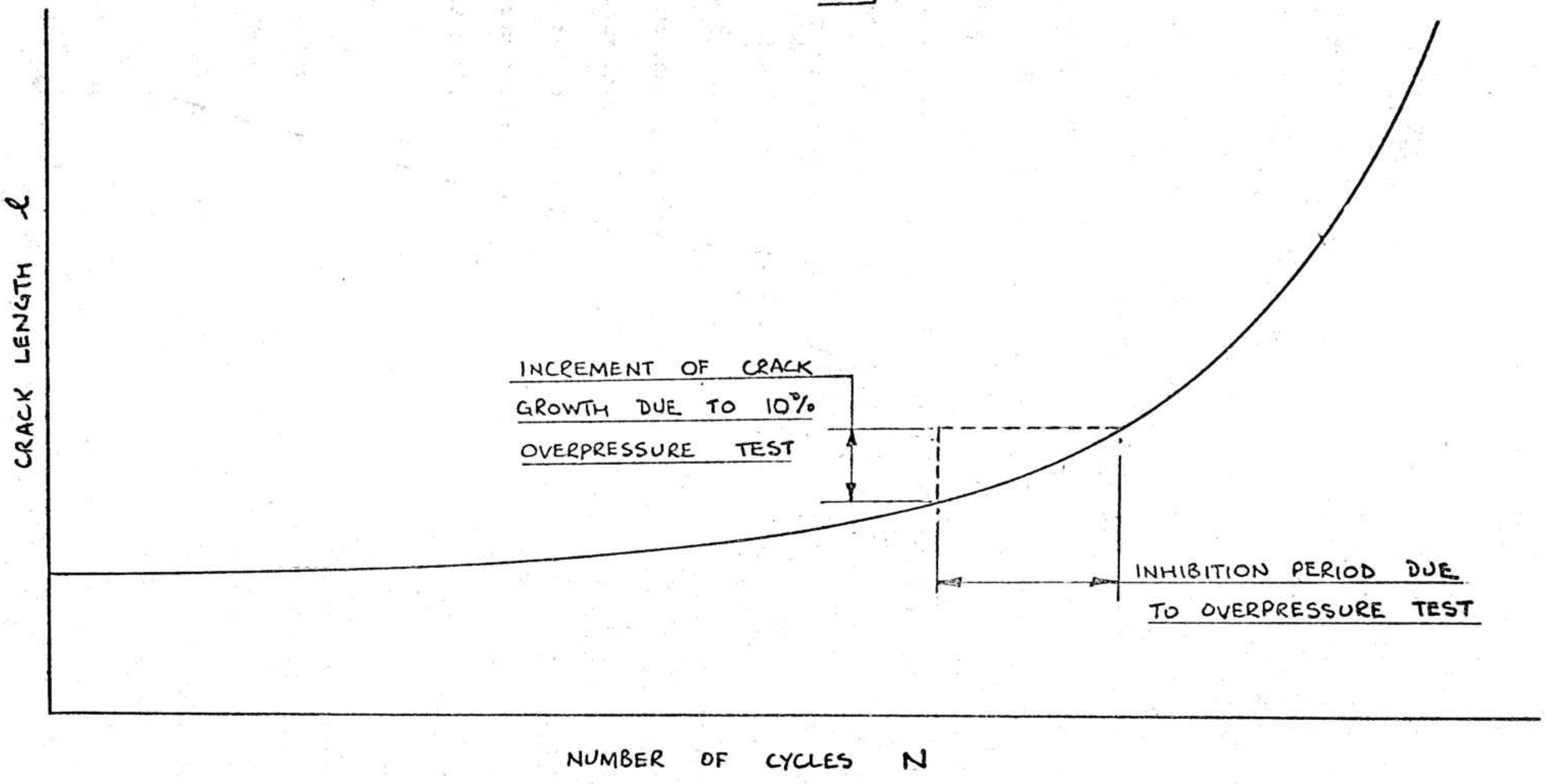

EFFECT OF ONE OVERPRESSURE CYCLE ON CRACK GROWTH CHARACTERISTIC

FIG. 3

LECTURE No. 5

ELASTO - PLASTIC THEORY

OF FRACTURE MECHANICS

Outline of Problem

1. In an ideally elastic material the theory of elasticity predicts that the stress at the tip of an infinitely sharp crack is infinite. Griffith avoided this difficulty by considering the relative rates of release of strain energy by the plate and absorbtion of fracture energy at the crack tip. In steels, yielding occurs at the tip of the crack as has been described in Lecture 3. The occurrence of this zone of plastic material, and the requirement that its volume must be constant, for a given size of zone,results in the yielded material contracting in the thickness direction. This contraction is resisted by the surrounding elastic material and a system of mutually opposing stresses is set up in the thickness direction, these being tensile in the plastic material and compressive in the elastic material. The plastic zone has been caused by the stresses in the plane of the plate which are tensile and hence this plastic zone material is subject to a triaxial stress system. The effect of this is, of course, to increase the flow stress of this material and this allows the stresses in the plane of the plate, in this zone, to rise appreciably above the uniaxial yield stress. As the external load condition is increased stress levels increase until the material in the immediate vicinity of the crack tip reaches the fracture stress and fast crack propagation ensues. The problem is thus to describe this situation in terms of nominal stress level, crack size and material properties.

Failure Conditions at the Crack Tip

2. If the conditions for equilibrium in the plane of the crack are considered then it will be seen that the load shed by one half of the cracked material must be carried by the material at the end of the crack and due to the increase in flow stress in the plastic zone referred to above, most of this load will be carried in the plastic zone. If initially the reduction in thickness at the crack tip is neglected then the situation may be represented as in Fig. 1 where

S is the reciprocal of A (mentioned in Lecture 3) and may be thought of either as the width of the plastic zone, or alternatively, as the mean width of zone of high stress at the crack tip. The equation of failure for constant material properties is then:-

$$F = f_y \left(\frac{1}{S} + 1 \right) \qquad \text{Eqn. (1)}$$

where the nomenclature is as given in Fig. 1.

Experimental results obeying this equation should fit a plot of the type shown in Fig. 2.

Quirk[1] has examined the experimental data for a number of materials and has found that this sort of straight line plot is obtained.

Eight results from the tests on the 5 ft. vessel experiments described in Lecture 3 (sets of data corresponding to nearly similar material properties) are plotted in Fig. 3.

In all the data examined, except certain Zirconium alloys, the parameter F is found to coincide with the ultimate tensile strength f_u of the material. Thus in order to correlate materials of differing U.T.S. the type of plot shown in Fig. 4 may be used. In this figure, the intercept of each of the straight line-constant material plots intersects the abscissa at a value of $\frac{f_g l}{F}$, corresponding numerically to the plastic zone size S, at which failure occurs for the particular material properties. Thus, such a diagram can contain all the relevant information concerning the onset of fast fracture in a material. Some data [2] from 5 ft. vessel tests on mild and low alloy steels is plotted in Fig. 5. Again, all the data available is not suitable - only where there are two or more points at similar material properties has it been possible to make a plot. These results also show a good fit to Equation (1)

<u>The Effect of Material Parameters on Stress Distribution in the Crack Tip Region</u>

3. From the above, it will be realised that the fast fracture behaviour of materials can be characterised by the parameters F and S. Since it would be prohibitively expensive to employ large scale testing for each new material, it is important to find correlations with small-size laboratory tests. Since F is equal to the U.T.S. for most materials of interest, the remaining problem is to obtain a suitable correlation for S.

The influence of the Charpy value on the fracture parameters is obvious from the experimental work described in Lecture 3. The proportionality between lateral deformation and energy absorbtion in the Charpy test demonstrated by Orner[3], Fig. 6, suggests that Charpy could provide a measure of lateral deformation at failure at the tip of a real crack. If this is so, then since this deformation controls the through thickness stress P_3 at failure the Charpy value must also control the shape of the stress distribution in the plastic zone and consequently the size of the plastic zone.

Correlation of Experimental Data Without Bulging

4. Irvine et al [4] and Quirk [5] have both suggested tentative empirical correlations of the form:-

$$\text{at failure} \quad S = \text{Constant} \times (\text{Charpy energy})^{\frac{1}{2}} \qquad \text{Eqn. (2)}$$

Fig. 7 uses some results of the 5 ft. vessel experiment with 0.36%C steel to demonstrate the degree of fit to this relationship. The eight results used in Fig. 3 are again included here. Only data for P_1 type failure is used.

It is also to be expected that the size of the plastic zone will vary inversely as the yield stress. Quirk [5] has analysed data for a number of materials and taking the Charpy dependence to be:

$$S = \frac{(\text{Charpy energy})^{\frac{1}{2}}}{a} \qquad \text{Eqn. (3)}$$

has given the relationship between a and f_y as shown in Fig. 8. Use of equations (1) and (3) gives reasonably accurate failure prediction for a wide range of materials. However, the large amount of scatter apparent in Fig. 8 and the unsatisfactory form of equation (3) has prompted a search for a better correlation for S. One suggestion put forward is that it should be of the form:-

$$S = \left(\frac{\text{Charpy energy}}{\text{yield stress}}\right)^{\frac{1}{3}} \qquad \text{Eqn. (4)}$$

giving S in the dimension $\left(\frac{\text{ins} \times \text{lbs}}{\text{lbs} \times \text{ins}^{-2}}\right)^{\frac{1}{3}} = \text{ins.}$

The data for 5 ft. diameter vessel tests on mild and low alloy steels already plotted in Figs. 3 and 5 has been used to check equation (4). Fig. 9 shows that with one exception the data is a good fit.

This one exception is the point for the 1501-151 mild steel. The only exceptional feature of this material is its tensile elongation at failure which is 40% compared with 28-33% of the other materials in this figure. When developing Eqn. (1) at the beginning of para. 2, the effect of the local reduction in thickness at the crack tip was neglected and it may be that when correlating fast fracture data on materials of different tensile ductility, allowance should be made for this when calculating S from $\frac{f_g l}{f_u - f_g}$. However, as yet, insufficient evidence has been collected to resolve this point.

The Effect of Plate Thickness

5. The data considered earlier in this Lecture has been relevant to P_1 mode failures in 1 in. thick plate. At Charpy values in excess of 30 ft. lbs. (yield strength 15 T.s.i.) a transition to the $P_1 - P_3$ shear occurs as described in Lecture 3. This transition may be thought of as a decrease in constraint in the plastic zone, a decrease in P_3 (decrease in tension) and therefore an increase in the shear stress $P_1 - P_3$. When this exceeds the ultimate shear stress, which is approximately one half of the U.T.S. a shear mode of failure results. For such failures, a slight modification of the parameter F is thus indicated. See Fig. 12 of Lecture 3. Increase in thickness will result in an increase in plastic zone constraint, an increase in P_3, a reduction in $P_1 - P_3$ and therefore a shift in the transition to the $P_1 - P_3$ shear mode to higher values of Charpy energy (higher values of $\frac{\text{Charpy}}{\text{Yield stress}}$). Reduction in thickness should have the converse effect. This is the only effect of thickness which can be foreseen and is in accordance with the experimental evidence, e.g., Yukawa, Ref. 7 , gives data on matched spin disc tests in which the fracture stress of a 3 in. thick specimen and a 72 in. thick specimen were comparable.

Modification to Flat Plate Equation to Allow for Bulging

6. When the stress at the crack tip due to the stress concentrating effect of the crack is augmented by other stresses, then this must be taken into account on the right hand side of Eqn. (1). A case of particular interest arises when the bending stress due to the action of the pressure along the unsupported edge of a crack, in an internally pressurised component, becomes significant.

There are two possible ways in which such stresses could affect the failure pressure. The first of these is that the bending stress acts in conjunction with the P_1 stress at the crack tip and is thus proportional to (crack length)^2. The second possibility is that the bending stress is further intensified by the presence of the crack. Analysis of the available experimental data [5] suggests that the former assumption best describes the actual behaviour and the controlling equation is:-

$$F = f_y \left(\frac{K}{D^2} l^2 + \frac{1}{S} l + 1\right) \qquad \text{Eqn. (5)}$$

Where D = diameter of cylindrical component.

K is a function of yield strength (See Fig. 10) Ref. 5.

F, f_g l and S are previously defined in Fig. 1.

This equation is mainly of use for pipes and tubes. The l^2 or bulging term becomes insignificant for most reactor pressure vessels and for this case Eqn. (5) reduces to Eqn. (1).

Table I shows the analysis of the data on 58 in. diameter spheres in ½ in. thick mild steel reported by Taylor and Burdekin.[6] The data is plotted in Fig. 11 in the form of a $f_g - f_g l$ plot. This is clearly non-linear and indicates the presence of appreciable bulging. Since there is no linear portion available to determine S, this is estimated from the material properties and Fig. 9, and a 'flat plate' line drawn on Fig. 11 through f_u = 27 T.s.i. In Fig. 12, $f_g(\frac{l}{S} + 1)$ is plotted against $f_g l^2$ giving a reasonable straight line passing through f_u = 27 T.s.i. at $l = 0$ and $f_g l^2 = 0$, thus demonstrating the validity of the form of Eqn. (5). Quirk [5] has suggested that to allow for spherical geometry the bulging term should be modified, if the K - f_g correlation derived from cylindrical tests (Fig. 10) is to be used. Thus for spheres:-

$$F = f_g \left[\frac{2K}{(\frac{D}{2})^2} l^2 + \frac{1}{S} l + 1\right] \qquad \text{Eqn. (6)}$$

Application to Cracks Present in a Stress Gradient

7. Using the same approach as in the derivation of Eqn. (1) for the case of a stress gradient, the equilibrium condition at failure may be written:-

$$S \ (F - f_{avS}) = \int_{o}^{l} f_{g\ nom} dl \qquad \text{Eqn. (7)}$$

An approximate procedure is shown in Fig. 13.

Application to Cracks Present in a Component of Non-Uniform Thickness

8. Where the component is of non-uniform thickness and the stress is uniform, then the condition for failure may be written:

$$\int_{o}^{l} f_g \, da = \int_{l}^{(l + S)} (F - f_g) \, da \qquad \text{Eqn. (8)}$$

Fig. 14 shows this applied to a circular shaft with a crack normal to the axis.

Behaviour of Partial Thickness Cracks

9. It is obviously unreasonable to expect the idealized through thickness crack model to work in other situations, except perhaps that of a penny shaped crack embedded in a relatively large volume. The partial thickness crack model is of particular interest, and the Cockenzie failure is a typical example of this.Fig. 15.

Examination of this, and other cases suggests that failure of the remaining ligament occurs when the average stress is approximately equal to the ultimate tensile strength. If the through thickness crack, which then results is of super-critical length, this will continue to propagate, as in the Cockenzie case. On the other hand, if it is sub-critical in size, the worst result will be leakage. Fig. 16.

TABLE I

"Unstable Fracture by the Shear Mode in Spherical Vessels with Long Flaws"(Ref. 6)

The reference tabulates results of fracture tests on spherical vessels, 58 in. diameter, ½ in. thick, fabricated from materials to B.S.1501-161:1968, Grade B. Through thickness defects were cut in the vessels prior to hydraulically pressurising the vessels to failure. Six tests in all were done on this size of vessel and in all cases the crack was cut parallel to the rolling direction. Test results, as tabulated, are:-

Vessel No.	Slit length 2l (ins)	Max pressure lbs/sq. in (f_g)	Temp. °C	Charpy Energy (ft.lbs)
1	3.375	1230	78	45
2	6.3	950	80	45
3	12.4	560	78	45
4	18.4	375	80	45
5	24	260	80	45
6	6	1100	0– 10	15–20

f_u at 80°C transverse to rolling direction 60,900 lb/sq.in.

f_y at 80°C transverse to rolling direction 36,000 lb/sq.in.

f_u at 15°C transverse to rolling direction 63,200 lb/sq.in.

f_y at 15°C transverse to rolling direction 37,860 lb/sq.in.

The following values are derived from this table using only tests at constant material properties, i.e., tests 1 to 5.

Vessel No.	f_g Tons/sq.in.	2l (ins)	$f_g l$	$f_g l^2$	$f_g(0.294l + 1)$
1	15.9	3.375	26.85	45	23.8
2	12.3	6.3	38.75	122	23.7
3	7.24	12.4	44.95	280	20.4
4	4.85	18.4	44.65	412	18.0
5	3.37	24	40.5	487	15.2

The results of the constant temperature tests (1-5) are presented as f_g v $f_g l$ in Fig. 11.

By comparison with typical f_g $f_g l$ plots obtained from the other experiments it may be deduced that all these tests failed under the influence of a bending stress. That is, the failure criterion given by Eqn. (6).

References

1. QUIRK, A. A Maximum Stress Theory for the Failure of Pressure Components Containing Through Thickness Defects. AHSB(S) R 134, 1967.

2. COWAN, A., AND KIRBY, N. The Application of C.O.D. Measurements to Large Scale Test Behaviour. Proc. Symposium on Fracture Toughness Concepts for Weldable Structural Steel, Risley, April, 1969.

3. ORNER, G. M., Charpy Brittle-Fracture Transitions by the Lateral Expansion Energy Relationship. The Welding Journal-Research Supplement, May,1958 p.201S.

4. IRVINE, W. H.. QUIRK, A., BEVITT, E. An Elasto-Plastic Approach to Fracture Mechanics. AHSB(S)R.142, 1968.

5. QUIRK, A. The Effect of Material Properties and Component Geometry on Fracture Behaviour. AHSB(S)R.149, 1968.

6. TAYLOR, T. E., BURDEKIN, F. M. Unstable Fracture by the Shear Mode in Spherical Vessels with Long Flaws. Jnl. Mech. Eng. Science, Vol.11, No. 5, 1969.

7. YUKAWA, S. "Fracture Design Practices for Rotating Equipment" in "Fracture" An Advanced Treatise, Vol. 5.

Uniform Gross Stress

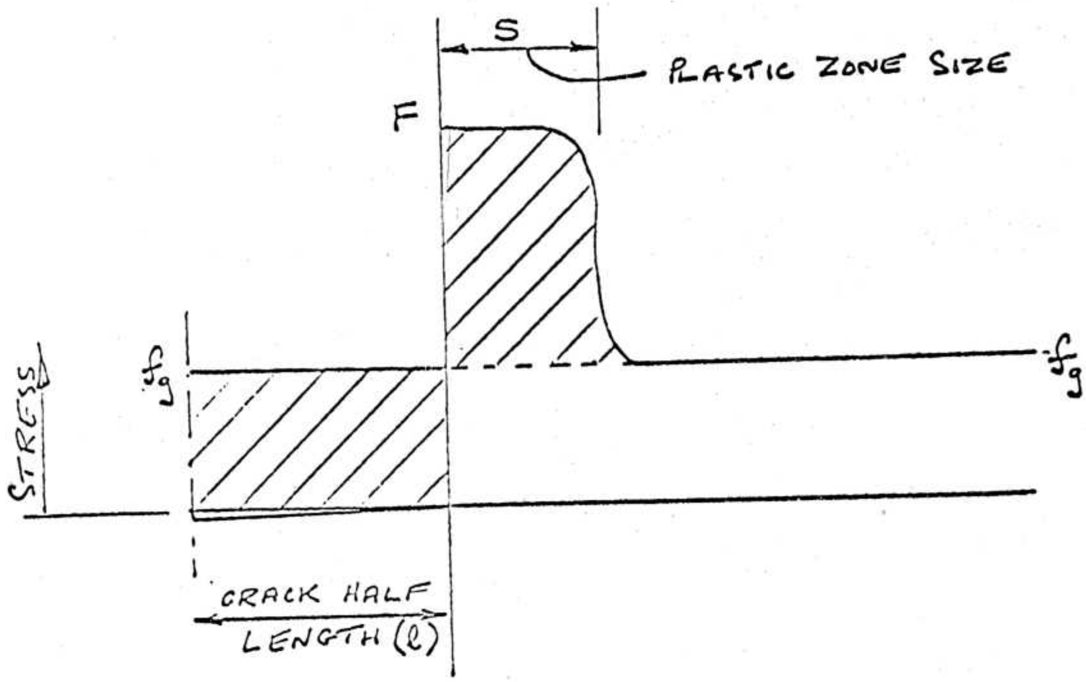

Fig. 1.

Considering equilibrium in plane of crack

$f_g l$ = load shed by cracked material

= extra load carried by crack tip material

$F - f_g$ is proportional to capacity of crack tip material to carry additional load at failure.

F is failure stress of material at crack tip.

∴ For crack which is just critical:- $f_g l \propto (F - f_g)$ for constant material properti

Diagramatically Fig. 2

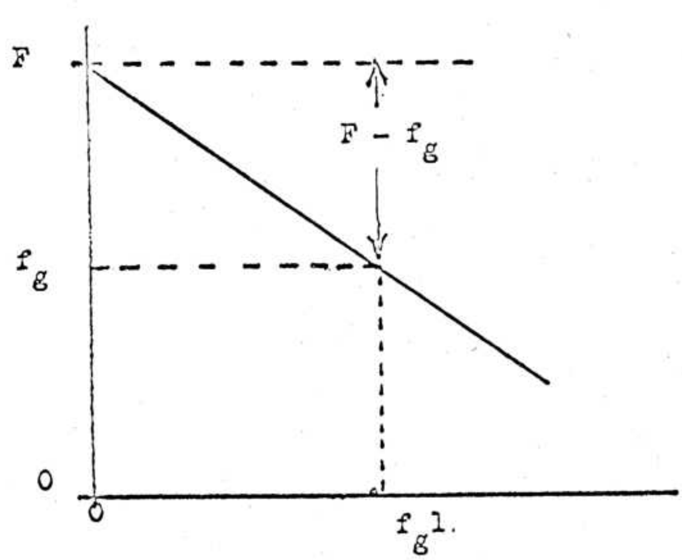

Re-write as:

$f_g l = S(F - f_g)$ equality of shaded areas in Fig. 1.

$F = f_g(l. \frac{1}{S} + 1)$

F = UTS (exp. evidence)

$\frac{1}{S}$ = A = a material constant.

i.e., plastic zone at failure is constant for constant material properties.

Charpy Energy	½ crack length l (ins.)	Failure stress f_g (Tons ins^2)	$f_g l$
7	12	4.3	51.6
7	3	12.3	36.9
12	12	5.2	62.4
12	6	8.4	50.4
12	3	13.4	40.2
17	12	5.8	69.6
17	6	9.4	56.4
17	3	14.5	43.5

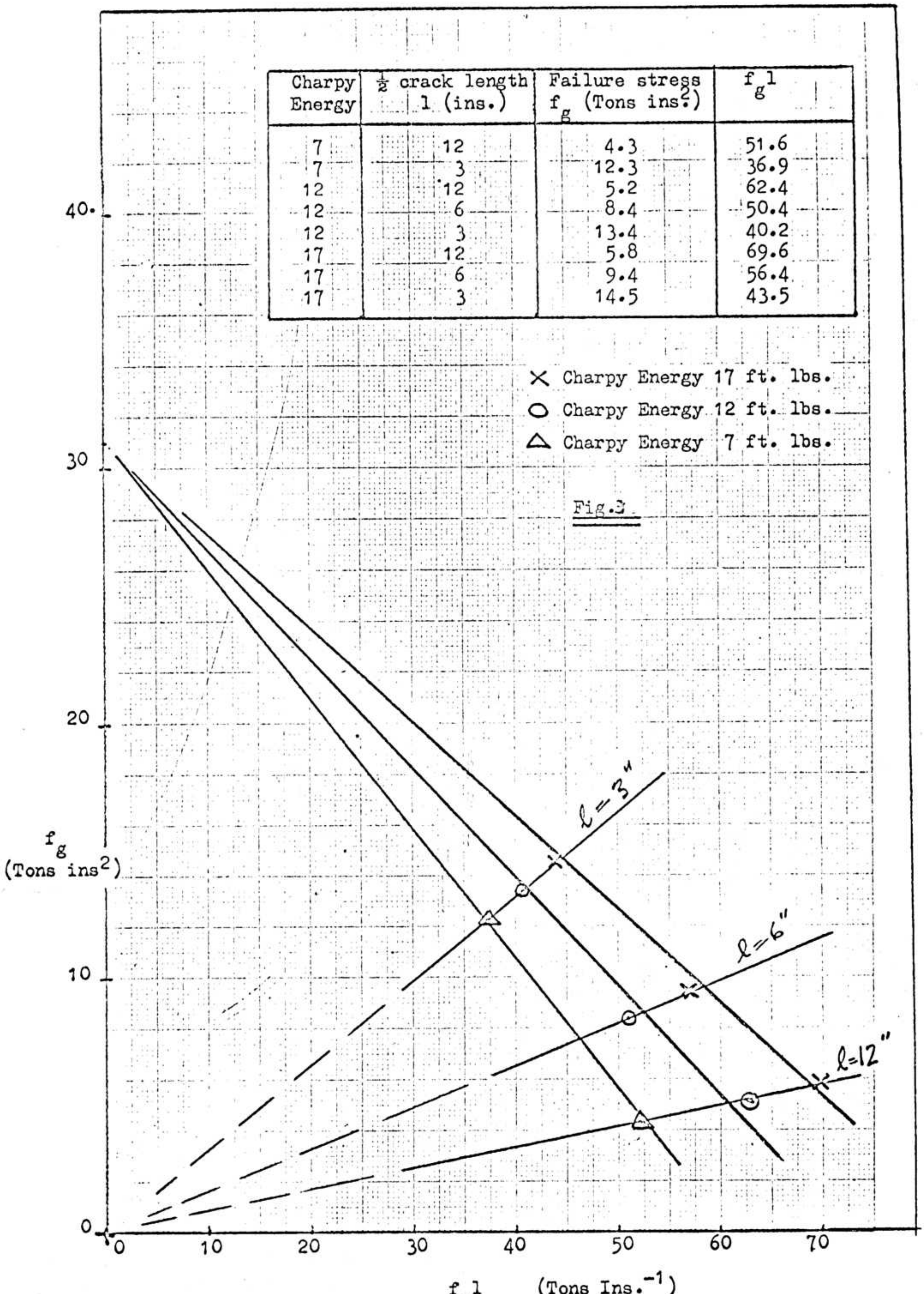

Fig.3

Plastic zone size at failure $= \dfrac{f_g l}{F - f_g} = S$

as $f_g \rightarrow 0$ $\qquad S \rightarrow \dfrac{f_g l}{F}$

Re-drawing Fig. 2

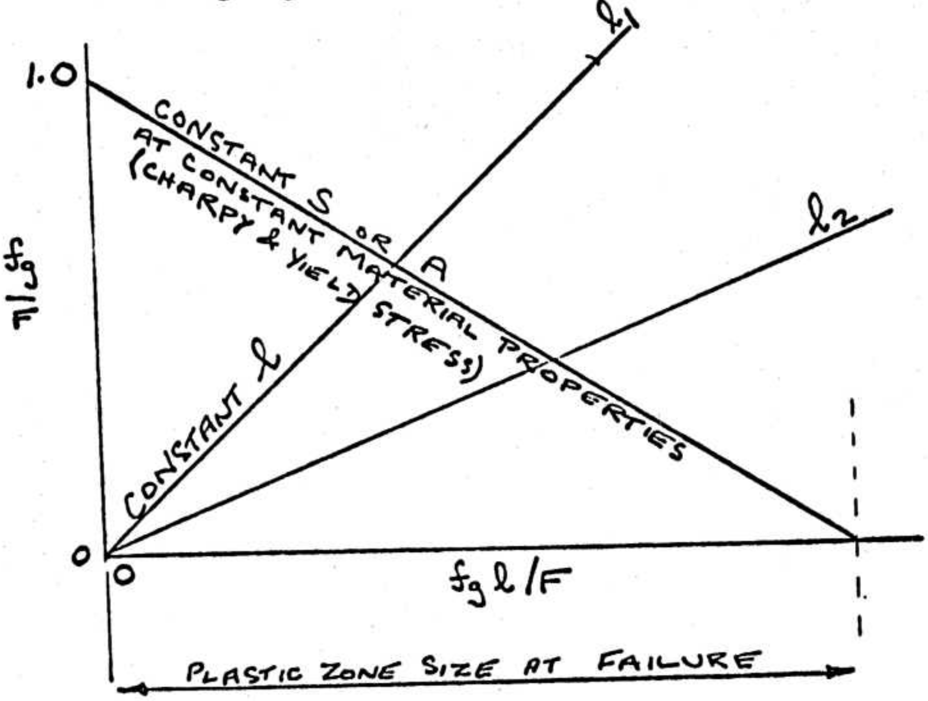

Then generalised diagram is as below :

FIG. 4.

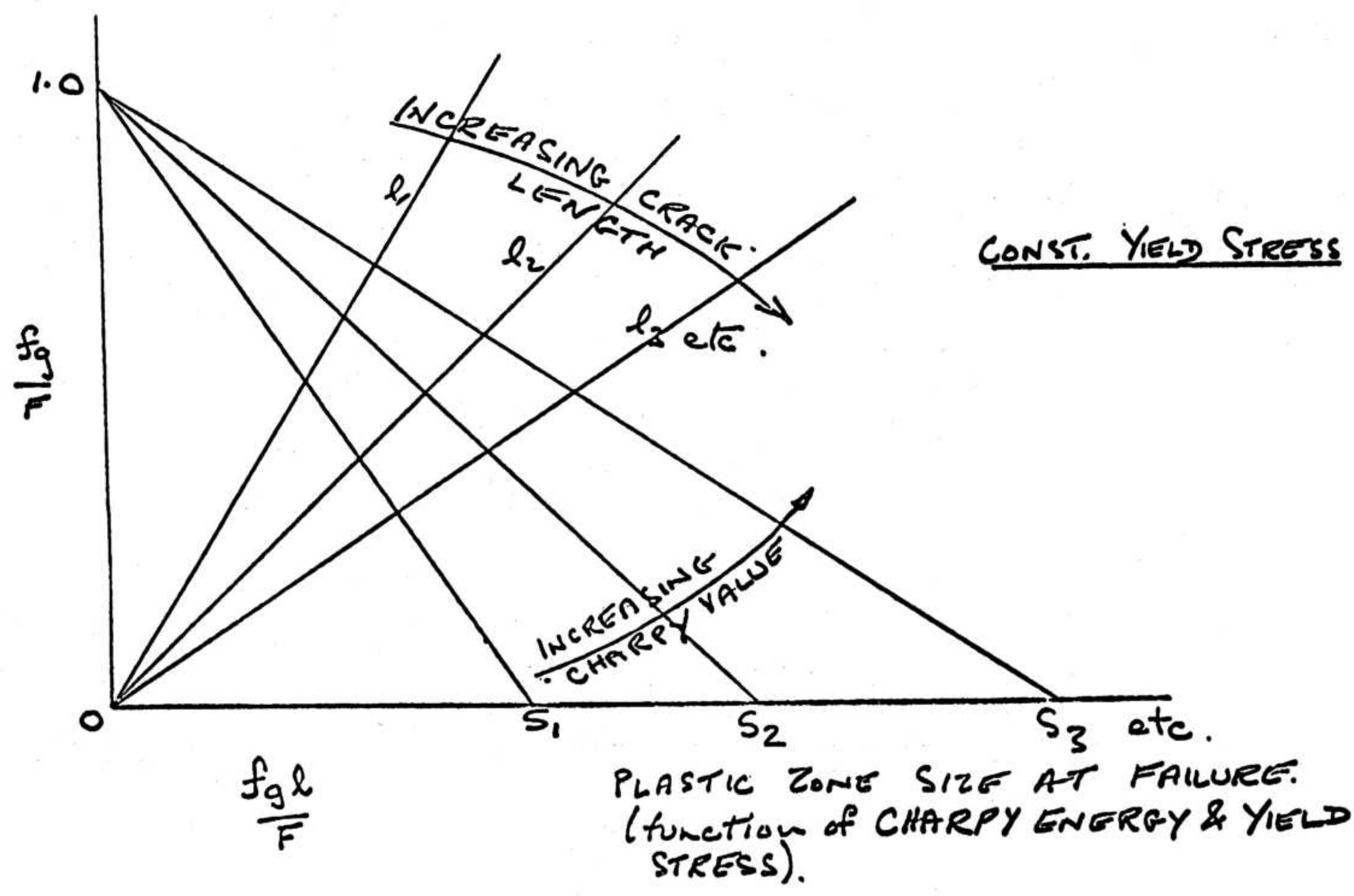

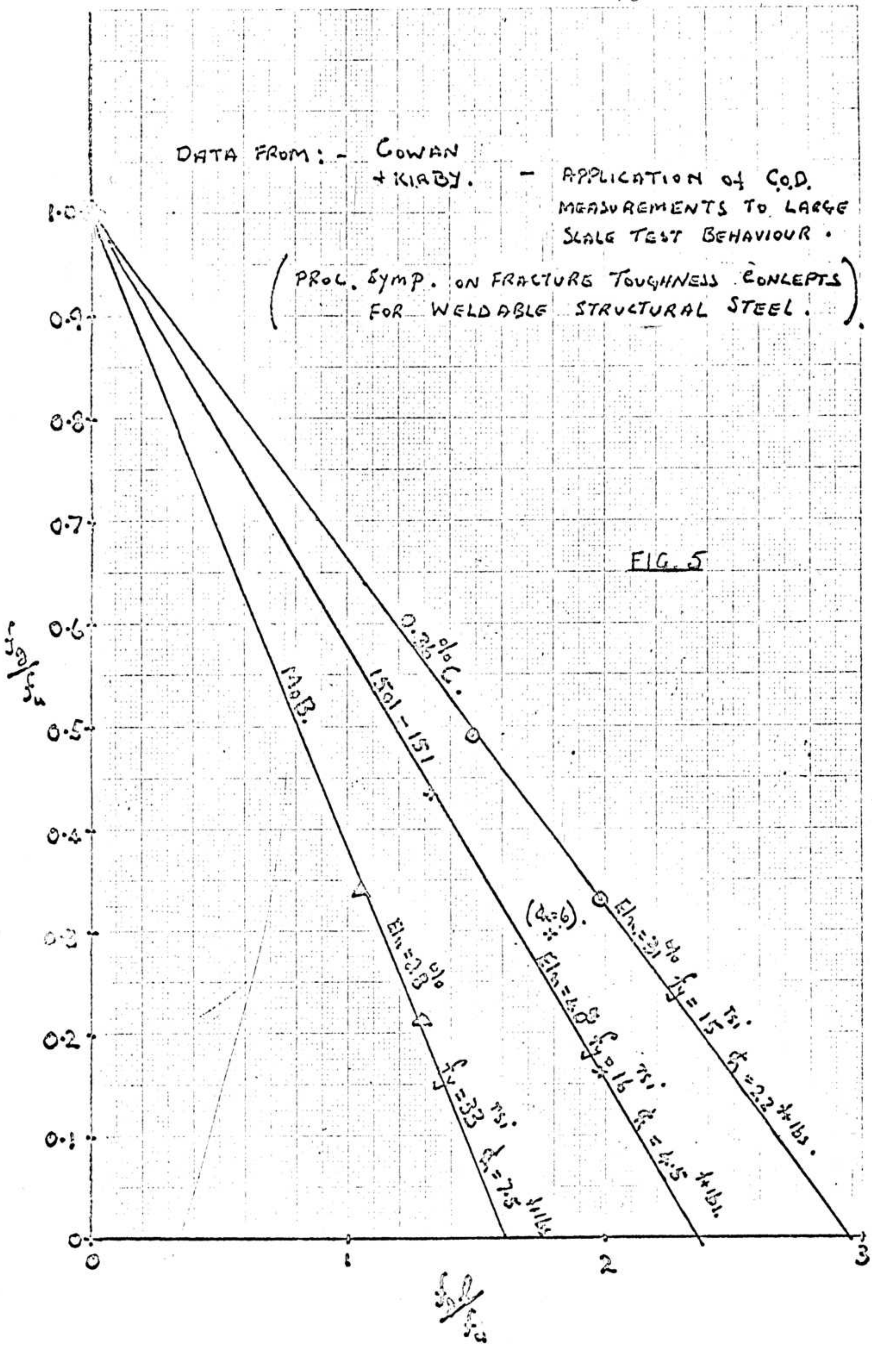
DATA FROM: - COWAN + KIRBY. - APPLICATION of C.O.D. MEASUREMENTS TO LARGE SCALE TEST BEHAVIOUR.
(PROC. SYMP. ON FRACTURE TOUGHNESS CONCEPTS FOR WELDABLE STRUCTURAL STEEL.)
0.2% C.
1501 - 151
MnB.
1.0
0.9
0.8
0.7
0.6
0.5
0.4
0.3
0.2
0.1
0
1
2
3

FIG. 5

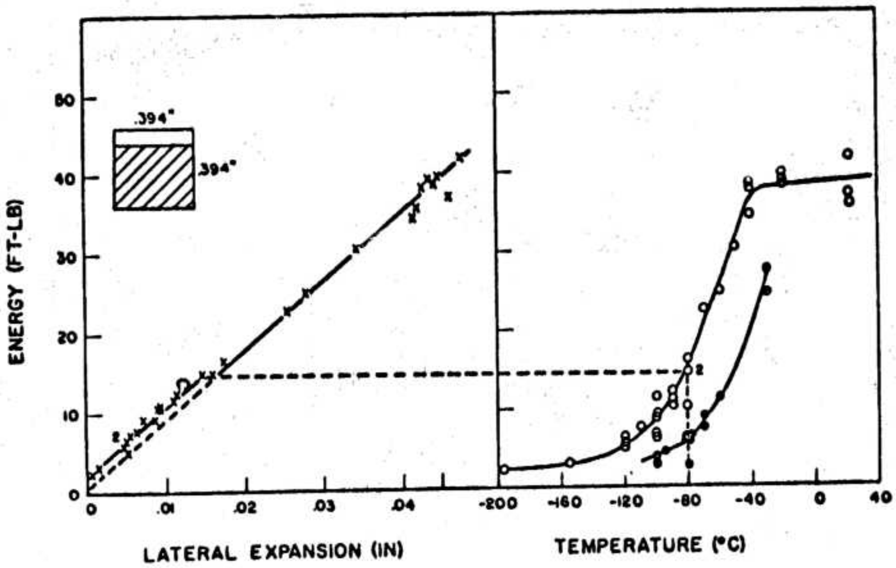

Fig. 6. Energy-expansion and energy-temperature curves from standard V-notch Charpy specimens

The energy-expansion (X) and one of the energy-temperature (O) curves were obtained from conventional (single-blow) tests. The energy-temperature curve (●) showing an inflection at —80° was obtained by the low-blow technique and represents the energy to propagate the initiated crack. Note the discontinuity in the energy-expansion relationship and that its horizontal projection cuts the conventional transition curve at —80° C, the low-blow transition temperature

Charpy Energy	f_g	$f_u - f_g$	$\frac{f_g}{f_u - f_g}$	l	$l\left(\frac{f_g}{f_u - f_g}\right) = S$	$(\text{Charpy})^{\frac{1}{2}}$
7	4.3	26.7	0.161	12	1.932	2.64
7	12.3	18.7	0.657	3	1.971	2.64
12	5.2	25.8	0.201	12	2.418	3.46
12	8.4	22.6	0.371	6	2.226	3.46
12	13.4	17.6	0.76	3	2.28	3.46
17	5.8	25.2	0.23	12	2.76	4.12
17	9.4	21.6	0.435	6	2.61	4.12
17	14.5	16.5	0.878	3	2.634	4.12
33	11.5	19.5	0.59	6	3.54	5.75
41	11.9	19.1	0.624	6	3.74	6.4

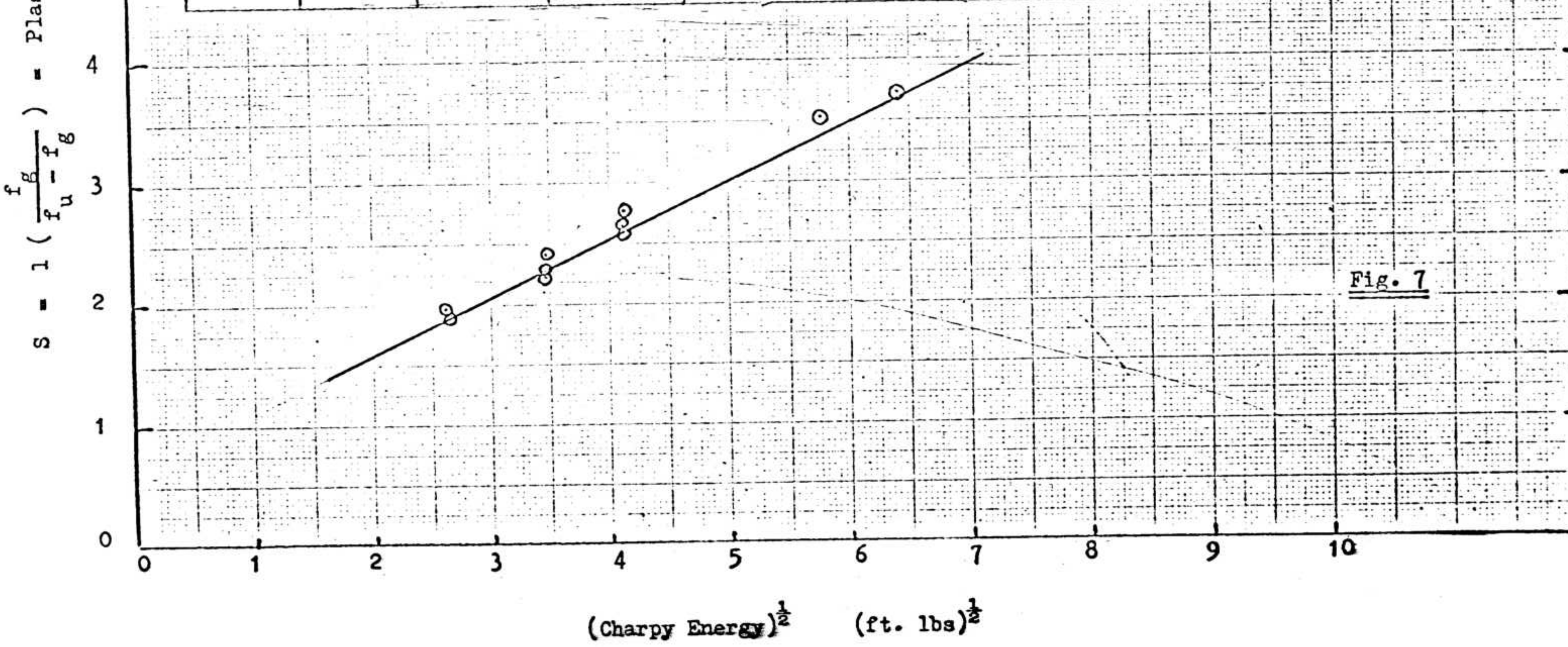

Fig. 7

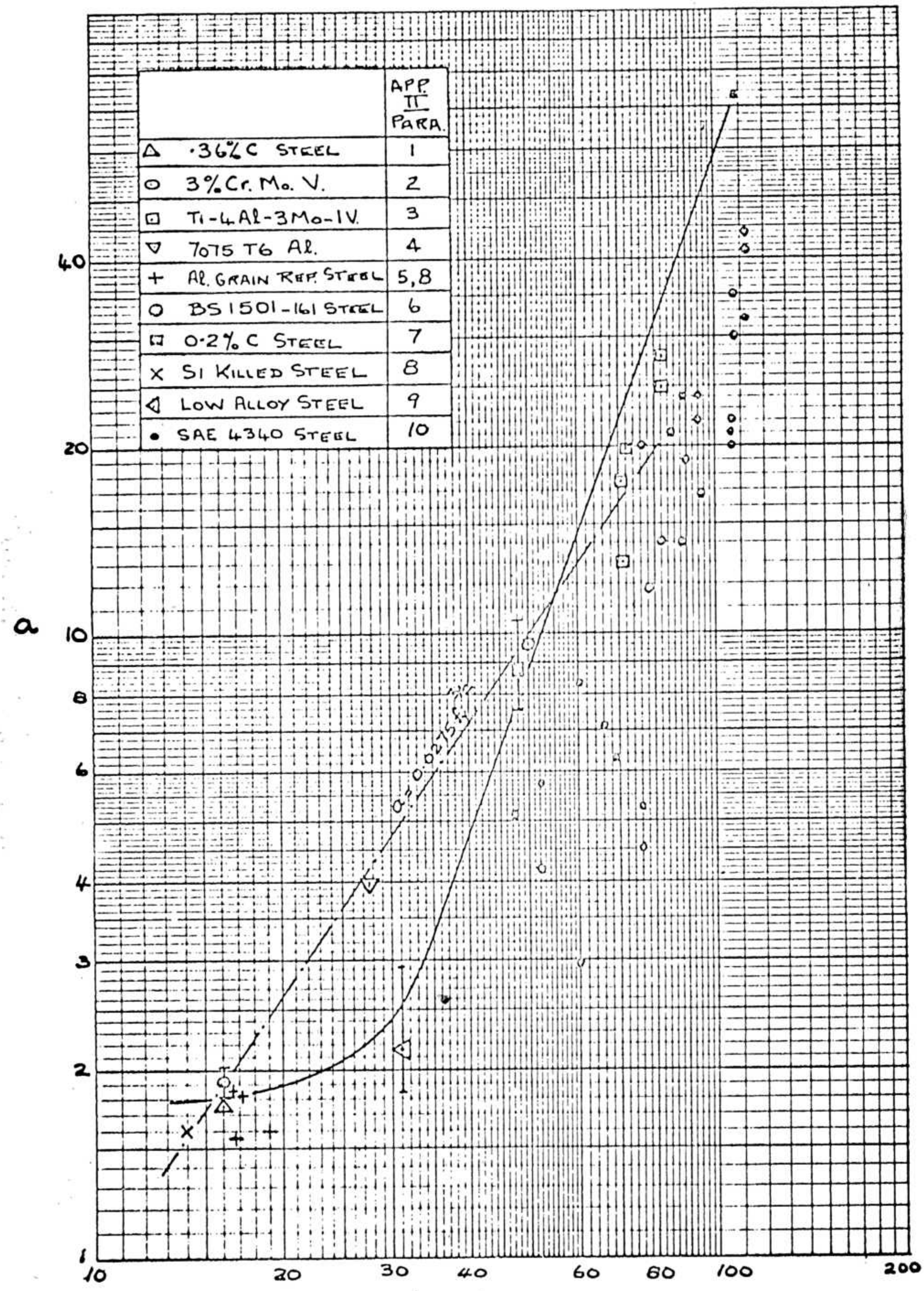

FIG. 8. SHOWING EFFECT OF YIELD STRENGTH ON PARAMETER 'a' EQUATION 4

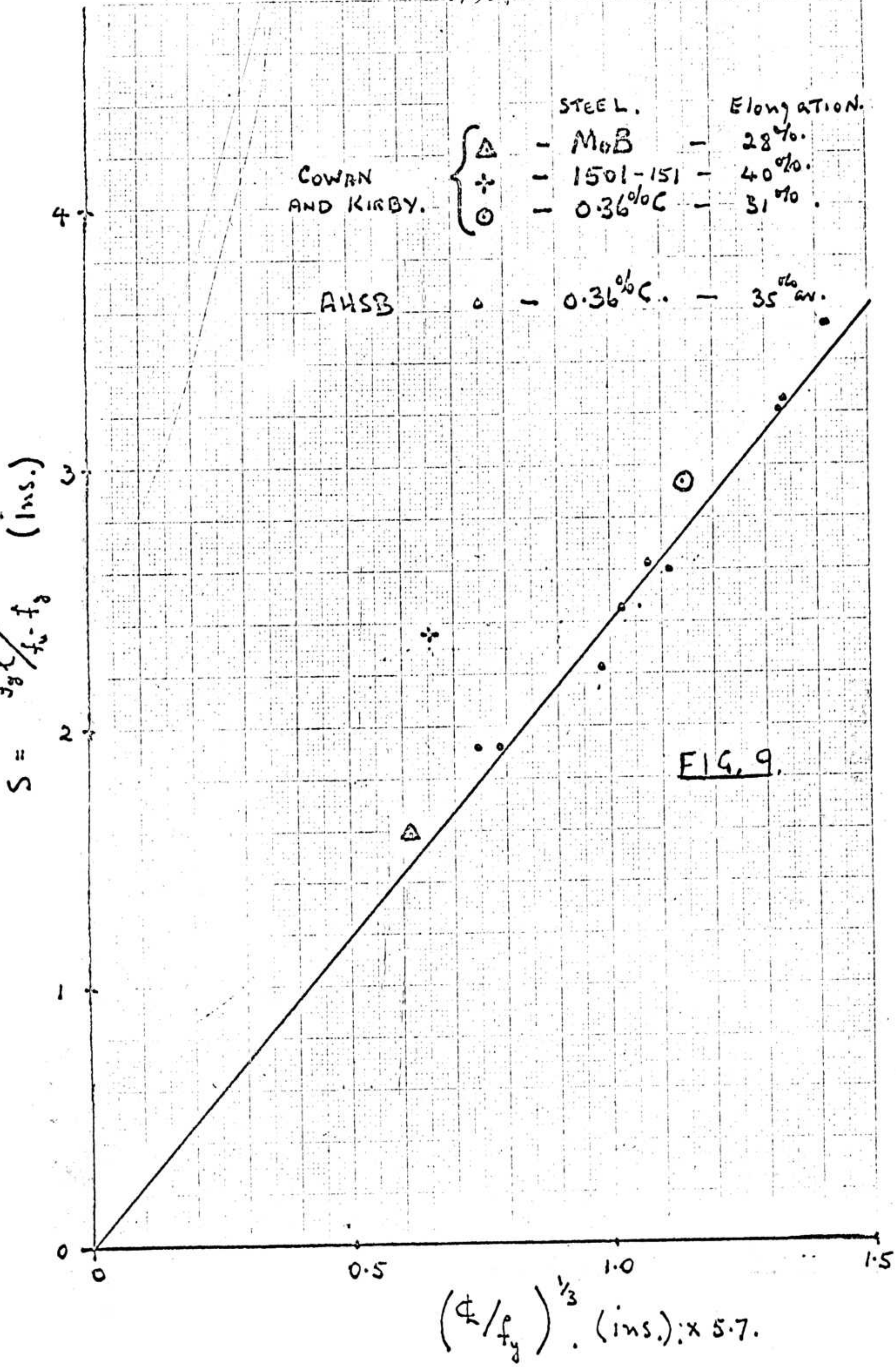
STEEL.
Elongation.
COWAN AND KIRBY.
Δ - MoB - 28%.
÷ - 1501-151 - 40%.
⊙ - 0·36%C - 31%.
AHSB ∘ - 0·36%C. - 35% av.
S = f_y l / (f_u - f_y) (ins.)
(ℓ/f_y)^(1/3) (ins.); x 5·7.
0
0·5
1·0
1·5
1
2
3
4

FIG. 9.

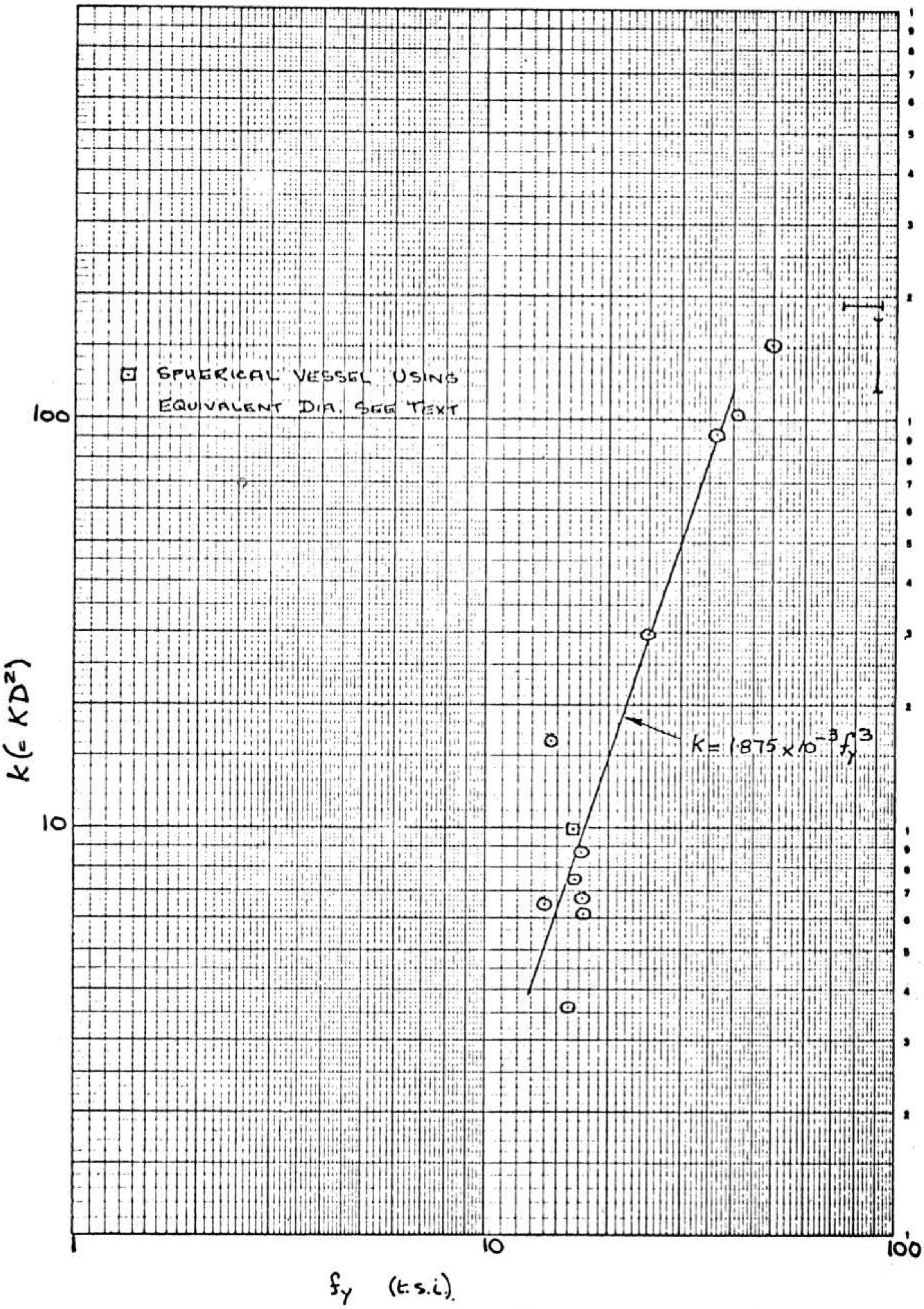

FIG. 10 RELATION BETWEEN YIELD STRESS AND K

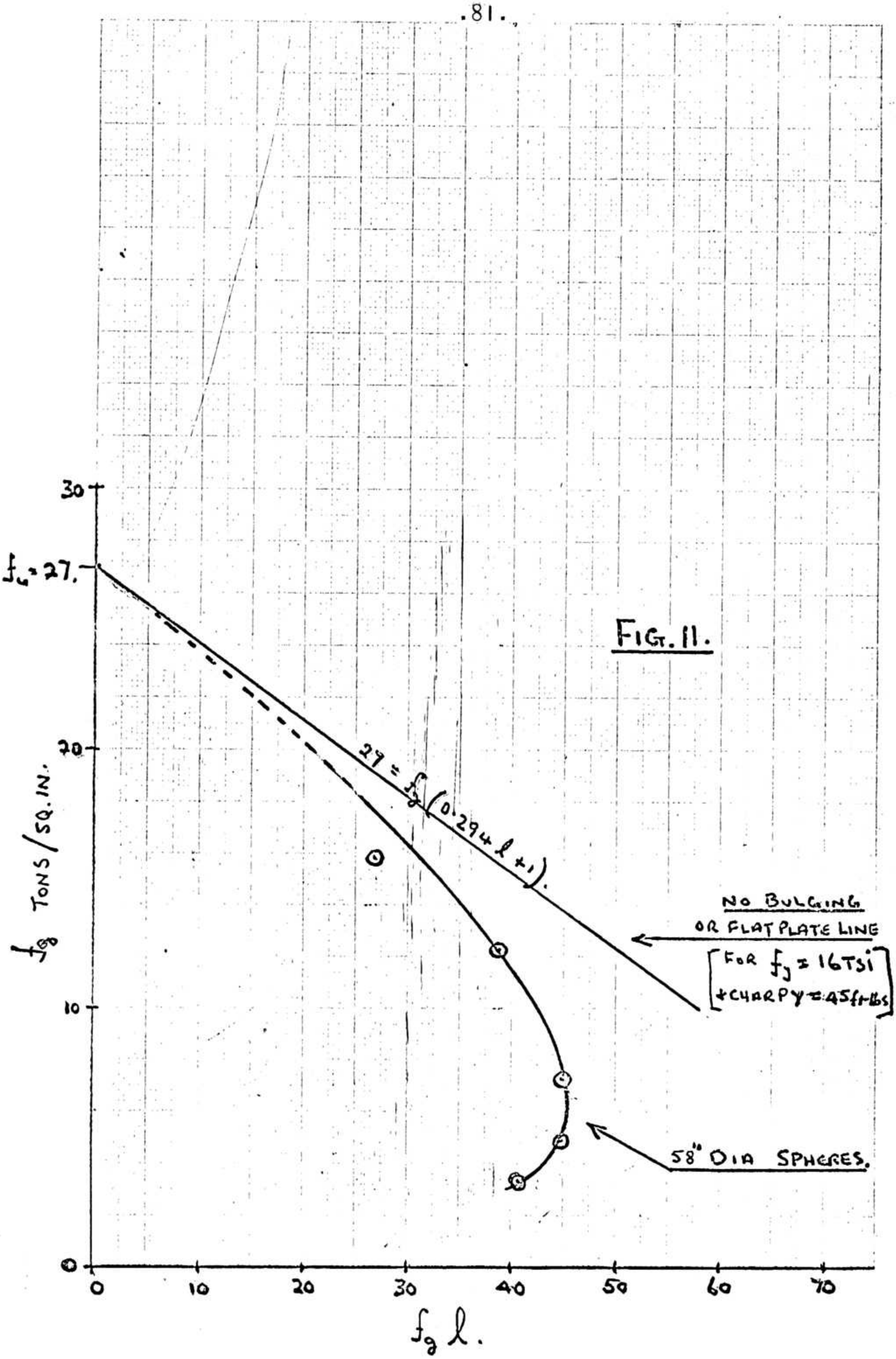

FIG. 11.
30
$f_u = 27.$
20
10
0
f_{go} TONS/SQ.IN.
$27 = f_g(0.294\,l + 1).$
NO BULGING
OR FLAT PLATE LINE
[FOR f_y = 16TSI
+ CHARPY = 45 ft-lbs]
58" DIA SPHERES.
0
10
20
30
40
50
60
70
$f_g\,l.$

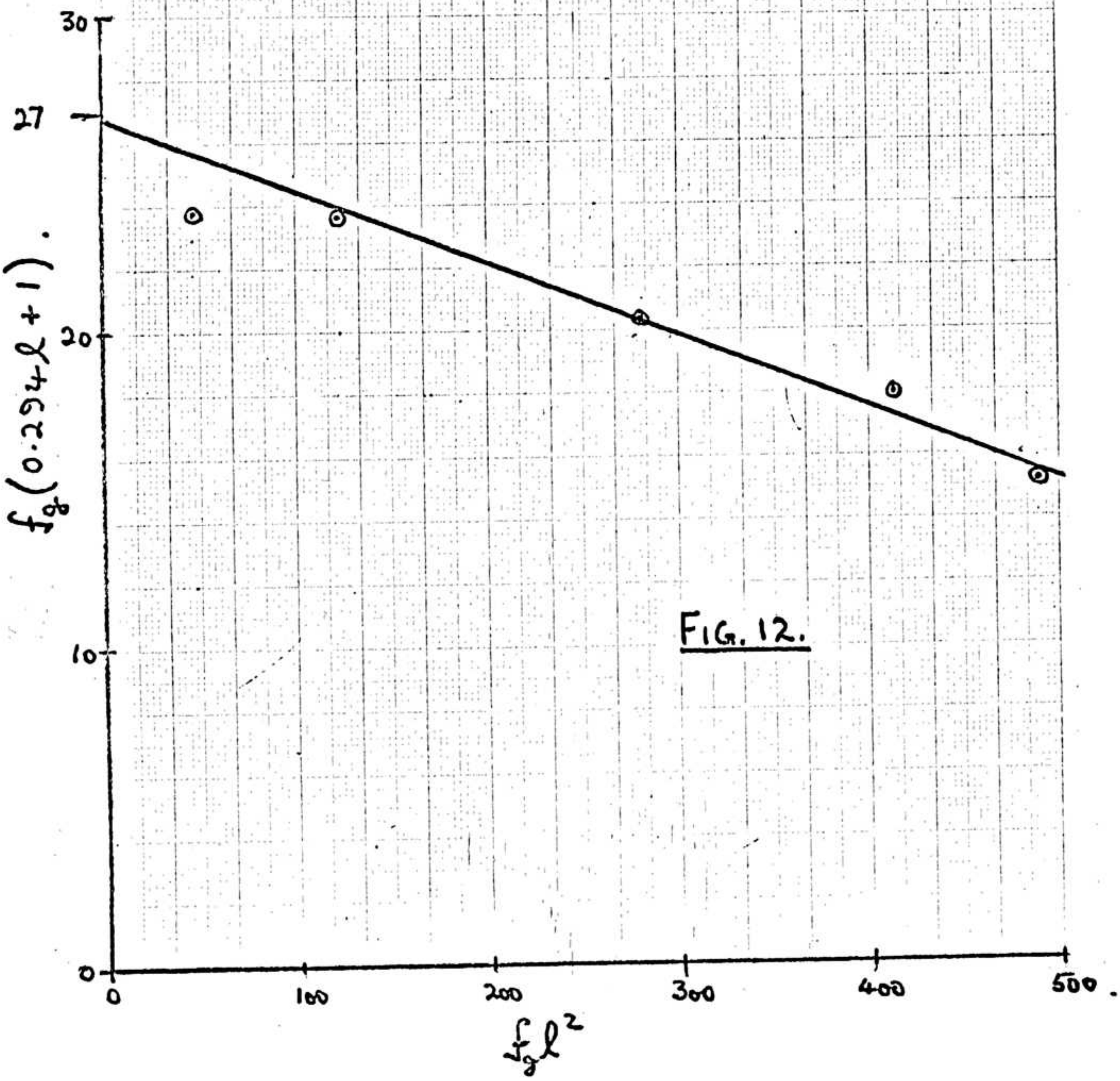

FIG. 12.

Non Uniform Stress

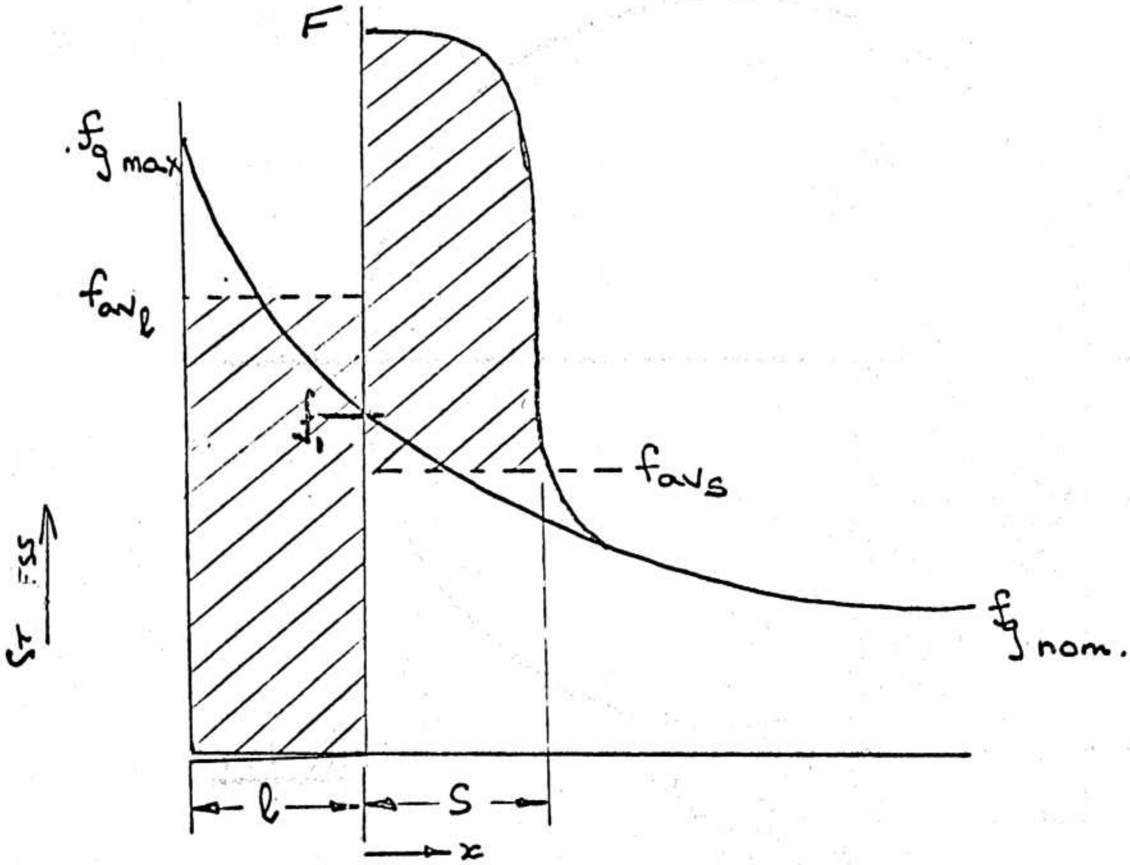

Fig. 13

At failure use of same principles as in Eqn. 1 gives approximately

$$A\, f_{av\ l}\, l = F - f_{avS}$$

$$A\, l \times \frac{f_{av\ l}}{f_{av\ S}} + 1 = \frac{F}{f_{av\ S}}$$

Just put

$$f_{av\ l} = \frac{f_{g\ nom} + f_{g\ max}}{2} \quad \text{and} \quad f_{av\ S} = f_{g\ nom}$$

then $\frac{1}{2}Al\,(1 + K) + 1 = \dfrac{F}{f_{g\ nom}}$

where $K = \dfrac{f_{g\ max}}{f_{g\ nom}}$

Hence l for specified values of A & F (U.T.S.)

then using this value of l in the first equation on this page obtain a more exact value of l.

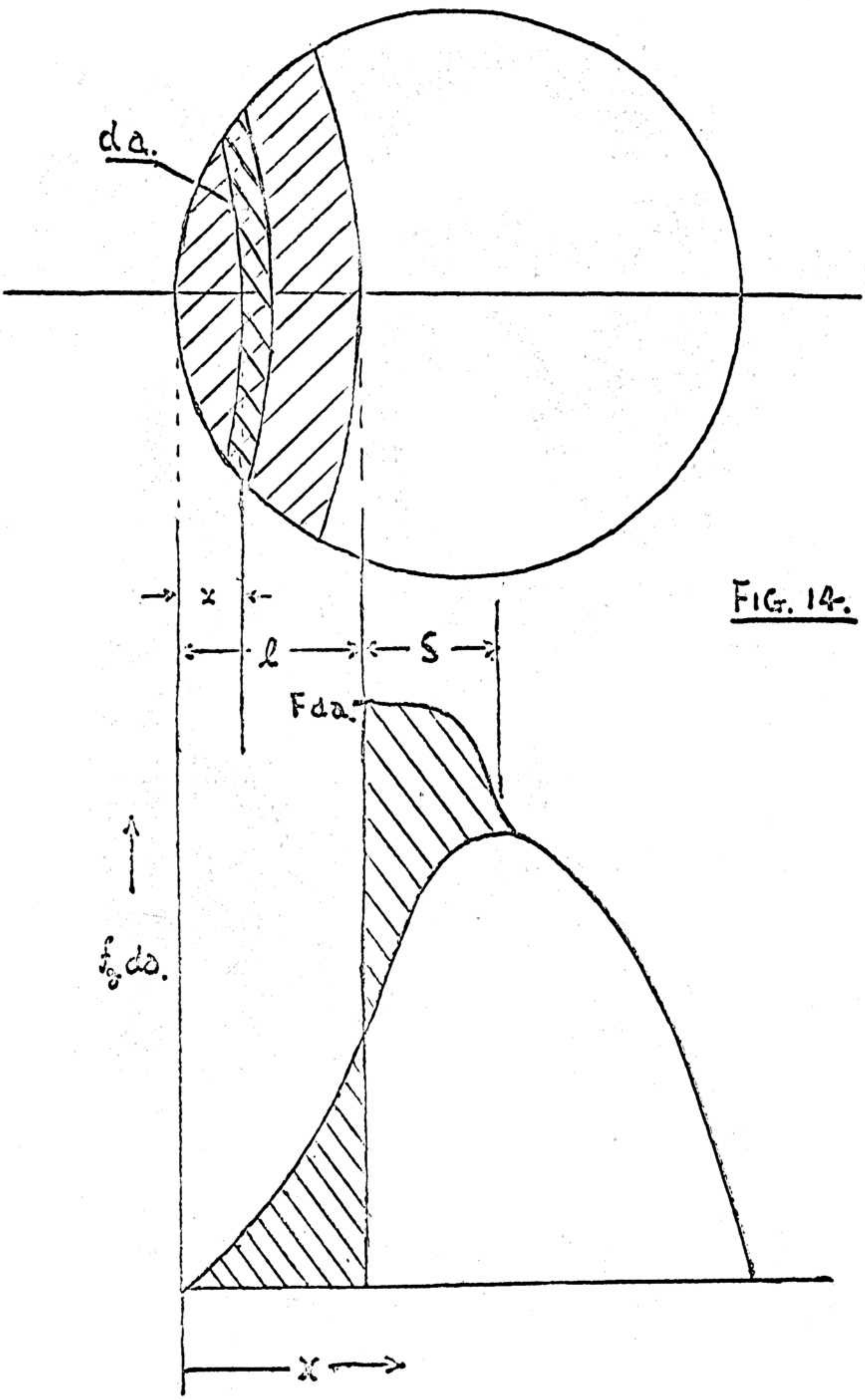

FIG. 14.

COCKENZIE BOILER DRUM FAILURE

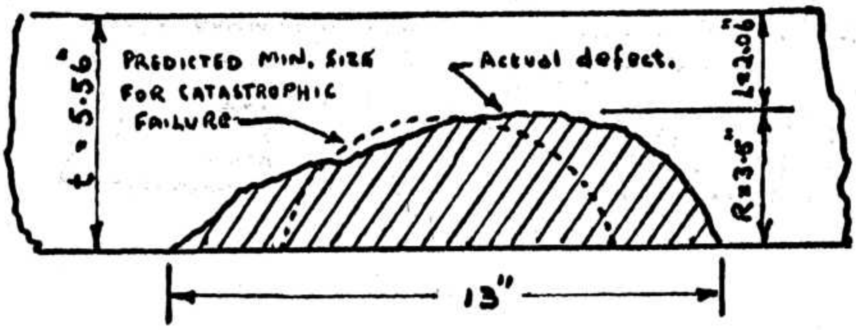

Failure Conditions

Failure Pressure P_F = 3,980 P.s.i.g.

Design Pressure P_D = 2,775 P.s.i.g.

Failure Stress f_{gF} = $9 \times \frac{3980}{2775}$ = 12.9 T.s.i.

Material

U.T.S. = 36 T.s.i.
Y.P. = 30 T.s.i.
Design Stress = 36/4 = 9 T.s.i.
Charpy value at test temperature = 20 ft.lbs.

Average stress on minimum remaining ligament at failure = $12.9 \times \frac{5.56}{2.06}$ = 35 T.s.i.

Failure Prediction

Assuming that snap-through occurs when average stress on remaining ligament reaches U.T.S. (f_u)

Then $f_{gF} \times t = f_u \times L$ at failure

and putting

$$L = t - R$$

$$R = t(1 - {}^{f_g}/{}_{f_u})$$

$$= 5.56\ (1 - 0.359) = 3.56$$

$$L = 2.0''$$

For a through crack, critical length is 8" from Eqn. (1)

Therefore fracture of 13" partial thickness defect will be catastrophic.

FIG. 15

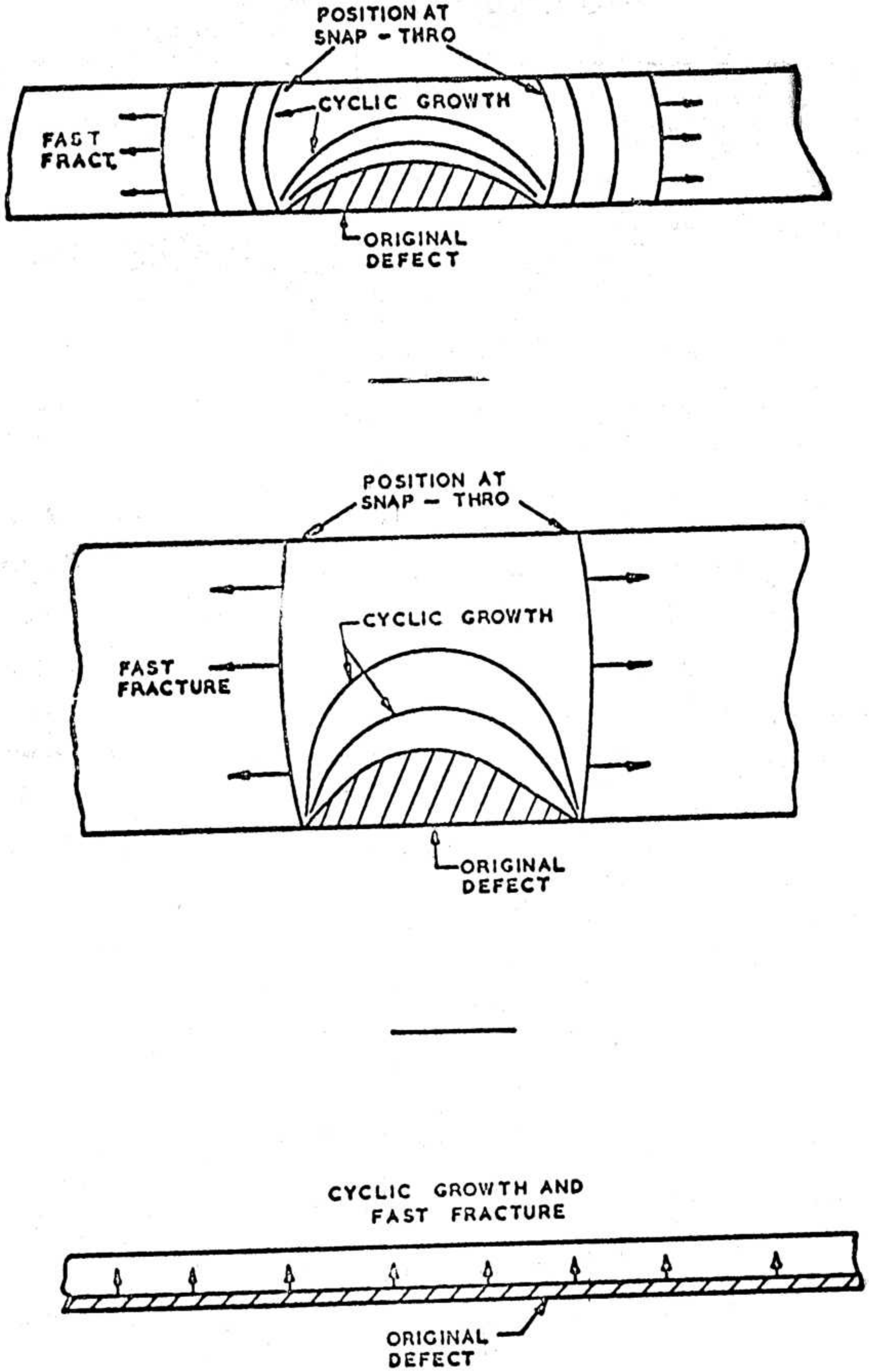
POSITION AT
SNAP - THRO
CYCLIC GROWTH
FAST
FRACT.
ORIGINAL
DEFECT
POSITION AT
SNAP - THRO
CYCLIC GROWTH
FAST
FRACTURE
ORIGINAL
DEFECT
CYCLIC GROWTH AND
FAST FRACTURE
ORIGINAL
DEFECT

FIG.16

LECTURE No. 6

Other Fracture Mechanics Approaches

1. The Griffith Approach

As has been explained in previous lectures, although Griffith [1] realised that failure at the crack tip in a brittle material would occur due to the action of the maximum principal stress at that point, he had to adopt an energy approach because of the theoretically infinite value of this stress predicted by elastic stress analysis.

The Griffith formula is:-

$$f_g^{\,2}\, l = \frac{EG}{\pi} = \text{material const.} \qquad \text{Eqn. (1)}$$

Where E = modulus of elasticity

and G = the energy required to form unit area of fracture surface.

G is usually referred to as fracture toughness.

The basic assumptions in the derivation of this formula are:-

(a) Infinite area of plate

(b) Perfect elasticity

(c) Loads and stresses acting only in the plane of the plate

(d) Uniform uniaxial tensile stress f_g.

2. Modifications to Griffith Equation - Linear Elastic Fracture Mechanics

In engineering the above assumptions are seldom satisfied and to deal with these practical situations various modifications to Eqn. (1) have been proposed. Irwin [2] realising that the occurrence of plasticity at the crack tip had invalidated Eqn. (1), proposed that the crack should be treated as though its tip was in the plastic zone and thus that the crack had a total equivalent length of $2(l + \Delta l)$, where Δl is a fictitious increase in crack length. See Fig. 1. He also proposed that in cases where the size of the crack was sufficiently large relative to the size of the plate as to invalidate assumption (a) in para. 1, a further modification should be made to allow for this.

However, instead of using the strain energy release rate G, Irwin suggested a stress intensity factor defined by:

$$K^2 = EG \qquad \text{Eqn (2)}$$

Where E is the modulus of elasticity.

Eqn. (2) is appropriate for the case of plane stress whereas in the case of plain strain the right hand side should be divided $1 - v^2$ where v is Poisson's ratio.

The exact addition to the real crack length was taken to be one plastic zone width, so that the equivalent crack may be visualised as extending between plastic zone centres, i.e.,

$$2l_e = 2l + S \qquad \text{Eqn. (3)}$$

where l_e = equivalent half length of crack

l = actual half length of crack

$2\Delta l$ = S = Plastic zone size. (See Fig. 1.)

The plastic zone size S is estimated roughly as $\frac{K^2}{\pi f_y}$ from the elastic stress field equations by assuming that the onset of plasticity at the crack tip caused little disturbance of the elastic stress field beyond the elasto-plastic boundary. Consequently,

$$l_e = l + \frac{1}{2\pi}\left(\frac{K_c}{f_y}\right)^2 \qquad \text{Eqn. (4)}$$

where f_y is the yield stress and K_c is the critical stress intensity factor.

However, Gerberich and Zackay [3] have shown experimentally on a number of high strength materials that the Dugdale equation:

$$S = l\left(\text{Sec}\,\frac{\pi f_g}{2f_y} - 1\right) \qquad \text{Eqn. (5)}$$

gives a better estimate of plastic zone size than $\frac{K^2}{\pi f_y}$. The finite width correction is usually attributed to Westergaard and in conjunction with Eqn. (5) this gives:

$$S = \frac{W}{\pi}\tan\left(\frac{\pi l}{W}\right)\left[\sec\left(\frac{\pi f_g}{2f_y}\right) - 1\right] \qquad \text{Eqn. (6)}$$

for a centre cracked sheet of width W.

It is possible that the expression may also be suitable for lower strength and higher toughness materials such as low alloy steel and mild steel and it has been suggested that for these materials the tensile strength f_u instead of the yield strength f_y, should be used.[4]

3. Neuber's Plastic Stress Concentration Factor Concept

Neuber's idea was that the average value of stress over a distance ε should control failure instead of the fictitiously high value f_m given by the theory of elasticity.[4] See Fig. 2. It has obvious similarities to the approach of Lecture 5 where ε is analogous to S.

4. Crack Opening Displacement Approach - C.O.D.

Here the basic idea is that the onset of fast crack propagation occurs when a critical strain is reached at the c rack tip. This critical strain is thus a material parameter rather like G or K and the basic assumption is that crack opening displacement C.O.D., is simply related to this strain. The relation as given by a number of authors [5], [6] and [7] for a flat plate is:-

$$\text{C.O.D.} = \frac{8 f_y l}{\pi E} \log \sec \frac{\pi f_g}{2 f_y} \qquad \text{Eqn. (6)}$$

This is, of course, only the C.O.D. which takes place during deformation prior to any crack extension. As mentioned above the critical value is a material parameter, e.g., it will vary with temperature in the transition range of a mild steel.

The model from which Eq. (6) is derived is shown in Fig. 3. The model consists of a crack of length 2l in an infinite plate which is subjected to a uniform tensile stress applied in the y direction at infinity. Under the action of the stress f_g, the slit extends to a length $2l_e$ and opens, but is partially constrained from extending and opening by a uniformly distributed internal tension, T, acting only on parts of the slit from $x = \pm l$ to $x = \pm l_e$ and $= (l_e - l)$. The basic argument is that if T is equated to f_y (the uniaxial yield strength of the material), the internal tension closely simulates the local support derived from similar shaped wedges of yielded material. The opening referred to in this equation is that occurring at the tip of the real crack.

5. Relationships Between Linear Elastic Fracture Mechanics and C.O.D. Approaches

If Eqn. (6) is expanded it becomes:-

$$\text{C.O.D.} = 8\frac{f_y l}{\pi E}\left[\frac{1}{2}\left(\frac{\pi}{2}\frac{f_g}{f_y}\right)^2 + \frac{1}{12}\left(\frac{\pi}{2}\frac{f_g}{f_y}\right)^4 + - - -\right] \quad \text{Eqn. (7)}$$

Considering only the first term:

$$\text{C.O.D.} = \frac{\pi f_g^2 l}{E f_y} \quad \text{Eqn. (8)}$$

From Eqn. (1) $$G = \frac{\pi f^2 l}{E} \quad \text{Eqn. (9)}$$

Combining equations (8) and (9) gives:-

$$G = f_y \times \text{C.O.D.} \quad \text{Eqn. (10)}$$

Equation (10) emphasises the fact that the model of material behaviour embodied in this analysis is a very simple one, makes no allowance for work hardening and is equivalent to assuming that fracture occurs at f_y.

6. Modifications to C.O.D. Equations to Allow for Bulging

The main work on bulging has been carried out by Folias[8] and his treatment has been used in conjunction with the C.O.D. flat plate equation (6) to give:-

$$\text{C.O.D.} = \frac{8f_y l}{\pi E}\left(\log \sec \frac{\pi}{2}\frac{f_g}{f_y}\right)\left(1 + 1.6\frac{l^2}{Rt}\right. \quad \text{Eqn. (11)}$$

where R is the radius of the cylinder

t is the thickness

and f_g is the hoop stress

The same device may be used for the Griffith type equation.

7. Plastic Collapse Approach

Hahn and his co-workers [9] have suggested that in the ductile region failure may be considered as being due to plastic collapse and therefore that the effect of the crack is to simply cause a magnification of the general or gross stress - failure being assumed to occur at a value of flow stress which is empirically determined. The Folias bulging correction factor has also been applied to this and the resulting relationship is:-

$$f_g = f_u = \bar{f}\left(1 + 1.61\ \frac{l^2}{Rt}\right)^{-\frac{1}{2}} \qquad \text{Eqn. (12)}$$

One empirical relation which has been determined is:-

$$\bar{f} = 1.04\ f_y + 10 \qquad \text{Eqn. (13)}$$

where f_y is in 10^3 lb/in^2

8. Inter-relation of the Various Approaches

There appears to be a concensus of opinion (10) that the approaches reviewed above are, in fact, all complementary, as follows:-

(a) The Griffith - Linear Elastic Fracture Mechanics equations being most suitable for very brittle materials where the plastic zone size is small compared with crack length.

(b) The C.O.D. type of analysis being suitable for intermediate situations such as in the brittle ductile transition in mild steel where C.O.D. is neither too small to be measured not so large as to be indefinite.

(c) The plastic collapse type of approach being suitable for the fully ductile region where the dependence of failure conditions on plastic constraint, triaxiality, and hence plastic zone size are at a minimum.

9. Conclusions Regarding the Adequacy of the Various Approaches

In all the approaches reviewed above, the common area of difficulty and uncertainty, when they are being used for practical applications, is the behaviour of the plastic zone.

(a) Linear Elastic Fracture Mechanics

Here the occurrence of crack plasticity is allowed for by adding a fictitious increment Δl to the real crack. When the 5 ft. diameter results described in Lecture 5 were examined for constancy of $f_g^2 l$ the result obtained in shown in Table I.

TABLE I

Variation of $2f_g^2 l$ @ Constant Temperature with Crack Length			
Total Crack Length (Inches)	Temperature		
	10°C	45°C	80°C
6	900	1260	-
12	770	930	1660
24	490	625	985

That $f_g^2 l$ is far from constant is not surprising; however, what is significant is that $f^2 l$ is largest for small crack lengths, i.e., the only way of modifying l to give constant $f^2 l_e$ is to put

$$l_e = l - \Delta l \qquad \text{Eqn.(14)}$$

Since it has been shown in Lecture 7, Fig. 11, that there is no effect of bulging up to about 45 ft. lbs., i.e., 80°C for the 0.36%C, 5 ft. diameter steel vessel tests, it must be concluded that the validity of Linear Elastic Fracture Mechanics in this region of intensive practical interest (5 - 45 ft. lbs) is open to serious doubt.

(b) C.O.D.

The drastic idealisation of material properties mentioned in para. 5, along with other aspects of the strip model make the absolute validity of the C.O.D. approach seem rather doubtful. It has been suggested (11) that these objections are avoided because of the comparative nature of the approach, i.e., the C.O.D. of a pressure vessel is compared with the C.O.D. on a laboratory sized specimen.

To provide a general check at constant material properties, Eqn. (11) may be re-written:-

$$\text{Constant} = A \times \text{C.O.D.} = l \log \sec \left(\frac{\pi}{2} \frac{f_g}{f_y} \right) \left(1 + 1.61 \frac{l^2}{Rt}\right) \qquad \text{Eqn. (15)}$$

since the parameter $\frac{\pi E}{8 f_y}$ will be constant

Then if Eqn. (11) does predict C.O.D. and C.O.D. at failure is constant, for constant material properties A x C.O.D., calculated from Eqn. (15) using experimental data obtained from tests on cylinders containing longitudinal slits should be constant. Figs. 4, 5, 6 and 7 are typical examples and show that this is not so. So that it would appear that either Eqn. (11) or C.O.D. = Constant at failure cannot be true.

(c) Plastic Collapse

This approach appears to be able to give quite good correlations in its limited range of applicability - probably due to its insensitivity to plastic zone behaviour. The principal difficulty is to know when a new problem is in this range, although this could be resolved by determining $\frac{S}{1}$ by the formula of para. 2. A fundamental objection to the Eqn. (12) type of formula is that it implies that for a given geometry and crack size the failure stress will increase with yield stress. This is in straight contradiction of the principle mentioned in Lecture 5 and verified by the observed behaviour of a large number of materials, that increasing the yield stress,concentrates more load at the crack tip and therefore causes failure at lower values of general field stress.

In general it must be concluded that the above approaches are inadequate, both from the point of view of the basic theoretical concepts on which they are based and the degree of practical substantiation by large scale pressure vessel tests.

Both Linear Elastic Fracture Mechanics and C.O.D. require special material test procedures, some of which are beset by the same fallacies and difficulties as the earlier Robertson test.

Use of the Folias bulging factor such as in Eqn. (12) can lead to a particularly dangerous conclusion, i.e., as R and t become large, so l becomes correspondingly large (everything else being constant). Thus it might be argued that in extrapolating to large vessels, critical crack lengths will be so large as to be unattainable, and therefore fast fracture will not be of interest. However, comparison of work on flat plate and spin tests with pressure vessel results has shown that what difference in behaviour does occur, may be fully explained using the approach of Lecture 5.

REFERENCES

1. GRIFFITH, A. A. The Phenomena of Rupture and Flow in Solids. Phy. Trans. Roy. Soc. 221 p.163, 1921.

2. IRWIN, G. R. Theoretical Aspects of Fracture Failure Analysis. Metals Engineering Quarterly, Vol. 3, No. 1, 1963.

3. GERBERICH, W. W., ZACKAY, V. F. On the Plane Stress Plastic Zone Correction in Fracture Mechanics.

4. NEUBER, H. Kerbspannungslehre, Springer, 1937.

5. BARANBLATT, G. I. Advances in Applied Mechanics, Academic Press, 1962.

6. HAHN, G. T., ROSENFIELD, A. R. Acta Met., 1966

7. BURDEKIN, F. M. STONE, D. E. W. Jnl. Strain Analysis 1. No. 2, Jan. 1966.

8. FOLIAS, E. S. The Effect of Initial Curvature on Cracked Sheets. Final Report to N.S.F., University of Utah, August, 1968.

9. HAHN, G. T., SARRATE, M., ROSENFIELD, A. R. Criteria for Crack Extension in Cylindrical Pressure Vessels. Int. Jnl. of Fracture Mechanics (S), 1969

10. General Discussion and Symposium on Fracture Toughness Concepts for Weldable Structural Steels, Risley, 1969.

11. CODA Report. Symposium on Fracture Toughness Concepts for Weldable Structural Steel, Risley, 1969.

CRACK WITH PLASTIC ZONE $\equiv$ LONGER CRACK WITHOUT PLASTIC ZONE

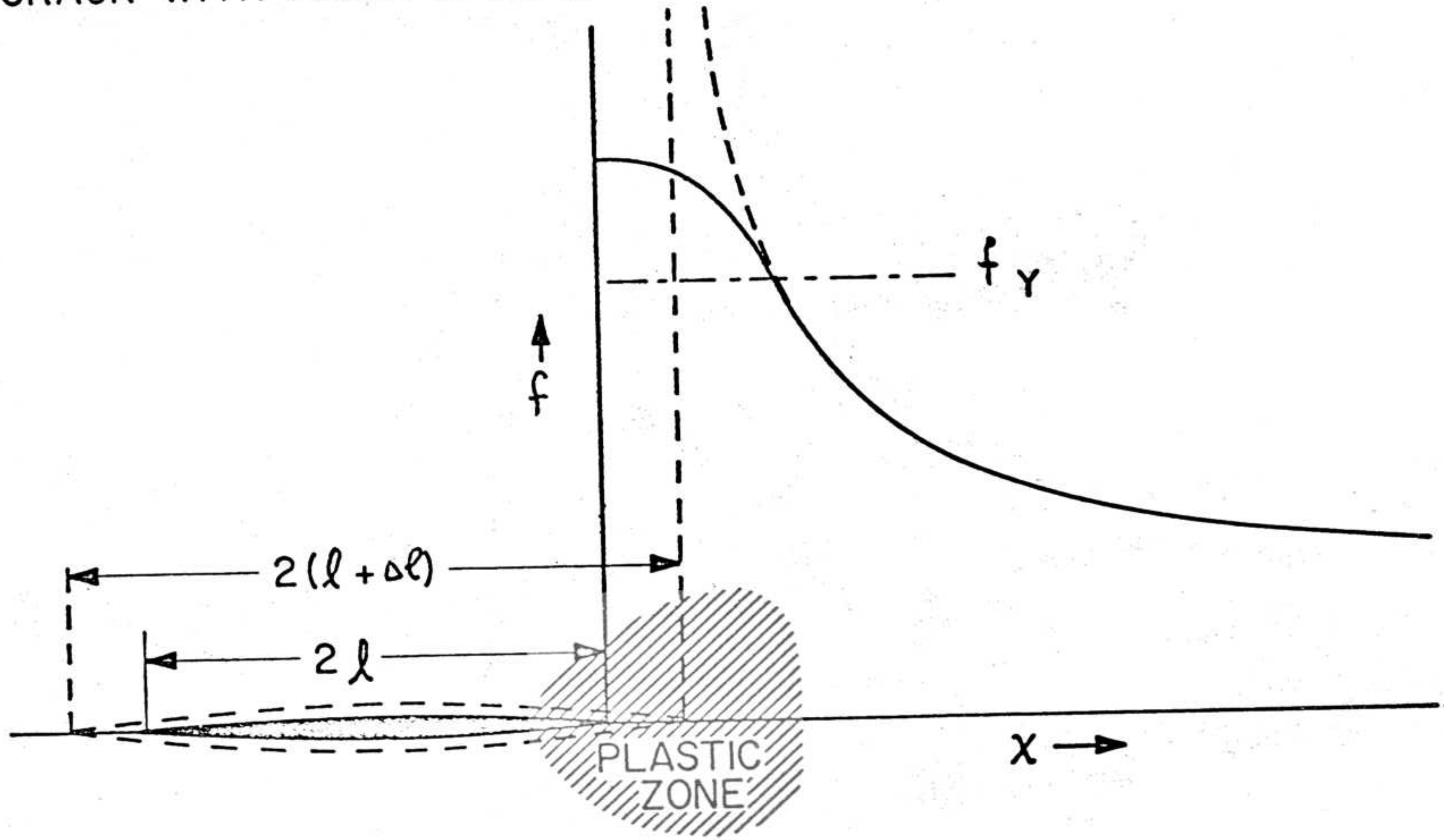

CRACK AUGMENTATION $2\Delta\ell = \frac{1}{\pi}\left(\frac{K}{f_Y}\right)^2 \simeq$ PLASTIC ZONE SIZE

(FIG.I.-)

CRACK EDGE
STRESS FIELD EQUATIONS

$$f_y = K \frac{\cos \theta/2}{\sqrt{2\pi r}} \left\{1 + \sin\frac{\theta}{2} \sin\frac{3\theta}{2}\right\} \quad (1)$$

$$f_x = K \frac{\cos \theta/2}{\sqrt{2\pi r}} \left\{1 - \sin\frac{\theta}{2} \sin\frac{3\theta}{2}\right\} - f_{ox} \quad (2)$$

$$f_{xy} = K \frac{\cos \theta/2}{\sqrt{2\pi r}} \sin\frac{\theta}{2} \cos\frac{3\theta}{2} \quad (3)$$

$$K^2 = E\mathcal{G} \quad (4)$$

E = MODULUS OF ELASTICITY

$\mathcal{G}$ = STRAIN ENERGY RELEASE RATE

K = STRESS INTENSITY FACTOR

"PLASTIC" STRESS CONCENTRATION FACTOR CONCEPT

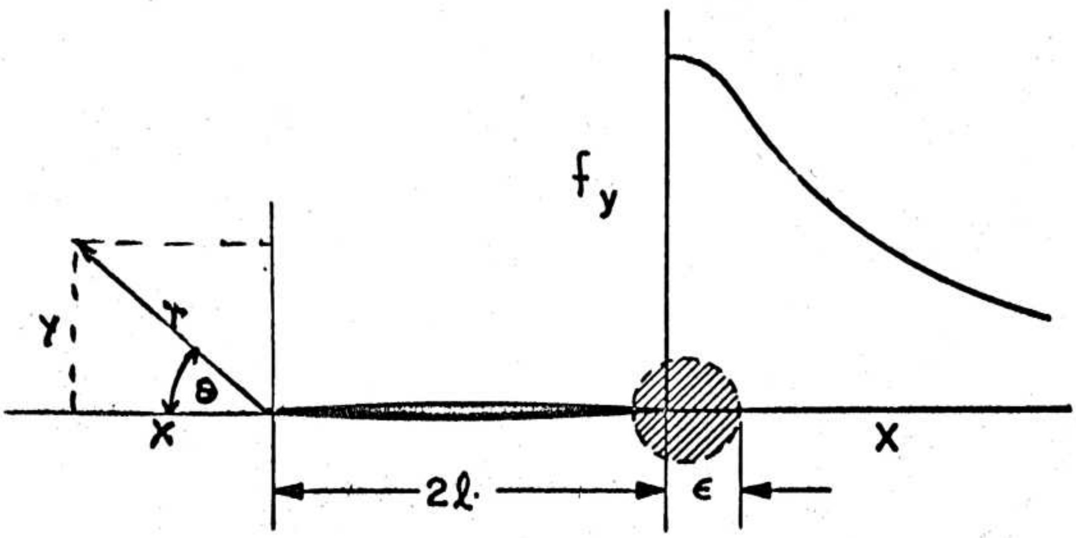

$$\bar{f} = \frac{1}{\epsilon} \int_0^{\epsilon} f_y \, dx \quad (5)$$

$$= K\sqrt{\frac{2}{\pi\epsilon}} \quad (6)$$ (After Irwin).

$$K = f\sqrt{\pi \ell} = \bar{f}\sqrt{\frac{\pi\epsilon}{2}} \quad (7)$$

$$\text{"PLASTIC" S.C.F.} = \frac{\bar{f}}{f} = \sqrt{\frac{2\ell}{\epsilon}} \quad (8)$$

FIG. 2.

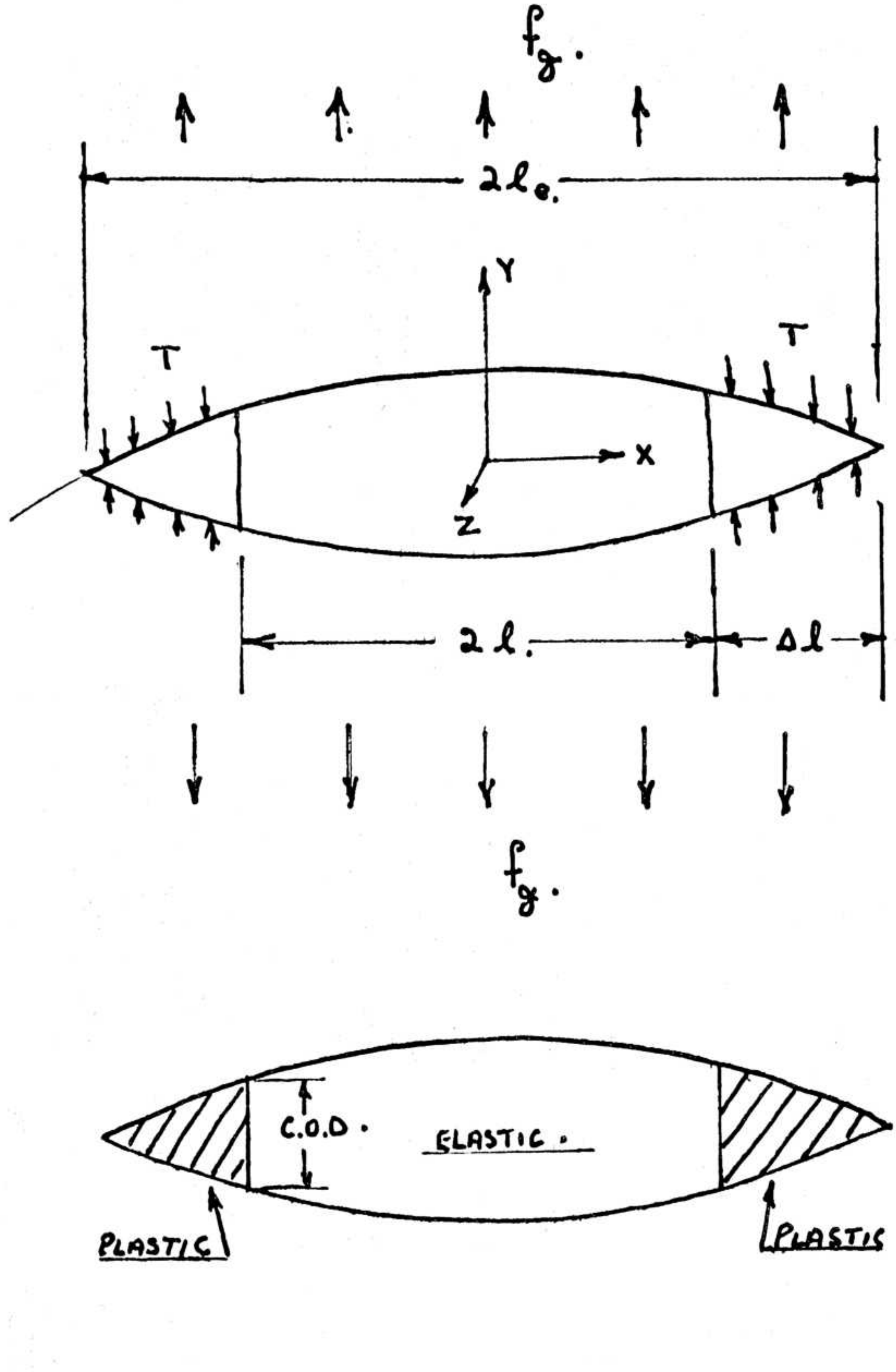

FIG.3.

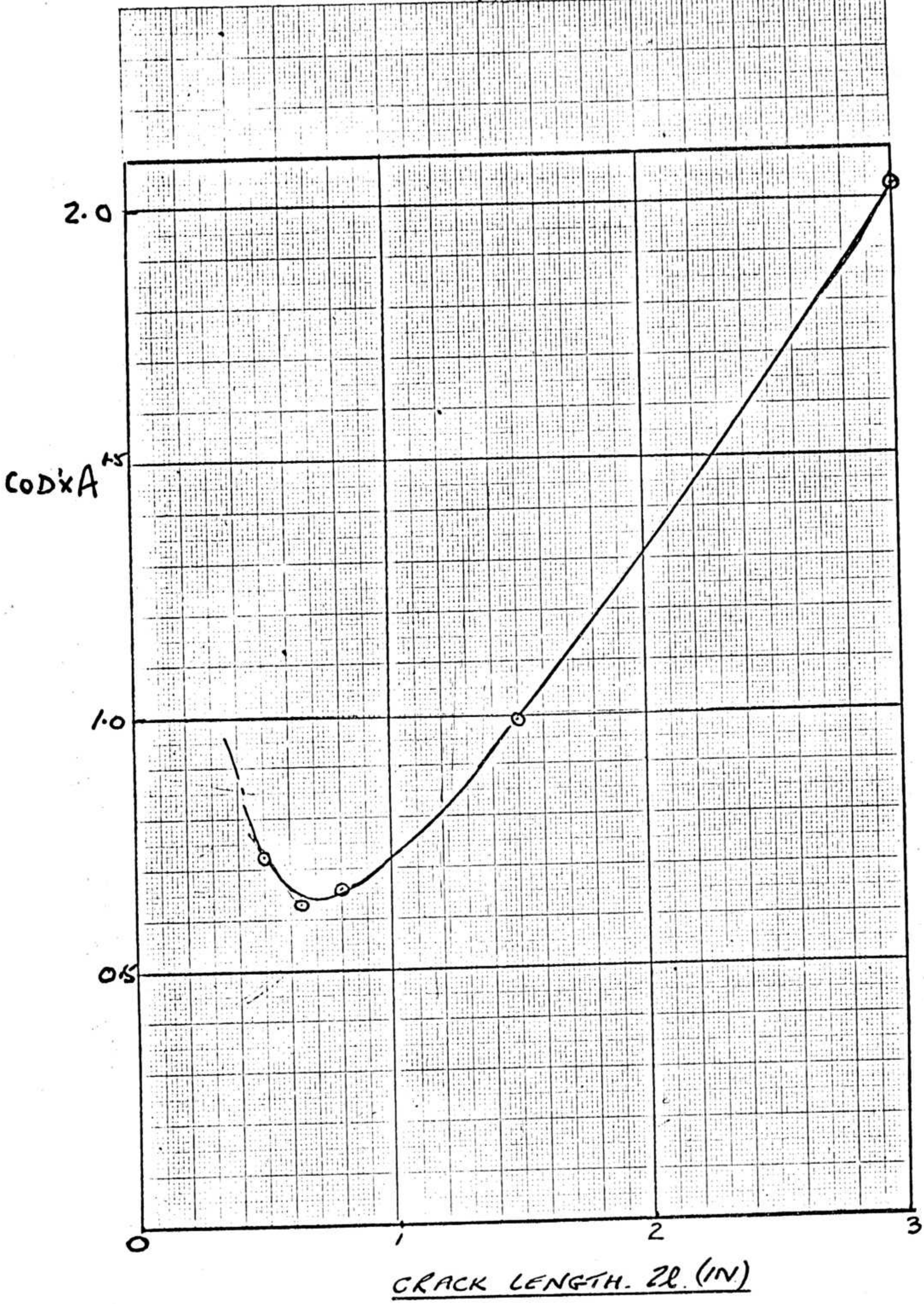

FIG. 4 CRITICAL COD – CRACK LENGTH AS CALCULATED FROM EQN. (11). ZIRCALOY-2. DATA p.5. AHSB (S) R134

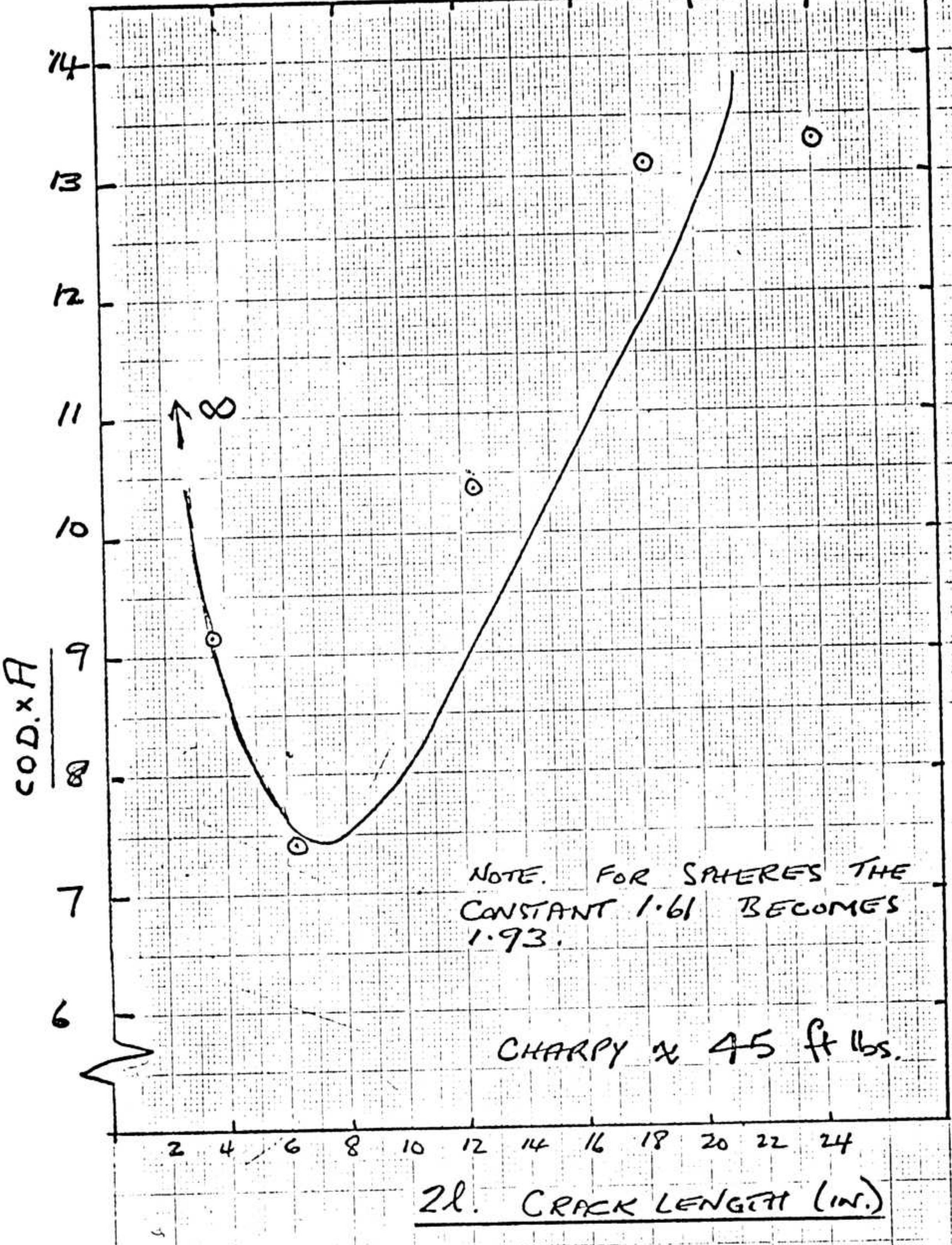

FIG. 5. CRITICAL COD – CRACK LENGTH. AS CALCULATED FROM EQ^{n}. 11. BS 1501–161 : 1958 GRADE B SPHERES. DATA p19. AHSB(S) R134

DO NOT PRINT BEYOND THIS LINE

GRADING

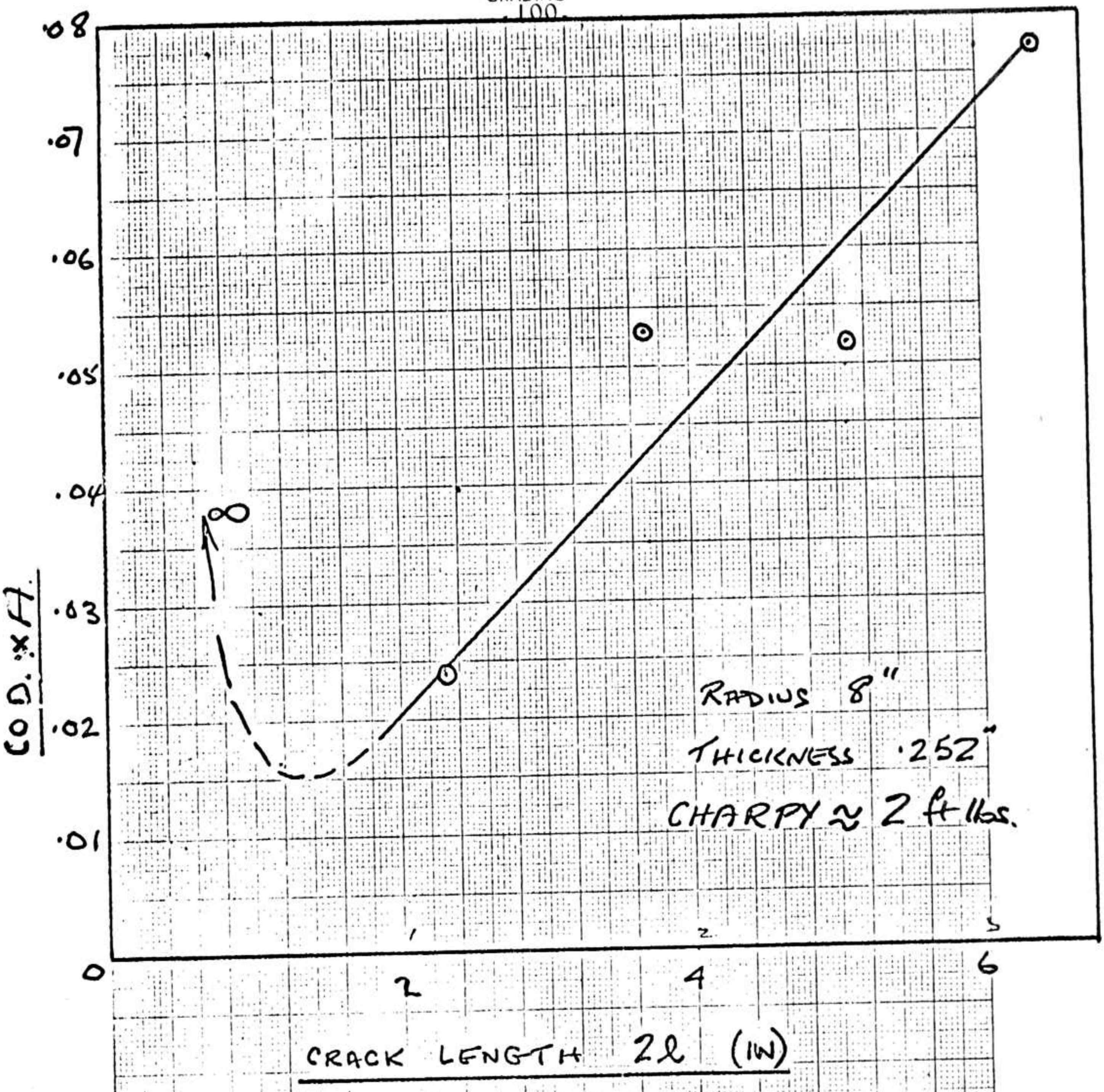

FIG 6. CRITICAL COD (EQN 11) – CRACK LENGTH. 0·21% STEEL PIPES TEMP. –196°C.

DATA: p. 21 AHSB (S) R149.

DO NOT PRINT BEYOND THIS LINE

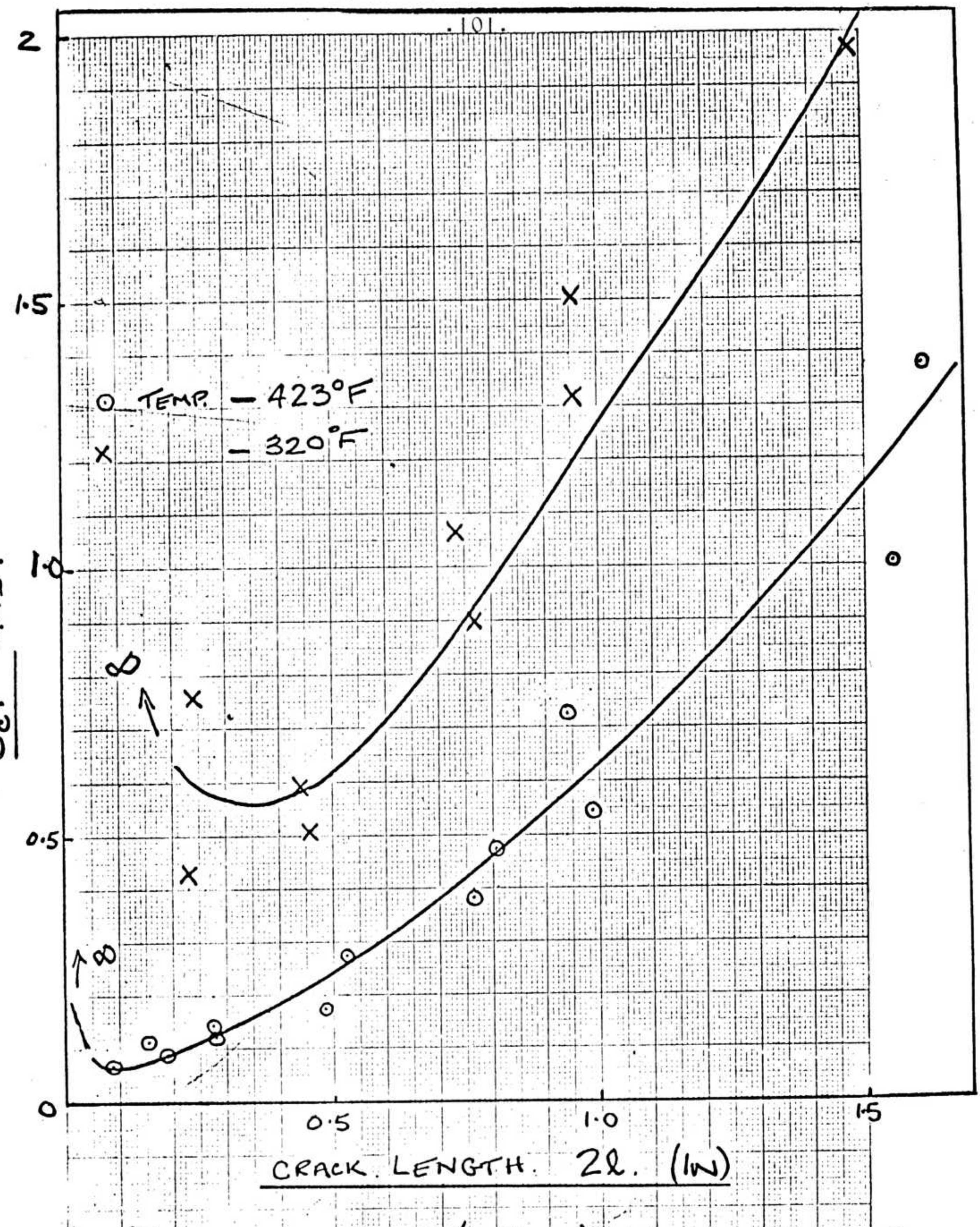

FIG 7. CRITICAL COD (EQN 11) − CRACK LENGTH.
5Al − 2.5Sn − Ti CYLINDERS. DATA: P11, AHSB(S) R134

LECTURE No. 7

APPLICATION OF FRACTURE MECHANICS

1. Types of Application

Fracture mechanics can be used in several different ways. First of all, in a rather qualitative way, such as to identify problem areas at the design or construction stages. Here only nominal values of material values and stress levels may be known, and so the objective is to obtain an approximate estimate of crack size and to use this to assess particular combinations of design detail and material properties, thus avoiding:-

(i) Situations which give rise to critical crack sizes below the level of discrimination of the inspection methods.

(ii) Situations which are unpredictable because either the stress level or the material properties are unpredictable.

Such an assessment may also be used to obtain assurance that leak before break behaviour has been achieved in certain cases.

Secondly, fracture mechanics may be used in a comparative way, such as fixing operational limits of temperature and pressure in a reactor vessel. Here the objective is to determine the level of structural strength at temperatures lower than those of normal operation by reference to previous satisfactory pressurisation at normal operating conditions and assuming constant crack length during depressurisation.

Finally, absolute values of permissible crack sizes may be defined. Thus the sensitivity of the inspection methods necessary during construction or again the amount of crack growth, which may be shown to be tolerable, bycarrying out a proof test, may be defined.

The applications mentioned above are in order of increasing accuracy of prediction and detailed examples of these is given, using the approach of Lecture 5.

2. Type of Material

The approach of Lecture 5 was developed specifically for low strength materials i.e., mild and low alloy steels with tensile strengths 20-40 T.s.i., yield strengths of 12 -30 T.s.i., and Charpy values of 5 - 120 ft. lbs. Cracking is, of course, most likely to be associated with weldments and it is sometimes the properties of these and the associated heat affected zones that are of most interest. In the primary circuit of a nuclear reactor the materials of construction are subjected to the effects of nuclear radiation. The direct influence of this on mild and low alloy steels is to increase the yield stress and generally reduce Charpy values. Indirect effects may also be present such as embrittlement by radiolytically produced Hydrogen. Other materials such as stainless steel may be embrittled by other mechanisms. Some steels are prone to strain ageing embrittlement, i.e., if the steel is strained plastically - say at the tip of a crack, then held at an elevated temperature for some time, and then again loaded, it will fail at a lower stress level than that which produced the plastic straining in the first place. Such a characteristic is obviously undesirable for high integrity components and such materials should not be used. The methods of fracture mechanics provide a suitable method of detection.

3. Geometry of Components

Components of simple geometry under uniform stresses are the most readily analysed. Methods of treatment for more complex cases have been outlined in Lecture 5.

The effect of radius and thickness of the component has also been discussed in Lectures 5 and 6. It may be summarised by saying that they can have an effect on the mode of failure but, except in the case of the bulging mode, have little effect on failure stress. For the materials mentioned above, it is not likely that shear mode failures will occur at thicknesses in excess of 3". This means that for most nuclear reactor vessels only the P_1 mode need be considered, although the shear modes are possible in piping and ducting. Indeed, in order to ensure leak before break behaviour in relatively thin small diameter piping, the material properties should be chosen to give the $P_1 - P_2$ (bulging mode), with its associated large crack opening and leakage. Thus the integrity of the reactor vessel will depend on not having any cracks approach the critical size, whereas the integrity of the piping can be made to depend on failure, if it occurs, being of a certain type. (Leakage is still classed as failure).

4. Determination of Material Properties and Stress Levels

The determination of material properties which realistically represent the component in its finally manufactured state is one of the most difficult aspects of applying fracture mechanics. Where the accuracy required is not great, such as in preliminary material assessment, nominal values of both material properties and stress level may be used. For example, to allow for possible local yielding in the proof test the stress level may be fixed at yield stress level, and material properties should represent the worst conditions which are possible in the weld, heat affected zone, or parent plate. This will result in a conservative assessment from the point of manufacture. It should be borne in mind however, that because of the strong dependence of crack growth rate on crack length, it is not conservative if used in a fatigue life assessment. Fig. 1 shows a $f_g - f_g 1$ plot (P_1 mode) for a low alloy weld metal using typical properties. At the other extreme, when an accurate assessment is required, such as that necessary to estimate the cover obtained from a repeat proof test in a nuclear reactor vessel, considerable effort may be required to obtain a full stress analysis. Specimens of the material will have to be installed in the vessel under conditions which are fully representative of the environment, so that they are available for withdrawal and testing at predetermined intervals throughout the life of the reactor. Lecture 5 explained how the parameter S could be determined from yield stress and Charpy value. The Charpy test is suitable for the measurement of the properties of local areas such as the weld heat affected zone. To determine the tensile properties miniature specimens such as the Houndsfield will be necessary. Where sufficient material is available, and if one is resigned to using a special test piece, the relationship between S and temperature may be determined directly by using a cracked tensile specimen. Such a procedure would work best at temperatures corresponding to low Charpy values. By also carrying out Charpy tests and making an S-Charpy correlation similar to that of Figs. 7 or 9 of Lecture 5, extrapolation to the more ductile range is possible.

5. Examples of Various Applications

(a) Material Selection or Assessment

Such guidance is normally contained in a Standard or Code of Practice.[1] Fig. 1 for low alloy weld metal has already been referred to above. Yield stress level in the parent plate is about 27 T.s.i., and Charpy value in the heat affected zone is 7 ft. lbs. at atmospheric temperature and therefore, from Fig. 1, 21 = 0.6" (14 m.m.). Fig. 2 shows a mild steel typical of the materials used in the construction of the primary circuits of Stage I Gas Cooled Reactors in the U.K. Yield stress is 15 T.s.i. and Charpy in weld metal could be as low as 25 ft. lbs. at atmospheric temperature and therefore, the total crack length is 6" (140 m.m.). It is obviously much easier to achieve an adequate standard of construction in the mild steel.

(b) Operational Limits - Low Temperature Protection

Once a vessel has been raised to its working pressure and temperature there is some evidence that it will not fail at lower temperatures, unless this value of pressure is exceeded. This hot pre-stress effect has been mentioned in Lecture 4. However, this effect is, as yet, incompletely understood and applications where complete reliance may be placed on it are ill-defined.

The other principle available for low temperature protection relies on the fact that if the vessel has survived a certain pressure, namely the working pressure at a high temperature without failure, then, because appreciable crack extension will not occur during reduction of pressure, permissible safe conditions can be defined by moving down a constant crack length line on a diagram of the type in Figs. 1 and 2. In moving down this line, values of Charpy energy can be read off, corresponding to various stress levels. If stress is then converted to pressure and Charpy to temperature (from Charpy-temperature characteristic), the curve defining the minimum safe temperature for a certain pressure is obtained. This is a limit approach, i.e., it is the limiting condition under which it is possible to show that the vessel cannot fail. There are some applications in which the most severe stress condition does not occur under maximum pressure. An example is the stress system produced by bolt pre-stress in a flange region. Here the condition that controls is at zero pressure and maximum temperature - maximum values of stress dropping off as pressure is applied.

(c) Proof Testing of Steel Containment Structures

Here, the same idea as in example (b) is used the reverse way round. When a large containment structure for say a nuclear reactor has to be fabricated, it is highly desirable to apply a proof pressure test as well as a leak test. However, often because of plant and equipment which are already inside, it is either difficult or impossible to apply a pressure equal to the accident pressure it is desired to contain. It can usually be arranged that the temperature of the containment shell is one which gives nearly upper shelf Charpy values.

By carrying out a combined pressure and leakage test at a pressure which is only a fraction of the accident pressure and a temperature which gives lower shelf Charpy values, see Fig. 3, an adequate pressure test can be obtained. The difference in temperature can increase the test severity by as much as a factor of 2 on stress.

The assumptions made are as follows:-

(a) The containment structure, once it has been tested, will normally be maintained at a constant or zero pressure difference until the occurrence of the accident.

(b) The structure contains cracks which do not increase in size during normal operation.

(c) It is possible, to ensure that at the time the structure has to function as a containment its temperature is significantly higher ($\approx 60^{\circ}C$) than the test temperature.

(d) Repeat Proof Testing Reactor Vessels

The main objective in carrying out a repeat proof pressure test on a reactor pressure vessel is to transfer the risk of failure to a point in time at which the consequences of such a failure may be prepared for and consequently minimised. The test is carried out by applying an overpressure such that, at the chosen test temperature, the size of crack required to cause sudden rupture is less than under normal operating conditions. Following such a test, the vessel will be safe for a period of operation which is just less than that which will cause a crack of a size equal to the critical crack length under test conditions, to grow to the critical crack size under operating conditions.

It follows from the above, that increasing the severity of the test, either in terms of pressure and/or temperature, decreases the critical crack size under test conditions, thus increasing the risk of failure during the test and increasing the immunity period. Therefore, it is desirable to strike a suitable balance between these factors to avoid either over-testing or under-testing for a given immunity period. It is suggested that this can be done by the use of fracture mechanics.

As mentioned above, the severity of the test controls the critical crack size under test conditions and therefore, the amount of crack growth available during the next period of operation. The relationship between the length of this period and the amount of crack growth depends on the rate of crack growth and hence on the mechanism of crack growth. For temperatures below 350°C and mild steel, crack extension will be by a fatigue type process, brought about by the major pressure cycles the vessel receives and experimental data on the growth of cracks in mild steel pressure vessels under various levels of cyclic stress may be used to derive the amount of crack growth required for a certain period of safe operation (immunity period).

Examination of the experimental data on crack growth suggests that the phenomena of crack growth and fast fracture are quite separate and independent.

The growth rate of a through thickness crack cycled at constant stress amplitude, appears to be exponentially dependent on the length of crack, e.g., a crack 2 or 3 inches half length, growing under a stress amplitude of 15 T.s.i., has a growth rate of a few thousandths of an inch per cycle. However, when this same crack has grown to a half length of 7 or 8 inches, it is growing at the rate of several tenths of an inch per cycle, under the same cyclic conditions. However, the "natural" growth of such a crack, in practical materials such as mild steel, will be cut short by the onset of fast fracture when the crack reaches its critical size, as determined by the stress level and material properties, (U.T.S., yield strength and Charpy). Thus two cracks in pressure vessels, one with a high Charpy value and the other with a low Charpy value, will have similar growth curves, except that the crack in the vessel with low Charpy will fail at a shorter length than the other. However, because of the strong dependence of crack growth rate on crack length, most of the cycling takes place at the shorter crack lengths, and therefore, the total number of cycles to failure is, for materials of reasonable notch ductility, (say 60-100 ft. lbs.), dependent only on initial crack length and stress level. This allows the derivation of Fig. 4 for through thickness cracks.

It has been explained above how the application of test conditions ensures that there are no cracks greater than a certain size in the vessel, this size depending on the stress level and material properties. This is the initial crack size referred to above. This size will vary for the different materials and different stress levels in the vessel, being large for areas where material is at a low stress level and has high notch ductility and smaller where there are local stress concentrations and brittle material. There may, of course, be no crack approaching these limiting sizes in a vessel which has successfully withstood the test and therefore, the approach is basically a limit approach and is inherently pessimistic.

A worked example is given in Appendix I.

(e) De-rating Procedures

Pressure vessel failure statistics show that failure rates are higher in early years of life and again towards the latter end of design life. The early peak is normally allowed for by more frequent inspection. In the later years it may be more convenient to de-rate rather than to increase operational inspection, or again, a de-rating procedure may be combined with a very slight overpressure test. The arguments are similar to those for repeat proof testing and Fig. 5 illustrates the procedure. First, the pressure is dropped gradually over a period of time down a curve dictated by the growth rate of a crack which is 90% of its critical size at operating conditions. When the pressure has dropped to about 90% of the original operating pressure it is then raised back to its original level. This really amounts to carrying out a 10% proof test. Alternatively, a 5% proof test can be carried out first and de-rating carried out from this datum until the pressure is 5% below normal operating pressure. A 10% proof test is then carried out and the cycle repeated.

6. Discussion

In the applications described in Section 5, the through-crack fracture model has been used. In the case of example (a), the idea of maximum acceptable crack size is notional and therefore the use of the through crack model is permissible. In example (b), it may be argued that low temperature protection is only necessary against the possible occurrence of through thickness cracks. In example (c), the application intended is thin shell structures and the argument is strictly valid only for through cracks. Obviously, it is not a conservative approach.

In examples (d) and (e), strictly speaking, the calculations should be carried out for both through and part-through cracks. However, experience indicates that the through crack model nearly always gives the least period of cover for a given overpressure and this is the one which should be used.

With regard to the required accuracy of critical crack length predictions, it will be obvious that in example (a) the crack sizes only need to be estimated roughly, whereas in contrast to this in examples (d) and (e), small inaccuracies will seriously affect the degree of cover predicted. In the case of the example in Appendix I, inaccuracies will affect the prediction of the test conditions required.

Reference 1

Specification for Carbon and Low Alloy Steel Pressure Vessels for Primary Circuits of Nuclear Reactors. British Standard 3915: 1965.

APPENDIX I

Material - Mild steel plate to BS 1501-151 Grade 28

Plate thickness - 2 in.

Stress level - 7 T.s.i. at operating pressure

Procedure:-

(a) Enter Fig. 4 at 10 cycles and read off the half crack length for a stress level of 7 T.s.i. as 9.25 in.

(b) Since this crack length is greater than three plate thicknesses, the through crack model is valid.

(c) The crack length obtained in (a) is the maximum size which can exist under test conditions in this particular material. Hence the product of gross stress under test conditions and half crack length can be obtained. e.g., for an overpressure ratio of 1.2

$$f_g l = 7 \times 1.2 \times 9.25 = 77.7$$

The point on Fig. 2 defined by $f_g = 7 \times 1.2 = 8.4$ and $f_g l$ corresponds to a Charpy value of 33 ft. lbs. and therefore, this is the maximum Charpy value which must occur under test conditions for this material to obtain an immunity period of 10 cycles.

(d) This process is repeated for different stress levels, overpressure ratios and numbers of cycles and the results plotted in Figs. 6 and 7.

(e) The maximum test temperatures can be derived from Figs. 6 and 7 and the Charpy-temperature curve.

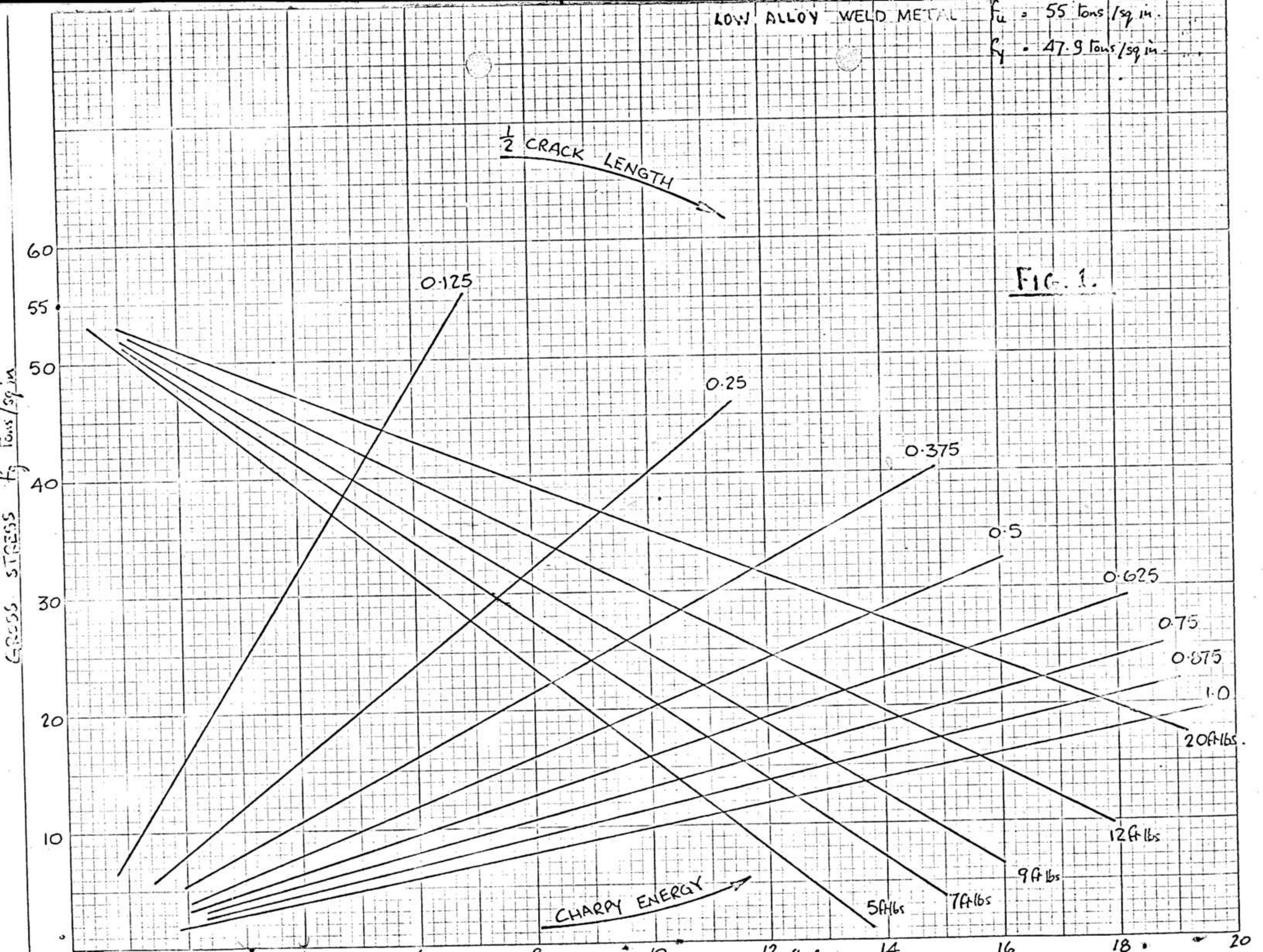
LOW ALLOY WELD METAL
f_u = 55 Tons/sq in.
f_y = 47.9 Tons/sq in.
½ CRACK LENGTH
CHARPY ENERGY
0·125
0·25
0·375
0·5
0·625
0·75
0·875
1·0
20 ft lbs.
12 ft lbs
9 ft lbs
7 ft lbs
5 ft lbs
GROSS STRESS f_g Tons/sq in
60
55
50
40
30
20
10
0
14
16
18
20

FIG. 1.

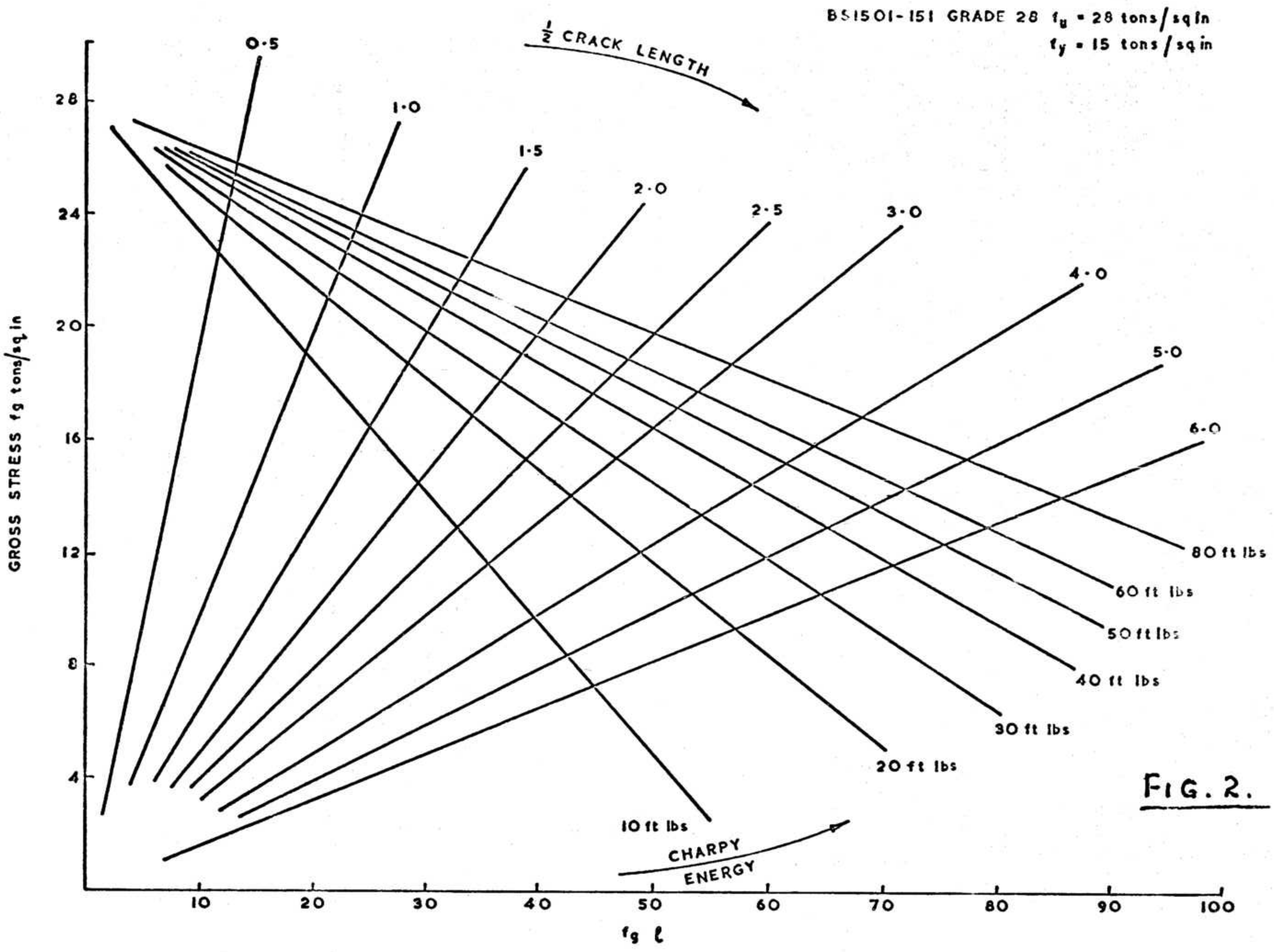

BS1501-151 GRADE 28 f_u = 28 tons/sq in
f_y = 15 tons/sq in
½ CRACK LENGTH
0·5
1·0
1·5
2·0
2·5
3·0
4·0
5·0
6·0
80 ft lbs
60 ft lbs
50 ft lbs
40 ft lbs
30 ft lbs
20 ft lbs
10 ft lbs
CHARPY ENERGY
GROSS STRESS fg tons/sq in
28
24
20
16
12
8
4
10
20
30
40
50
60
70
80
90
100
$f_g\,l$

FIG. 2.

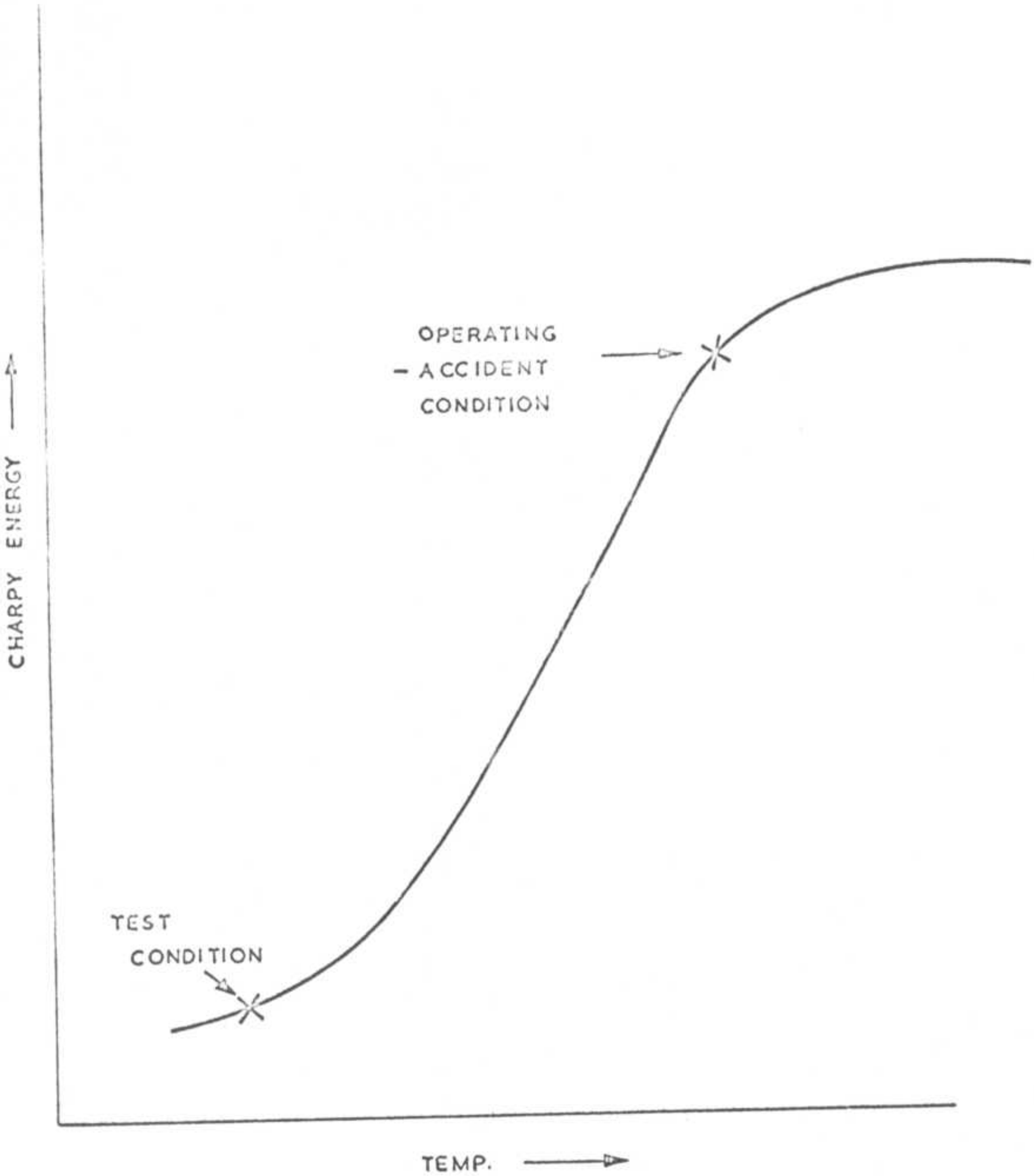
OPERATING
- ACCIDENT
CONDITION
CHARPY ENERGY
TEST
CONDITION
TEMP.

FIG. 3.

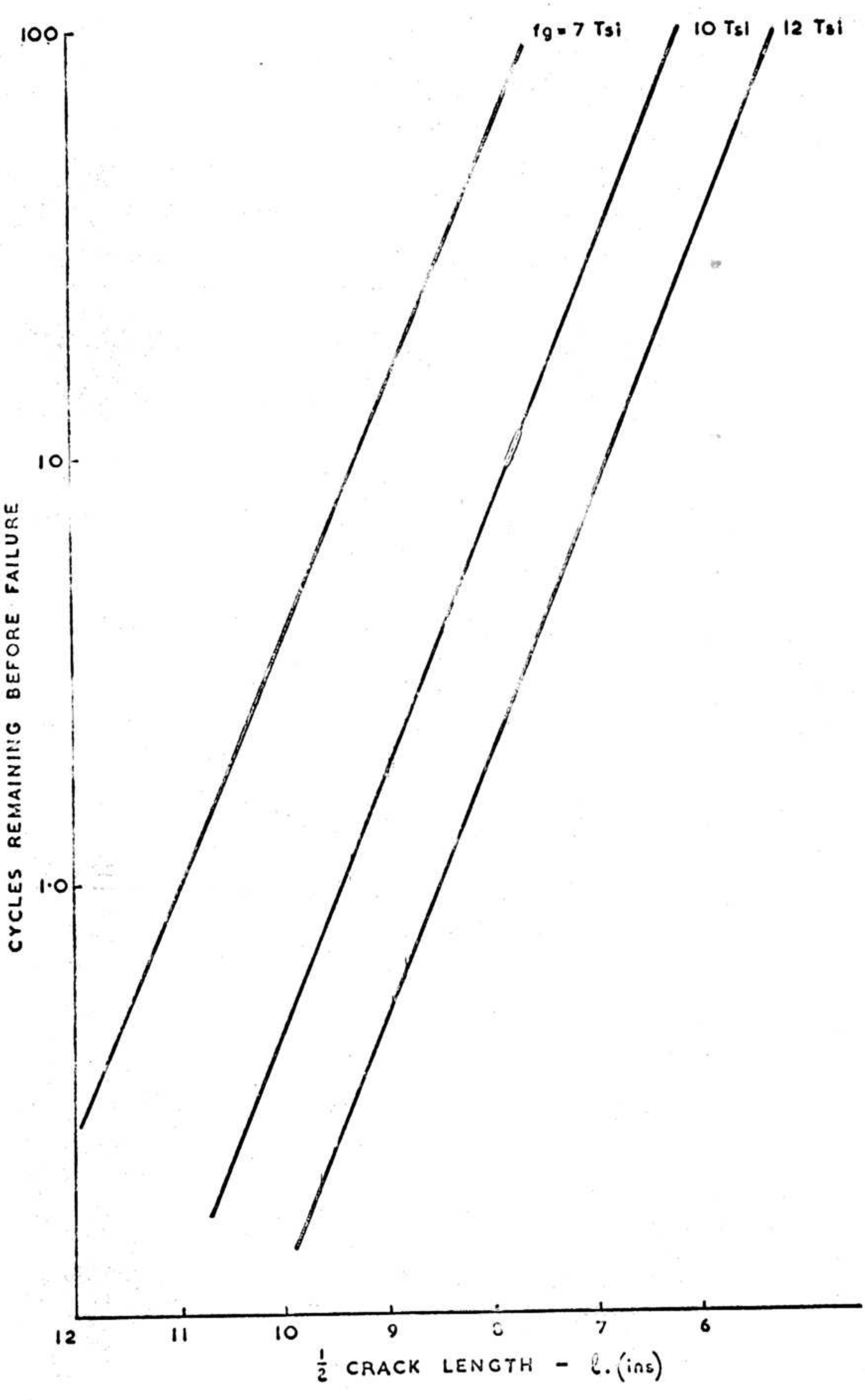
fg = 7 Tsi
10 Tsi
12 Tsi
100
10
1·0
CYCLES REMAINING BEFORE FAILURE
12
11
10
9
8
7
6
½ CRACK LENGTH – ℓ. (ins)

FIG.4.

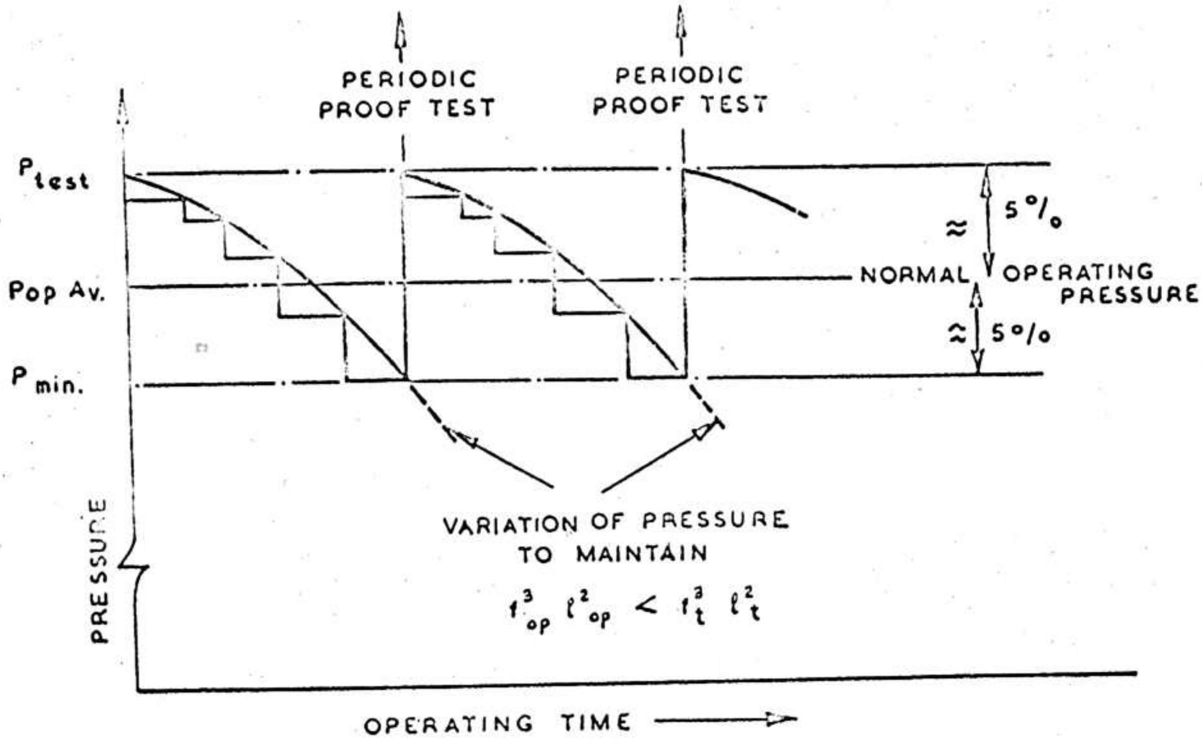

P test > NORMAL OPERATING PRESSURE

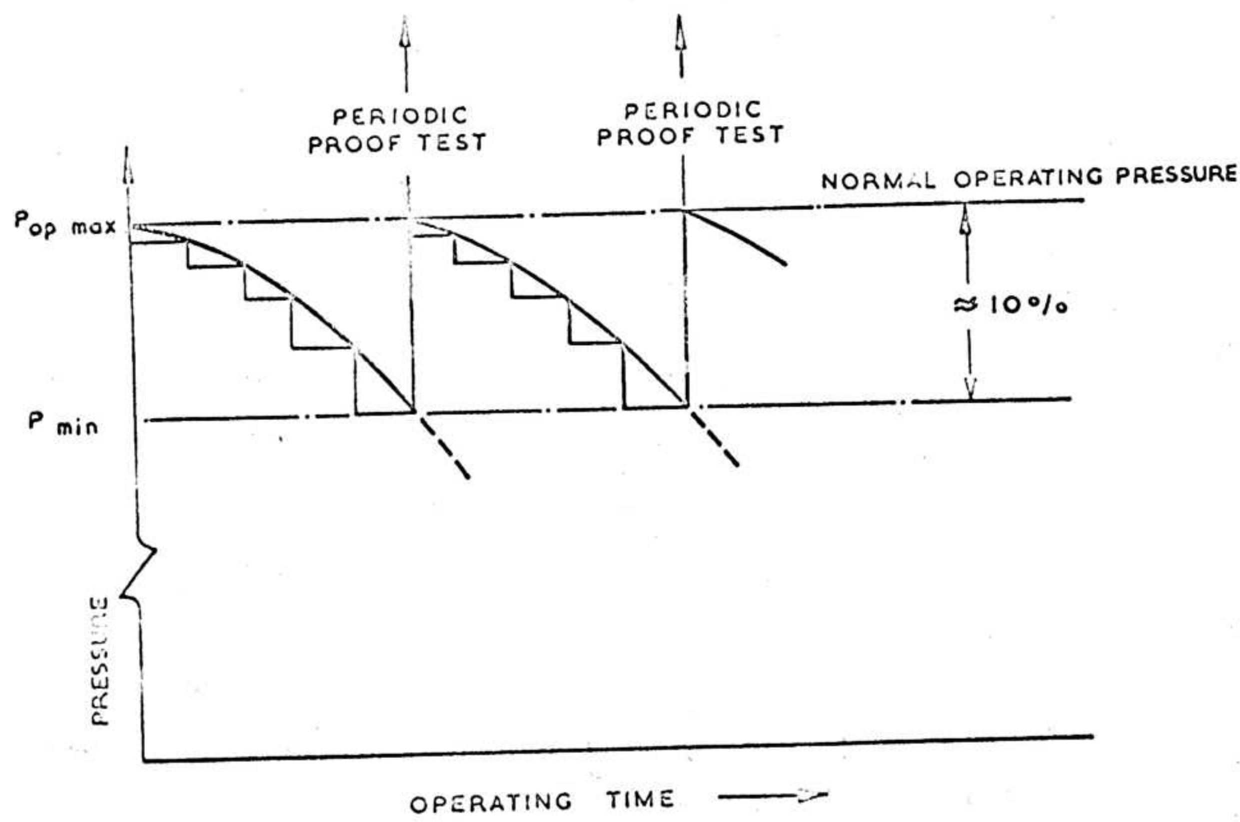

FIG. 5 Ptest = NORMAL OPERATING PRESSURE

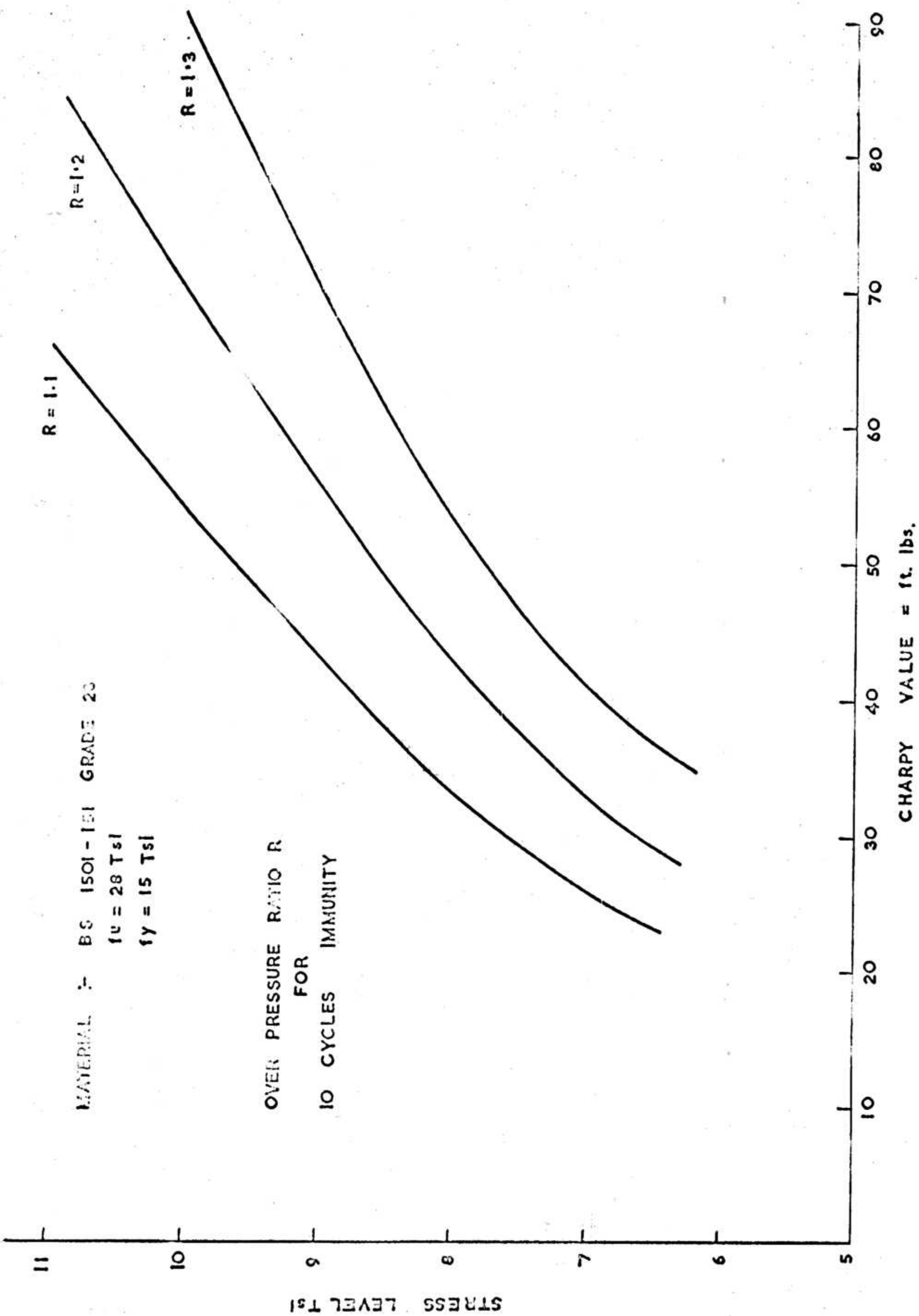
MATERIAL :- BS 1501 - 151 GRADE 28
fu = 28 Tsi
fy = 15 Tsi
OVER PRESSURE RATIO R
FOR
10 CYCLES IMMUNITY
R = 1.1
R = 1·2
R = 1·3
STRESS LEVEL Tsi
CHARPY VALUE = ft. lbs.
5
6
7
8
9
10
11
10
20
30
40
50
60
70
80
90

FIG . 6

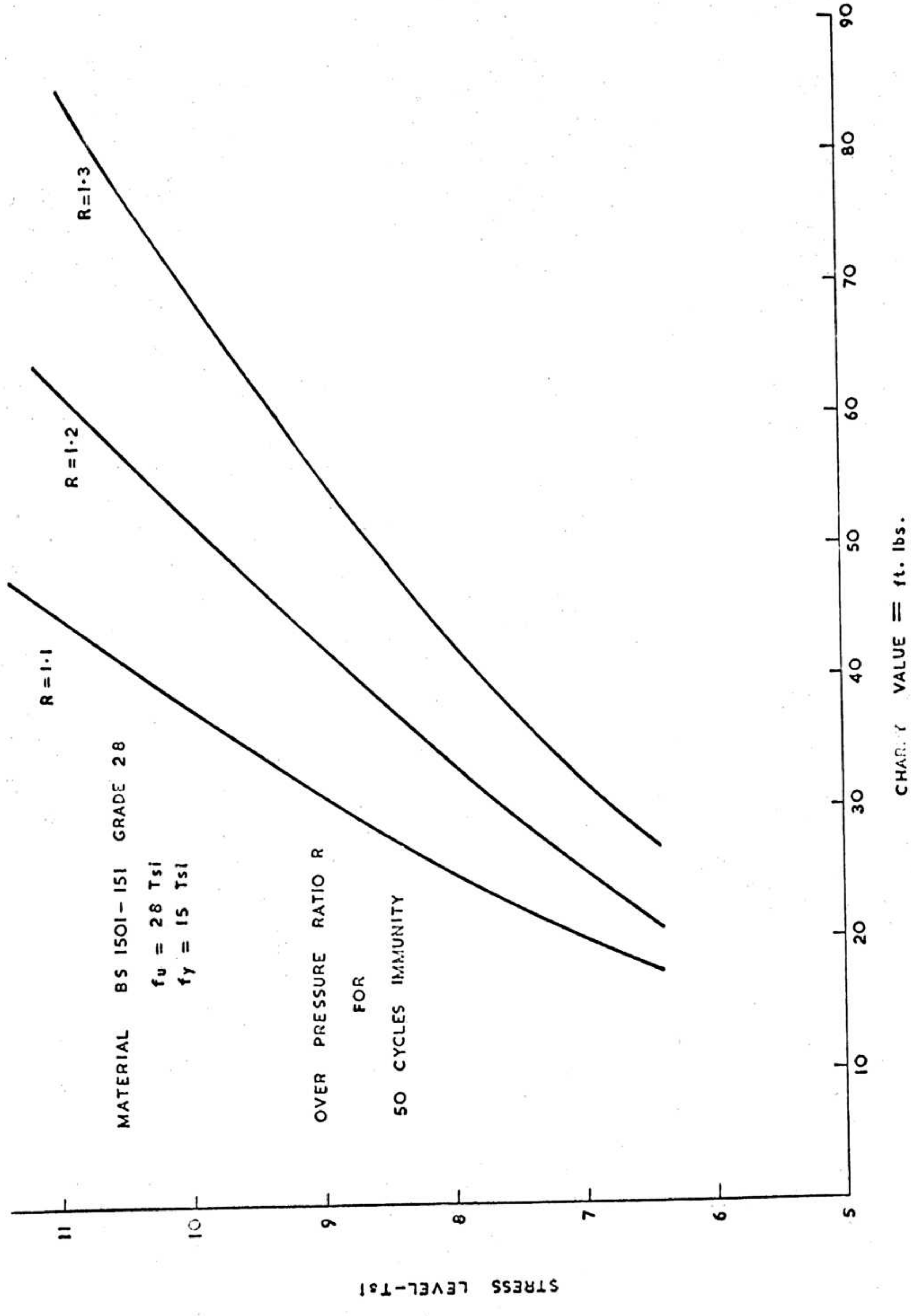
MATERIAL BS 1501 - 151 GRADE 28
f_u = 28 Tsi
f_y = 15 Tsi
OVER PRESSURE RATIO R
FOR
50 CYCLES IMMUNITY
R = 1·1
R = 1·2
R = 1·3
CHARPY VALUE — ft. lbs.
STRESS LEVEL-Tsi
10
20
30
40
50
60
70
80
90
5
6
7
8
9
10
11

FIG. 7